Int. J. Plant Sci. 180(5):411–457. 2019.
1058-5893/2019/18005-0006$15.00 DOI: 10.1086/702641

EXPLOITING NONDIETARY RESOURCES IN DEEP TIME: PATTERNS OF OVIPOSITION ON MID-MESOZOIC PLANTS FROM NORTHEASTERN CHINA

Xiaodan Lin,*,† Conrad C. Labandeira,[1,*,†,‡] Qiaoling Ding,*,§ Qingmin Meng,* and Dong Ren[1,*]

*Capital Normal University, College of Life Sciences, Beijing 100048, China; †National Museum of Natural History, Smithsonian Institution, Washington, DC 20013, USA; ‡Department of Entomology, University of Maryland, College Park, Maryland 21740, USA; and §School of Life Sciences, Sun Yat-sen University, Guangzhou 510275, China

Editor: Patrick H. Herendeen

Premise of research. Even though the fossil record of oviposition provides a rich archive of plant resource use, it is deficient for a fundamental reason. Very few analyzable oviposition data have been collected, particularly from the preangiospermous Mesozoic.

Methodology. From northeastern China, we investigated 1817 plant specimens of the Early Cretaceous Jehol Biota (125 Ma), of which 60 specimens exhibited ovipositional damage; 3886 specimens of the Middle Jurassic Yanliao Biota (165 Ma) revealed 296 specimens with ovipositional damage; and 408 specimens from the Late Triassic Beipiao Biota (205 Ma) yielded 19 specimens with ovipositional damage. First, we analyzed herbivore ovipositor structure of 68 Jehol and Yanliao insect species, resulting in nine ovipositor morphotypes. Second, we analyzed oviposition lesions of plant specimens from all three biotas, yielding 15 oviposition damage types (DTs). Third, we linked ovipositor morphotype to oviposition DTs.

Pivotal results. The most heavily oviposited Jehol plant group was conifers, particularly *Liaoningocladus boii*; *Equisetites* (horsetails) were subordinately attacked. For the Yanliao Biota, the most intensely oviposited plant group was bennettitaleans, particularly *Anomozamites*, responsible for 46.6% of all ovipositor associations in the total Jehol-Yanliao-Beipiao data set. The conifer *Yanliaoa* and the ginkgophyte *Ginkgoites* had subordinate levels of oviposition. The Beipiao Biota revealed a more balanced distribution of oviposition, with cycads and ferns having the greatest ovipositional damage.

Conclusions. These three time slices, separated by two 40-million-year intervals, indicate major shifts in oviposition preferences. An examination is warranted into the factors promoting the pronounced oviposition levels on Yanliao *Anomozamites*, a bennettitalean.

Keywords: bennettitalean, damage type, endophytic oviposition, Jiulongshan Formation, *Paleoovoidus*, Yixian Formation.

Online enhancement: appendix.

Introduction

Insects use plants as resources in a variety of trophic ways, the most common of which is the antagonism of herbivory (Singer 1984). Two other major trophic modes of resource use by insects are mutualisms that involve consumption of nectar and/or pollen essential in pollination (Bronstein 2015) and seed predation for dispersing plant embryos to new sites (Forget et al. 2004). Nontrophic uses of plants by insects include mimicry to avoid predation (Chopard 1938; Mugrabi-Oliveira and Moreira 1996; Barker et al. 2005) but also interactions such as domatia and leaf folds, rolls, and cases that combine provision for shelter with access to food (Johnson and Lyon 1976; O'Dowd and Willson 1989). Perhaps most important in the use of plants primarily as shelter is oviposition. For oviposition, plant surfaces and deeper tissues are substrates for egg laying (Hinton 1981; Braker 1989) but advertently incur a wealth of microecological processes and their associated feedbacks that determine how the egg-laying and egg-reposing processes are deployed in time, space, and host plant substrate. The process of oviposition incurs the twin liabilities of dealing with host plant protective responses and avoidance of predators and parasitoids (Chew and Robbins 1984; Janz 2002). For oviposition, female insects access the costs and benefits of life-history traits such that only those sites are selected for oviposition that favor growth and survival of offspring

[1] Authors for correspondence; email: labandec@si.edu, rendong@mail.cnu.edu.cn.

ORCIDs: Labandeira, https://orcid.org/0000-0002-4838-5099; Ren, https://orcid.org/0000-0001-8660-0901.

Manuscript received October 2018; revised manuscript received November 2018; electronically published April 23, 2019.

(Denno and Dingle 1981). As ovipositing insects occur in virtually all terrestrial and some aquatic habitats (Wesenberg-Lund 1943), the availability of plants at local sites determines choices for food, shelter, and oviposition (Craig et al. 1988; Lambret et al. 2015). Because there often are elevated levels of insect-mediated ovipositional damage on plants, many plants respond by producing an armamentarium of corresponding chemical (Janz 2002; Hilker et al. 2005) and physical (Constant et al. 1996; Lokesh and Singh 2005) defenses against insects to seal off intrusions into tissues and to avoid future attack.

Although insects lay eggs in plant tissues as a nonnutritive plant resource, the nature of the oviposition-plant interaction and its subsequent effects is analogous to that of herbivory (Scheirs and De Bruyn 2002). As in herbivory, there is modification of pristine photosynthetic tissue into a metabolically marginal or useless by-product, such as production of callus and scar tissue and subsequent necroses from pathogens (Sinclair et al. 1987). The emission of airborne volatiles that are detected by predators and parasitoids minimizes the ovipositional load on host plants (Feeny et al. 1983; Dwumfour 1992). The record of oviposition and mouthpart-inflicted damage is significant in revealing patterns of host plant use based on a variety of timescales and the presence of culprit insect-ovipositing lineages (Labandeira 2006*a*, 2006*b*). As in herbivory, the pattern of insect egg laying is divided into two major modes. There is more or less the passive deposition of eggs on plant surfaces, known as exophytic oviposition, commonly with some modification of surface tissues (Severson et al. 1991). The second mode is penetrative intrusion into living, and rarely dead (Martens 1992), plant tissues, known as endophytic oviposition (Guido and Perkins 1975; Corbet 1999). It is for these reasons that oviposition has informally been considered a token for herbivory and that the rich fossil record of oviposition is comparably as valuable as other forms of herbivory, such as surface feeding, piercing and sucking, and leaf mining (Labandeira et al. 2007) in deciphering how insects have historically used live plants.

Paleobiological approaches of examining oviposition in the deep fossil record provide a methodology that is complimentary in many ways to biological approaches of examining modern oviposition. Recent paleobiological methods in studies of plant-insect interactions (Labandeira et al. 2007; Gnaedinger et al. 2014) emphasize broad synecological patterns of oviposition within (Schachat et al. 2014; Labandeira et al. 2018; Xu et al. 2018) and across (Ding et al. 2015; Labandeira et al. 2016) biological communities. These patterns document plant hosts and their insect-inflicted damage but not insect culprits. By contrast, modern biological methods stress an autecological approach wherein the focus is on the physiological, behavioral, and ecological aspects of oviposition facilitated by individual insects (Sankaran et al. 1966). Such methods often delve into the particular nature of the plant host response (Shively 1948; Mumm et al. 2003). Nevertheless, given a major literature of insect body fossil descriptions extending for about 150 years in the recent expanding field of plant-insect interactions, there has not been a study linking ovipositor structure of specific insect taxa with plant damage occurring in the same deposit. Few localities meet the criteria for such studies, and fossil deposits necessarily require three conditions that would suffice for associating ovipositional lesions on plants with ovipositor structure. First, both plant and insect fossils need to be present in sufficient abundance and diversity in the same strata. Second, the deposit should represent a time interval and location that would provide a tractable answer to an interesting evolutionary or ecological question. Third, the deposit should be of sufficient preservational quality of plant and insect fossils that robust data could be obtained. Two of the three mid-Mesozoic deposits of northeastern China, mentioned below, meet these requirements and follow the broad outlines of a previous study that examined patterns of herbivory on broad-leaved conifers from the same three deposits (Ding et al. 2015).

The formal classification of insect feeding on fossil plants initially was based on ichnotaxonomic nomenclature (Vjalov 1975). Since Vjalov's (1975) seminal work, the compass of investigation has been expanded considerably (Straus 1977; Givulescu 1984; Zherikhin 2002) and continually has been updated (e.g., Krassilov et al. 2008). For oviposition, the history of discovery has involved descriptions of single occurrences of plant damage, with a sustained focus on Mesozoic European material (Roselt 1954; Kelber and Geyer 1989; Grauvogel-Stamm and Kelber 1996; van Konijnenburg-van Cittert and Schmeißner 1999; Béthoux et al. 2004; Pott et al. 2008; Laaß and Hoff 2015). This approach has been complemented by more synthetic contributions (Vasilenko and Rasnitsyn 2007; Sarzetti et al. 2009; Gnaedinger et al. 2014). Two recent proposals, however, are relevant for recent and future studies of oviposition in the fossil record. The first suggestion is that complete descriptions should be available to document and describe the morphology of ovipositors from suspected producers of insect damage on fossil plants (Zherikhin 2002). A second proposal is that distinctive oviposition damage on plants should be accepted as valid ichnotaxa and described within the formal system of fossil insect traces (Vasilenko 2005). Such proposals would validate almost all of the damage type (DT) assignments mentioned in this report, found in the current version of the *Damage Guide* (Labandeira et al. 2007) and its supplements. These two steps, as well as more extensive documentation of insect ovipositor structure and ovipositional damage in fossil biotas, would provide a more complete and rigorous approach toward understanding the relationship between oviposited plants and their insect culprits in deep time (Le Pape and Bronner 1987). Fossil insect oviposition data—from both insect causation and plant response perspectives—can provide ecological and evolutionary links among plant-insect relationships, insect reproductive biology, plant physiological and biochemical responses, and understanding of paleoenvironments in deep time (Vasilenko and Rasnitsyn 2007; Krassilov and Shuklina 2008; Na et al. 2014).

In this report, we expand on previous studies by tracking the frequency and diversity of oviposition DTs and assess the degree of plant host specificity across three Mesozoic time slices in northeastern China. In our account of the patterns of oviposition on these vascular plant hosts, we establish new records through examination of ovipositional damage and document specifically the targeting of particular plant groups and the responsible insect lineages. This linkage will be accomplished by describing the uniqueness of ovipositor lesions on plants with reference to the DT system (Labandeira et al. 2007) and by reference to known ovipositor shapes, sizes, lengths, denticulation, and other features causing the ovipositional damage. Last, we evaluate patterns of ovipositional damage to host plants in each of three

time slices, examining features such as culprit insect lineages, host plant specificity, and tissue partitioning. Documentation of the deep evolutionary history of associations between vascular plants and their ovipositing insect interactors is an essential prerequisite for testing hypotheses about the macroevolutionary dynamics of this fascinating plant-insect interaction (Labandeira 2002*a*).

A Brief Overview of Fossil Oviposition

The fossil record of insect oviposition commences during the Pennsylvanian Subperiod (Late Carboniferous) of the late Paleozoic. Pennsylvanian oviposition occurrences have been documented on stems of *Calamites cistii* and other calamite sphenopsids (Weiss 1876; Béthoux et al. 2004; Xu et al. 2018). This distinctive oviposition pattern was caused by an unknown insect lineage, most likely large paleodictyopteroids or odonatopteran dragonflies (Labandeira 2006*a*), given the exceptionally large oviposition lesion lengths of up to 4 cm. A single damselfly-like cluster of oviposition lesions also was recorded on a cordaite leaf at the end of the Pennsylvanian (Laaß and Hoff 2015). Permian occurrences were more varied and overwhelmingly targeted leaves rather than stems, a pattern that mirrors the occurrences of insect galls during the same time interval (Schachat and Labandeira 2015). From the Cisuralian of north-central Texas, major oviposition occurrences were on callipterid peltasperm and taeniopteroid foliage (Schachat et al. 2014, 2015), the former a seed fern and the latter either a fern or a seed plant. Also from the Cisuralian, in Germany, oviposition scars have been documented on cordaitalean foliage, other seed plant stems, and a distinctive oviposition scar that appears on the sphenophyte *Equisetites foveolatus* (Potonié 1893; Roselt 1954). Later during the Permian, a variety of oviposition DTs were found on glossopterid foliage in Gondwana, initially with occurrences from the Cisuralian of South America that range from oviposition marks parallel to secondary veins (Adami-Rodrigues et al. 2004*a*, 2004*b*) to very distinctive U-shaped scars on midribs (Gallego et al. 2014). Other patterns in younger mid-Permian floras from the La Golondrina Formation of Santa Cruz Province, Argentina (Cariglino and Gutiérrez 2011), include at least seven oviposition DTs on pteridosperm leaves of *Kladistamuos* and *Glossopteris* (Cariglino 2018). Later Guadalupian to Lopingian deposits exhibit a variety of ovipositional types on glossopterid foliage from South Africa (Prevec et al. 2009, 2010; McLoughlin 2011), India (Srivastava 1987; Shah 2004; Srivastava and Agnihotri 2011), and Australia (Beattie 2007). Considerably less oviposition is documented from the later Permian; most of what is known comes from the northern continent of Laurussia, including a notable record of oviposition on a leaf of the possible peltasperm *Pursongia* (Vasilenko 2011). It is notable, though, that the mid- to late Permian of Gondwana exhibits a high level of oviposition but low levels of herbivory on glossopterids (Prevec et al. 2009). This pattern is in distinct contrast to an opposite condition on plants of similar age in Laurussia, such as ferns, seed ferns, cycadophytes, conifers, and plants of uncertain affinities (Labandeira et al. 2016).

For the Mesozoic, a variety of ovipositional damage has been described from Triassic stems and foliage, principally sphenopsids and seed plants, from deposits in Gondwana or along equatorial Pangaea bordering the Tethys Ocean. The Middle to Upper Triassic of European Pangaea has been intensively studied. Several examples of oviposition were recorded from Germany on different taxa of Middle Triassic sphenopsids (Roselt 1954; Geyer and Kelber 1987; Kelber and Geyer 1989) and on foliage of the seed plant *Taeniopteris angustifolia* Schenck from Germany (Kelber 1988) and France (Grauvogel-Stamm and Kelber 1996). Also from the Middle Triassic, several Anisian and Ladinian floras from the Bletterbach Area of northeastern Italy indicate a broad spectrum of six oviposition DTs, principally on cycadophytes and pteridosperms and marginally on ferns and conifers and indicating a more expanded pattern of host targeting compared to earlier Permian floras in the same region (Labandeira et al. 2016). An oviposition association between a lycopsid host *Isoetites madygensis* Moisan et Voigt, a quillwort, and a damselfly has been described from the middle to upper Madygen Formation of southwestern Kyrgyzstan (Moisan et al. 2012). From the lower Carnian of Austria are exquisitely preserved, distinctive egg-containing ovipositional lesions on the bennettitalean *Nilssoniopteris haidingeri* Stur ex Krasser, which likely were caused by a dragonfly (Pott et al. 2008). From probably slightly younger deposits from the Carnian Molteno Formation of South Africa, there are host presumptive circular leaf mines on broad-leaved conifer foliage (Scott et al. 2004) that more likely are attributable to ovipositional damage (Labandeira 2006*b*). Currently, the most documented Molteno site for oviposition is the 188 occurrences at Aasvoëlberg 411 (Aas411), a speciose and abundant Molteno site from the Eastern Cape Province. Aas411 provides evidence for four ovipositional DTs: DT72 and DT108 that occur on sphenopsid stems, responsible for 44.1% of the oviposition, and DT76 and DT100 on the broad-leaved conifer *Heidiphyllum elongatum* (Morris) Retallack, consisting of 55.9% of ovipositional occurrences (Labandeira et al. 2018). *Equisetites bradyfi* Daugherty from the late Carnian or more likely earlier Rhaetian of the United States exhibits a few oviposition types on various hosts (Ash 2005, 2009). Webb (1982) also documented one of the few examples in the fossil record of exophytic oviposition on a leaf surface of the Middle Triassic fern "*Dictyophyllum*." Single occurrences of oviposition from the Middle Triassic include the seed plant *Taeniopteris parvilocus* Anderson and Anderson from Australia (McLoughlin 2011) and the broad-leaved conifer *H. elongatum* from Chile (Gnaedinger et al. 2007). A flora that represents the Rhaetian Stage of the Upper Triassic at Yangcaogou, in northeastern China, preserves ovipositional damage on broad-leaved conifers (Ding et al. 2015) and other plant hosts reported below.

Evidence for Jurassic ovipositional damage on plants has come from single occurrences, particularly from Western Europe on bennettitalean hosts and from China on ginkgophyte and conifer hosts. Lower Jurassic ovipositional damage has been found on bennettitaleans as clusters of lesions from Germany (Krausel 1958; van Konijnenburg-van Cittert and Schmeißner 1999), Romania (Popa and Zaharia 2011), and Australia (McLoughlin et al. 2015). Oviposition interactions of DT76, DT100, DT101, and DT175 were documented from the latest Middle Jurassic Jiulongshan Formation of Inner Mongolia, in northeastern China, affecting all major foliar tissues—epidermis, parenchyma, xylem, and phloem—of the *Podozamites-Lindleycladus* broad-leaved conifer species complex (Ding et al. 2015). Other single oviposition associations reported from this deposit include DT100 ovipositional damage on leaves of the ginkgophyte *Sphenobaiera* (Na

et al. 2014, 2017) and DT272 on the fructification of another ginkgophyte, *Yimaia capituliformis* Zhou, Zheng and Zhang (Meng et al. 2017). Damage from the Jiulongshan Formation represents by far the richest spectrum of oviposition DTs of any Jurassic flora, as documented by this report that accounts for 15 DTs hosted by sphenophytes, ginkgophytes, bennettitaleans, conifers, and other plant groups. Plants with damage caused by ovipositing insects were reported from the Late Jurassic–Early Cretaceous boundary interval of Russia, occurring on a *Pityophyllum* sp. conifer leaf (Vasilenko 2005).

During the first 20 million years of the Cretaceous, horsetails, ferns, and gymnosperms had oviposition associations that later included some angiosperm groups during the Aptian-Albian Gap from 125 to 95 million years ago (Labandeira 2014). After this time interval, oviposition interactions were predominantly with angiosperms to the end of the period (Labandeira 2006*a*). For recognition of several primary types of oviposition, the 125–90-million-year-old (Aptian to Turonian) Hatira and Ora Formations, in the central Negev region in Israel, are an important series of localities that straddle the Aptian-Albian Gap (Krassilov et al. 2008). At these localities, various single or clustered, patterned or unpatterned oviposition associations have been documented on 10 angiosperm species (Krassilov and Shuklina 2008; Krassilov et al. 2008). In their exhaustive consideration of the oviposition ichnology and associated nomenclature from these several Israeli floras, an ichnological group, Ovisignata, was erected. Within the Ovisignata, six oviposition ichnogenera (*Catenoveon*, *Sertoveon*, *Costoveon*, *Margoveon*, *Massoveon*, and *Transpiroveon*) and their 12 oviposition ichnospecies were formally erected to describe the broad variety of egg-laying patterns on leaves, stems, roots, and other plant elements (Krassilov et al. 2008). Most of these ichnotaxa have extant morphological equivalents with modern taxa that produce the same or nearly exact oviposition patterns. For individual associations from the Early Cretaceous, smaller contributions describe oviposition on an angiosperm from India (Banerji 2004). From the Czech Republic, the earliest Late Cretaceous, the Cenomanian, records ovipositional damage on an unknown angiosperm (Hellmund and Hellmund 1996*b*). By contrast, a profusion of ovipositional damage has been recorded from the latest Late Cretaceous (Maastrichtian) of North Dakota, stratigraphically adjacent to the Maastrichtian-Paleocene boundary, consisting mostly of ovipositional plant damage found generally on sycamore (Platanaceae) and laurel (Lauraceae) angiosperm hosts (Labandeira 2002*b*). Oviposition also has been described on foliage of the aquatic plant *Quereuxia* from the Upper Cretaceous of Russia (Vasilenko 2008).

Ovipositional damage is extensive on angiosperms during the Cenozoic (Labandeira 2006*a*), of which only a broad outline will be presented here. From the Eocene of Patagonia, Argentina, the Laguna del Hunco and Río Pichileufú localities have provided three ichnospecies of *Paleoovoidus*, two newly described as highly stereotyped damage on dicotyledonous angiosperms and attributed to modern dragonflies of Lestidae (spreadwings) and Coenagrionidae (narrow-winged damselflies; Sarzetti et al. 2009). The Cenozoic record of odonatan endophytic oviposition is abundant and typically exhibits very modern patterns deployed on foliage. Eocene plant hosts with modern-aspect ovipositional damage also are known from North America. There are occurrences on various floras from the Pacific Northwest (Lewis and Carroll 1991; Lewis 1992; Labandeira 2002*b*), the Tallahatta Flora of Mississippi (Johnston 1993), and Paleocene and Eocene floras, including those from the Paleocene-Eocene boundary interval from the Western Interior, particularly Wyoming (Labandeira et al. 2007; Wilf 2008). A considerable number of descriptions have been made of oviposition types on angiosperms from the early-middle Eocene boundary to the middle Miocene interval of Germany (Hellmund 1987; Hellmund and Hellmund 1996*c*, 2002*c*). One of the more noteworthy deposits is Messel, a deep maar lake from the early to middle Eocene boundary that shows a broad variety of oviposition styles on angiosperms (Scharschmidt 1992; Labandeira et al. 2007). The somewhat younger middle Eocene Braunkohle (brown coal) deposit at Geiseltal shows evidence for oviposition inflicted by Lestidae (Hellmund and Hellmund 2002*b*). In a younger maar lake deposit from the early Oligocene of Hammerunterweisenthal, oviposition has been documented implicating coenagrionid damselflies (Hellmund and Hellmund 1998). The noted deposit at Rott has received considerable attention for its diverse and broad spectrum of oviposition patterns (Hellmund 1988; Hellmund and Hellmund 1993, 1996*a*, 1996*b*, 1998; Wappler 2010; Petrulevičius et al. 2011). At Vogelsberg, in Salzhausen, damselfly oviposition was documented on a few angiosperms (Hellmund and Hellmund 2002*a*). Other discoveries from Europe include oviposition at Ribelsalbes, from Castellón, Spain (Peñalver and Delclòs 2004), and from the Neogene of Argentina (Horn et al. 2011). Following the extensive mid-Cenozoic record of oviposition, especially from northern Europe, there is a sparse record of oviposition from deposits of late Miocene to Holocene age.

Material and Methods

Localities, Material, and Methods

Localities. In this study, all of the materials were assembled from localities in Liaoning Province and the Inner Mongolia Autonomous Region, in northeastern China (fig. 1). The fossils were collected from three stratigraphic units. The oldest unit is the Yangcaogou Formation, of latest Late Triassic (Rhaetian) age, at about 205 Ma (Zhou 1981; Liu 1987; Yang et al. 2000), representing the Beipiao Biota. The middle unit is the Jiulongshan Formation, of latest Middle Jurassic (Callovian) age, at 165 Ma (Wang et al. 2001; Shen et al. 2003; Chen et al. 2004), representing the Yanliao Biota. The youngest unit is the Yixian Formation, of mid-Early Cretaceous (Barremian) age, at 125 Ma (Swisher et al. 1999; Wang et al. 2001; Zhou et al. 2003), representing the Jehol Biota. These stratigraphic units, with the possible exception of Yangcaogou, have extensively studied biotas and are well placed biostratigraphically with well-established radioisotopic dates. The data from these localities were based on insect-oviposited plants housed at the Key Laboratory of Insect Evolution and Environmental Changes, College of Life Science, Capital Normal University, Beijing, China (CNU; D. Ren, curator).

The Beipiao Biota (Yangcaogou Formation: Yangcaogou locality). The Beipiao locality, near Beipiao City in Liaoning Province, is near the stratotype section for the Late Triassic (T_3) Yangcaogou Formation. The Beipiao locality is adjacent to Yangcaogou village, not far from Beipiao City, along the southeastern part of Beipiao County of Liaoning Province, in northeastern China. The sedimentary environment at this site of the

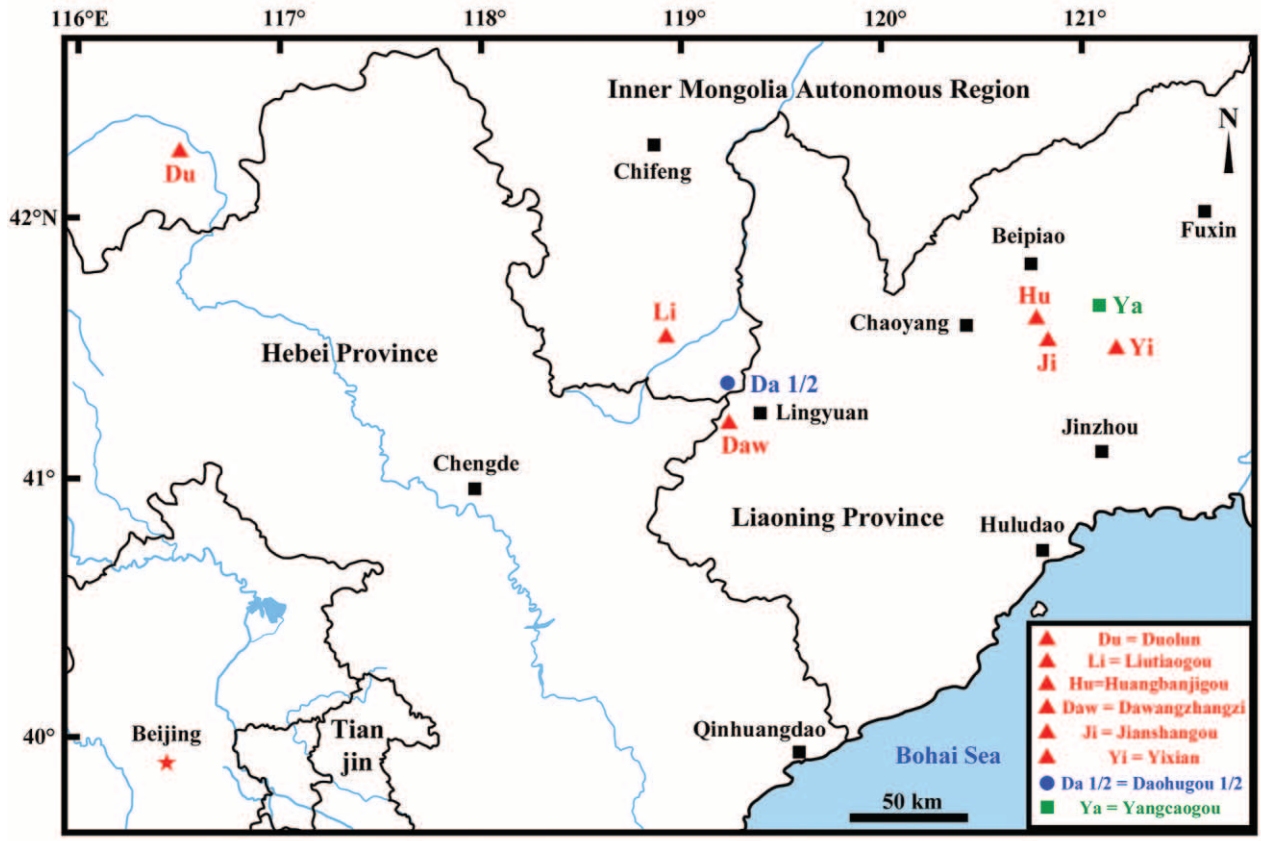

Fig. 1 Map of Yangcaogou (Late Triassic), Jiulongshan (Middle Jurassic), and Yixian (Early Cretaceous) localities in northeastern China. The red triangles denote Jehol Biota (Yixian Formation) localities, the blue circles denote Yanliao Biota (Jiulongshan Formation) localities, and the green squares denote Beipiao Biota (Yangcaogou Formation) localities.

latest Triassic Yangcaogou deposits consists of intermontane fluvial assemblages that contain strata typical of stream, flood plain, and swamp depositional environments. Examination of conchostracan fossils suggests that the age of the Yangcaogou deposits is Late Triassic to Early Jurassic (Liu 1987). However, plant megafossil and palynological studies support a Late Triassic age (Zhou 1981). A Late Triassic date is used here, corresponding to the Rhaetian Stage and an approximate age of 205 Ma (Walker et al. 2013). Consistent with this age, the Yangcaogou megaflora was dominated by certain ginkgoalean and conifer taxa as dominant elements and sphenopsids and ferns as subdominant components. Rare taxa were principally cycads, bennettitaleans, corystosperms, and other seed plant groups (Sun et al. 2016; Wang et al. 2016). Bivalves are present but have not been used in assessing a date for this deposit. These organisms of the Yangcaogou Formation are regionally known as the Beipiao Biota. However, insects are not known from the Beipiao Biota (Ren 1995) and thus are not part of this study.

The Yanliao Biota (Jiulongshan Formation: Daohugou 1 and Daohugou 2 localities). The latest Middle Jurassic (J_2) Jiulongshan localities are Daohugou 1 and Daohugou 2. Located near the village of Daohugou, near Chifeng City in Ningcheng County, Inner Mongolia Autonomous Region of China, these deposits have yielded a considerable diversity and abundance of plant and animal taxa. The lithology of the Jiulongshan Formation consists of gray, green-hued, purple, to almost black siltstones and reddish mudstones that sporadically are interbedded with fine-grained sandstones, tuffs, and taupe-hued conglomerates. Jiulongshan strata at the Daohugou localities range from 55 to 1520 m thick (Ren et al. 2002) and represent a series of regionally extensive lake deposits (Huang 2016). The well-characterized biota consists of a very diverse assemblage of vascular plants, insects, and vertebrates historically known as the Yanliao Biota. Plant taxa include ferns, such as the filicalean Dicksoniaceae; rare cycads; and conifers, especially the abundant *Yanliaoa sinensis* Pan emend. Tan, Dilcher, Wang, Zhang, Na, Li, Li and Sun (Pan 1977; Wang et al. 2016; Tan et al. 2018). Other seed plants were bennettitaleans, of which *Anomozamites kornilovae* Orlovskaia is particularly abundant; ginkgophytes, including *Yimaia capituliformis* Zhou, Zheng et Zhang, that exhibit a wide range of external form; and other seed plant taxa such as caytonialeans, corystosperms, and czekanowskialeans (Huang 2016; Sun et al. 2016; Wang et al. 2016). Vertebrates such as anurans, dinosaurs, and early mammals are present and are of major importance in understanding mid-Mesozoic vertebrate evolution (Huang 2016). The large numbers of conchostracans differentiate the beds of the Daohugou 1 locality from the stratigraphically distinct Daohugou 2 locality; both localities were used for both aspects of the study using ovipositor morphology and ovipositional damage. Radioisotope age analyses of zircon minerals provide an age date

for the Jiulongshan Formation at 165 Ma (Chen et al. 2004; He et al. 2004), equivalent to the late Callovian Stage of the latest Middle Jurassic (Walker et al. 2013). Other sources of evidence indicate a Middle Jurassic age (Ren et al. 2002; Shen et al. 2003; Yuan et al. 2004; Jiang 2006). Of particular importance are well-preserved insect body fossils that provided material for a large literature of species descriptions that document major ovipositor morphologies used in this study.

The Jehol Biota (Yixian Formation: Dawangzhangzi, Duolun, Huangbangigou, Jianshangou, Liutiaogou, and Yixian localities). The Early Cretaceous (K_1) late Barremian Yixian localities are Dawangzhangzi, Duolun, Huangbangigou, Jianshangou, Liutiaogou, and Yixian. These localities were used for both the ovipositor morphology and ovipositional plant damage aspects of this project. The Yixian Formation is exposed at these localities, which are situated in western Liaoning Province and the adjacent Inner Mongolia Autonomous Region, in northeastern China. Like the Jiulongshan Formation below, the Yixian Formation is rich with a diverse biota of plants, insects, and vertebrates, known as the Jehol Biota. Fossil plants include a few uncommon horsetails, gymnosperms such as the nilssonialean *Baikalophyllum lobatum* Bugdaeva, 1983, a broad spectrum of conifers that prominently include *Liaoningocladus boii* Sun, Zheng et Mei, the ginkgophytes *Baiera valida* Sun et Zheng and *Czekanowskia rigida* Heer, and the generally rare bennettitalean *Tyrmia acrodonta* Wu. The early angiosperm *Archaefructus liaoningensis* Sun, Dilcher, Zheng et Zhou (Sun et al. 2001; Ding et al. 2003) is present but because of its rarity is ecologically unimportant. The presence of an early angiosperm was initially controversial for the age of the Yixian Formation. The age of the Yixian Formation has been established as mid-Early Cretaceous (125 Ma), based on radioisotopic age dates, with which this report concurs. Additionally, given the pollen record of early angiosperms (Friis et al. 2011), the occurrence of *A. liaoningensis*, a very early, nearly entire angiosperm (Sun et al. 1998), is consistent with a mid-Early Cretaceous age. The age date of ca. 125 Ma was established on radioisotopic evidence (Swisher et al. 1999), buttressed by other biostratigraphic data (Wang et al. 2001; Zhou et al. 2003). The age date of 125 Ma corresponds with the later phase of the Barremian Stage (Walker et al. 2013), although other localities of the Yixian Formation are known to be of early Aptian age (Swisher et al. 1999; Xing et al. 2005). As in the Jiulongshan Formation, the Yixian Formation offers an extensive literature of insect species descriptions that have provided ovipositor morphology data for this study.

Identification of Oviposition Lesions in the Fossil Record

Two general aspects of oviposition lesion morphology on plants are important for their accurate identification. The first feature is the differentiation of oviposition lesions from similar structures, such as feeding damage attributable to detritivory and other forms of herbivory, as well as physical damage from nonbiological processes. The second feature involves discerning the structural difference between oviposition lesions and the very similar feeding punctures of piercing and sucking.

Distinguishing oviposition from detritivory, herbivory, and physical damage. Four important distinctions that differentiate oviposition from detritivory, herbivory, and physical damage are required for a preliminary assessment of ovipositional lesions in fossil material. Single or multiple combinations of these four major types of evidence are important to determine whether insect oviposition is present. First is the recognition of reaction or scar tissue, such as callus, a response to ovipositor insertion into live tissue. For example, lesions of the two-spotted treehopper *Enchenopa bionotata* Say (Hemiptera: Membracidae) on black walnut, *Juglans nigra* L. (Juglandaceae), in Missouri are enveloped by wound periderm that surrounds cambial zone disruption, eventually resulting in wound closure (Armstrong et al. 1979). During the interval between oviposition and mature reaction tissue development, necrotic tissue can result from distinctive colonizing fungi such as the ascomycete *Hypoxylon mammatum* (Wahl) Mill. (Xylariales: Xylariaeae) that invade surface tissues of trembling aspen, *Populus tremuloides* Michx. (Salicaceae). This prominent oviposition damage is caused by the 17-year cicada, *Magicicada septendecim* L. (Hemiptera: Cicadidae), in Wisconsin (Ostry and Anderson 1983). A second line of evidence involves small structures of the host plant associated with ovipositional damage (Beamer 1928). A noticeable instance of this are thin, woody splinters that emerge from oviposition lesions of the bladder cicada, *Cytosoma schmeltzi* Distant (Hemiptera: Cicadidae), on twigs of cultivated olive, *Olea europaea* L. (Oleaceae), in Australia (Spooner-Hart et al. 2007). Another type of distinctive damage are patterns of egg placement within the disrupted tissue of the central part of the lesion (Beamer 1928). An example of this are the inclined, en echelon, stereotypical placement of elongate eggs in lesions on coffee, *Coffea arabica* L. (Rubiaceae), by the giant cicada, *Quesada gigas* (Oliver) (Hemiptera: Cicadidae), in Brazil (Decaro Júnior et al. 2012).

Whereas the first two categories present micromorphological features of oviposition lesions, the two categories mentioned below involve broad patterns of oviposition stereotypy and feeding specificities on plant hosts. A third category of evidence is stereotypy of the oviposition pattern. The most conspicuous examples involve distinctive damselfly oviposition patterns in stems and leaves of plants associated with aquatic vegetation. One example is the conspicuous zigzag pattern of large redeye, *Erythromma najas* Hansemann (Odonata: Coenagrionidae), on the yellow water lily, *Nuphar lutea* (L.) Sm. (Nympheaceae), in Germany (Wesenberg-Lund 1913*b*; Grunert 1995). Commonly, a stereotyped pattern occurs mostly internally, in tissues, such as the overlapping positioning of several elongate eggs along a row in the pith tissue of apple, *Malus pumila* Miller (Rosaceae), by the buffalo treehopper, *Stictocephala bisonia* Kopp et Yonke (Membracidae), in Utah (Sorenson 1928; Yothers 1934). The fourth criterion is host specificity, a pattern that, like the other three criteria, would be expected of a persistent biological association on particular live plant tissues but not by feeding or physical damage on dead plant tissues. One genus-level, host-specific interaction is oviposition by the leafhopper *Erythroneura lawsoni* Robinson (Hemiptera: Cicadellidae) in the sycamore *Platanus* (Platanaceae) from Illinois (McClure 1974). A probable species-level, host-specific relationship is demonstrated by the olive fruit fly, *Batrocera oleae* Rossi (Diptera: Tephritidae), on cultivated olive, *O. europaea*, in Turkey (Genç 2016). The above four categories, used singly or jointly, would resolve ambiguities involved in the separation of oviposition lesions from other forms of analogous plant damage (Vincent 1990).

Distinguishing ovipositional from piercing-and-sucking damage. A second major issue for identification of oviposition

involves differentiation from the superficially similar herbivore damage of piercing and sucking. Both ovipositional lesions and piercing-and-sucking punctures occur as lenticular, elliptical, ovate, or circular cross-sectional shapes on plant surfaces (Carbonell 1957; Isenhour and Yeargan 1982; Childers 1997). Lenticular cross-sectional outlines with acute to acuminate ends are found as oviposition lesions (Beamer 1928; Yothers 1934) and as piercing-and-sucking punctures (Vidano 1963; Lopez-Abella et al. 1988). Another shape is broadly to narrowly elliptical, with rounded ends, which occurs in oviposition lesions (Fulton 1915; Sanford 1964; Grunert 1995) but also piercing-and-sucking punctures (Lodos 1967; Lopez-Abella et al. 1988). A third cross-sectional shape is ovate, with a broadened end and an oppositely placed narrowed end, present in some oviposition lesions (Smith and Linderman 1974) and piercing-and-sucking punctures (Günthart and Günthart 1983; Roversi et al. 1989). Most common of all are circular or near-circular cross-sectional outlines that are found in oviposition lesions (Sorenson 1928; Hilliard 1982) and in piercing-and-sucking punctures (Hori 1968; Chisholm and Lewis 1984; Childers and Achor 1991), the latter rarely with a central constriction (Backus 1985). These shapes of ovipositional lesion surfaces are illustrated best by the cross-sectional outlines of slicing or piercing ovipositors in plant-feeding Hemiptera (aphids, scale insects, whiteflies, cicadas, hoppers, psyllids, and true bugs). Hemipteran ovipositor cross sections range from the approximately circular in the periodical cicada, *M. septendecim* (Cicadidae) (Marlatt 1907), to the broadly ovate in the leafhopper *Cuerna sayi* Nielson (Cicadellidae; Readio 1922), to narrowly thin the leafhopper *Abana gigas* Fowler (Cicadellidae; Snodgrass 1933).

The stylate mouthparts of plant-feeding Hemiptera (Snodgrass 1935; Chaudonneret 1990) provide the analogous cross-sectional outlines of stylet ensembles that parallel in many ways those of the ovipositor. These mouthpart cross sections range from circular in the squash bug, *Anasa tristis* (De Geer) (Hemiptera: Coreidae; Tower 1914), to dorsoventrally compressed but broadly ellipsoidal in the periodical cicada, *M. septendecim* (Snodgrass 1935), to laterally compressed and broadly ellipsoidal in the green pea louse, *Acyrthosiphon pisum* Harris (Aphididae; Weber 1928). Hemipteran piercing-and-sucking mouthparts, however, lack more narrowly compressed outlines with shape aspect ratios greater than 1.5 that, nevertheless, are present in many piercing and all slicing ovipositors. More important are the frequent narrower shape outlines of ovipositors (Fulton 1915; Weltz and Vilhelmsen 2014). Compared to stylate mouthpart punctures, the internal structure of tissues from an ovipositional lesion is characterized by mangled and disrupted tissue compared to piercing-and-sucking punctures. Plant tissues resulting from ovipositional damage display tufts of hyperplasic or hypertrophic tissue that typically surround a slit-like structure that may contain a round feature indicating an inserted egg or its histological remnants (Beamer 1928; Labandeira and Currano 2013). A prominent, dark-colored ridge of callus or similar response tissue with a botryoidal surface surrounds this lenticular to circular area of inner disturbed tissue (Sanford 1964; Hilliard 1982). By contrast, lenticular to circular punctures from piercing-and-sucking activity typically are simpler structures consisting of empty, dark holes (Childers and Achor 1991) surrounded by an encircling rim of stylet-sheath material or callus with a smooth surface, imparting a cratered or, inversely, a domed appearance to the puncture (Hori 1968; Childers 1997; Freeman et al. 2001). Finally, oviposition structures typically are significantly larger than piercing-and-sucking structures, although there is some overlap between the two types of damage.

Determination of Ovipositor Morphotypes

The ovipositor is an egg-laying device confined to Insecta sensu stricto (Snodgrass 1933). The most phylogenetically basal occurrence of an ovipositor lies among Archaeognatha (bristletails; Smith 1969) and consists of a sword-like structure that is the primitive condition for the diverse spectrum of derived ovipositor morphologies seen throughout Insecta (Scudder 1961, 1971; Mickoleit 1973). The basic form of the ovipositor is a modified pair of ventral elements on the eighth abdominal (first genital) and a second pair on the ninth abdominal (second genital) segments (Scudder 1971). The ventral aspect of each of these two segments bears a pair of modified gonocoxae, homologous to the first segments of the thoracic legs, which are modified into a pair of lateral plate-like structures. These gonocoxae of the eighth abdominal segment, in turn, support a pair of typically elongate, lateral processes, the gonapophyses, which also are known as the first (outer) valves of the ovipositor. Similarly, the ninth abdominal segment gives rise to gonocoxae that support elongate structures that are the second (inner) valves of the ovipositor. Other structures, such as the appendicular gonoplac of the ninth abdominal segment, can form other structures, such as a sheath to confine the first and second ovipositor valves to a functioning unit for laying eggs. Once eggs are generated internally, they are pushed out through a median channel between the second valves for eventual deposition on or insertion into an appropriate substrate. Exophytic ovipositors are generally associated with plant substrates and include Lepidoptera (moths and butterflies) that attach eggs variously on plant surfaces (Chew and Robbins 1984; Thompson and Pellmyr 1991). Plant-penetrating endophytic ovipositors include Odonata (dragonflies and damselflies) and related extinct Paleodictyopteroidea, both with short triangular to elongate and blade-like ovipositors for insertion of eggs mostly into aquatic plant stems (Wesenberg-Lund 1943; St. Quentin 1962; Carpenter 1970; Bechly et al. 2001; Labandeira 2002*a*). Unlike their modern descendants that bear leathery egg cases (oothecae), Pennsylvanian to mid-Mesozoic Blattodea, the cockroaches and "roachoids," bore protuberant, generally straight ovipositors that were circular in cross section (Hörnig et al. 2018). By contrast, the ovipositors of Orthoptera (grasshoppers, crickets, and relatives) form curved, blade-like ovipositors with a saw-like edges (Carbonell 1957; Gwynne 2001), a form that also is repeated in ovipositors of Hemiptera such as the cicada (Readio 1922). Uncommonly, highly abbreviated ovipositors can abrade the surface of plant epidermis that produce two short, linear, and parallel slice marks (Ventura and Panizzi 2000), found in certain Hemiptera. The diversity of ovipositor structure is immense and can be linked directly and indirectly to particular types of ovipositional damage.

We consulted the pertinent literature that illustrated and discussed ovipositor-bearing insect taxa from the Jiulongshan and Yixian localities. The Yangcaogou locality, spotlighting the Beipiao Biota, unfortunately lacks documented insects, and, consequently, ovipositor morphology data from the Late Triassic was not part of this study. In the Yixian (Jehol Biota) and Jiulongshan

(Yanliao Biota) substudy, ovipositor morphotypes were selected that were most likely to use host plants for endophytic insertion of eggs. We excluded morphotypes inconsistent with penetration of dead plant tissues. We did not consider insects that oviposit in substrates such as detritus, wood, and soil; groups that penetrate the body cavities of other insects, such as parasitoid wasps possessing very long ovipositors surmounted by a drill; or insects such as vespid wasps with ovipositors modified into a sting.

Ovipositor morphotypes were determined by relevant publications on fossil insects, sourced from the primary descriptive literature (figs. A1–A12, available online). From this literature, 68 fossil insect taxa were sufficiently well preserved and documented that they were selected and categorized into basic morphotypes. Eight features of ovipositor structure were used to define ovipositor morphotypes. These features are (i) length; (ii) width or depth, depending or ovipositor orientation; (iii) aspect ratio; (iv) cross-sectional area, ranging from circular to narrowly lenticular; (v) number of plant-penetrating valve units; and (vi) and ovipositor form, ranging from straight to moderately curved. Other features mostly of the ovipositor tip and margin were used, such as (vii) terminus type, from a spectrum of round to acute to acuminate, and (viii) presence or absence of a saw-like margin, such as denticles or blunt teeth. The first six most important of these ovipositor characterizations are shown in table 3. Characterization of ovipositor morphotypes was carried out independent of a complimentary but separate substudy that characterized oviposition lesions by DT on plant hosts co-occurring in the same deposits. A data set of images with taxonomic identifications (figs. A1–A12) represented those insect taxa from the literature with ovipositors capable of piercing or cutting into plant tissues. From this data set of morphotypes, we established nine basic morphotypes responsible for creation of the oviposition lesions. The oviposition lesions were characterized by their DT assignments (figs. 5–14), indicated below.

Determination of Oviposition DTs

The terminology and classification system used to characterize oviposition in the fossil record in our study of the mid-Mesozoic of northeastern China follows the standard system for categorizing arthropod and pathogen damage by functional feeding group (FFG) and DT (Labandeira et al. 2007 and addenda). Currently, for the oviposition FFG, 41 DTs are documented in the fossil record globally, including additions to the existing version 3 of the *Guide to Insect (and Other) Damage Types on Compressed Plant Fossils* (Labandeira et al. 2007). Of this compendium and its additions, 36.6% are represented in the current data set from the mid-Mesozoic of northeastern China (table A4; tables A1–A4 are available online). Morphological features important for assignment of lesions to a particular DT include (i) lesion shape, (ii) lesion size, (iii) internal structure of parenchymatous tissues, (iv) callus and other reaction tissue, (v) mode of emplacement on a particular plant tissue, and (vi) overall pattern of the lesion on the plant surface (Wesenberg-Lund 1913*a*, 1913*b*; Bogdanov-Kat'kov 1947; Labandeira et al. 2007). Of these morphological features, lesion size and lesion shape are probably the most critical in controlling the appearance of the oviposition lesion, principally through the important role of lesion width. Structural details of the individually inserted eggs, such as size, shape, chorion sculpture, and insertion mode (Bogdanov-Kat'kov 1947), are preserved rarely in the fossil record (but see Pott et al. 2008) and typically are rarely used for DT assignments. Although broadly circumscribed ichnological classifications of fossil oviposition traces are known (Krassilov et al. 2008; Vasilenko 2008), the DT system (Labandeira et al. 2007 and addenda) is more finely tuned for resolving minute morphological details of oviposition on fossil plant surfaces.

Oviposition damage on plant specimens from Yangcaogou, Jiulongshan, and Yixian strata were resolved to particular DTs by microscopic examination and tabulated as raw data (table A4). The raw data, recorded on Microsoft Office Excel spreadsheets, compiled information on all megalocalities and included sublocality, CNU specimen number, plant host identification, oviposition DT, status regarding macrophotography or microphotography, and relevant comments. Macrophotographic images of ovipositional damage were taken on a Nikon D100 camera. Microphotographic and some macrophotographic images of oviposition damage were taken on a Leica MZ12.5 dissecting microscope. We measured length and width of representative samples of oviposition lesions along the midline from the anterior to posterior apices, and the width was measured across the broadest aspect (data not shown). Data of all localities, specimen numbers, plant host morphotype, oviposition types, and photo log and specimen comments initially were recorded on Microsoft Office Excel spreadsheets and reformatted as table A4.

Specimens

Insect-mediated DT data assigned to particular host plant species were recorded for the Early Cretaceous Jehol Biota of the Yixian Formation (table A1), latest Middle Jurassic Yanliao Biota of the Jiulongshan Formation (table A2), and Late Triassic Beipiao Biota of the Yangcaogou Formation (table A3). We retrieved 375 specimens that displayed oviposition from a total pool of 6111 specimens (6.1%; table 1). Of the 6.1% of specimens with oviposition damage, 29.7% was from the Jehol Biota, 63.6% from the Yanliao Biota, and 6.7% from the Beipiao Biota. Oviposition is a major but highly variable part of the total arthropod-mediated portfolio that includes herbivory within each of these biotas. For the Jehol Biota, oviposition is responsible for 30.3% of all interactions; for the Yanliao Biota, oviposition accounts for 11.2%; and for the Beipiao Biota, oviposition is 52.7%, although the latter figure could be an effect of small sample size (table 1). This comparison of ovipositional damage to total damage indicates that oviposition does not represent a consistent fraction of the total damage in each of the three studied biotas.

Data and Analyses

Occurrences of DTs on particular plant groups and species for each of the three biotas are provided in tables A1–A3. These data are derived from the raw data in table A4 for the 375 specimens with oviposition DTs, which originate from the larger sampled data set of 6111 plant specimens (not shown). A more detailed breakdown of localities within each of the three biotas is supplied in table 1. For an assessment of particular herbivore interactions, table 2 shows a rank ordering of DTs from commonest to rarest and furnishes DT, plant host, locality, and age data for each oviposition-plant DT interaction. Table 3 furnishes ovipositor morphological data for each of the 68 species of

Table 1

Summary of Specimens Studied and Their Total Damage and Ovipositional Diversity Data by Locality, Relative to the Total Data Set

Megalocalities and localities	Age, biota	Specimens studied		Oviposition DTs		Total DTs		Oviposition–to–total damage ratio (%)
		No.	%	No.	%	No.	%	
Yixian	K_1: Barremian	**1817**	**29.7**	**60**	**16.0**	**198**	**6.9**	**30.3**
Dawangzhangzi	(Jehol Biota)	(995)	(54.8)	(31)	(57.4)	(97)	(49.0)	
Duolun		(132)	(7.3)	(2)	(3.7)	(11)	(5.6)	
Huangbangigou		(57)	(3.1)	(2)	(3.7)	(6)	(3.0)	
Jianshangou		(14)	(.8)	(4)	(7.4)	(10)	(5.1)	
Liutiaogou		(619)	(34.0)	(15)	(27.8)	(74)	(37.4)	
Jiulongshan	J2: Callovian	**3886**	**63.6**	**296**	**78.9**	**2646**	**91.9**	**11.2**
Daohugou 1	(Yanliao Biota)	(2386)	(61.4)	(182)	(65.0)	(1816)	(68.6)	
Daohugou 2		(1500)	(38.6)	(98)	(35.0)	(830)	(31.4)	
Yangcaogou	T3: Rhaetian	**408**	**6.7**	**19**	**5.1**	**36**	**1.3**	**52.7**
Beipiao	(Beipiao Biota)	(408)	(100.0)	(19)	(100.0)	(6)	(100.1)	
Summaries		**6111**	**100.0**	**375**	...	**2880**	...	

Note. Numbers and percentages in bold refer to megalocalities, whereas those in parentheses refer to locality subtotals. See tables A1–A3, available online, for a breakdown of damage type (DT) ovipositional data by plant host group and species for each of the three megalocalities. Data for oviposition DTs were derived from table A4. For total damage DTs, nonoviposition DT data are not shown.

ovipositor-bearing insects examined and assigns for each insect species one of the nine ovipositor morphotypes to one or more DTs inferred to have been created by the particular ovipositor morphotype.

The frequency distributions of ovipositor morphotypes, oviposited plant specimens, and oviposition DTs for each plant species are provided, respectively, in figures 2, 3, and 4, which provide data for the Early Cretaceous Jehol, Middle Jurassic Yanliao, and Late Triassic Beipiao Biotas. For ovipositor morphotypes, frequency distributions are given for the Jehol and Yanliao Biotas in figure 2*A* and figure 2*B*, respectively. Figure 2*C* lists the frequency distributions of ovipositor morphotypes for each of the eight insect taxonomic orders detailed in figures A1–A12 of the appendix (available online). Of these taxonomic orders, extinct taxa are designated by a superscript dagger (†). (Unfortunately, the Beipiao Biota of the Yangcaogou Formation lacked available insects for the ovipositor substudy.) The frequency distributions of the eight plant groups with oviposition

Table 2

Rank List of Oviposition Frequencies by Plant Host Genus at the Jehol, Yanliao, and Beipiao Biotas

Damage rank	DT	Total DTs		Higher			Age
		No.	%	Plant host	Taxon	Biota	
1	DT76	103	40.1	*Anomozamites*	Bennettitales	Yanliao	J_2
2	DT76	19	7.4	*Yanliaoa*	Coniferales	Yanliao	J_2
3	DT101	17	6.6	*Anomozamites*	Bennettitales	Yanliao	J_2
4	DT101	15	5.8	*Ginkgoites*	Ginkgoales	Yanliao	J_2
5	DT226	13	5.1	*Anomozamites*	Bennettitales	Yanliao	J_2
6	DT101	12	4.7	*Liaoningocladus*	Coniferales	Jehol	K_1
7	DT76	12	4.7	*Pterophyllum*	Bennettitales	Yanliao	J_2
8	DT101	11	4.3	*Pterophyllum*	Bennettitales	Yanliao	J_2
9	DT101	11	4.3	*Yanliaoa*	Coniferales	Yanliao	J_2
10	DT72	10	3.9	*Equisetites*	Equisetales	Jehol	K_1
11	DT175	10	3.9	*Liaoningocladus*	Coniferales	Jehol	K_1
12	DT76	6	2.3	Y-cycad foliage[a]	Cycadales	Yangcaogou	T_3
13	DT72	6	2.3	*Equisetites*	Equisetales	Yanliao	J_2
14	DT137	4	1.6	*Ginkgoites*	Ginkgoales	Yanliao	J_2
15	DT76	4	1.6	*Nilssoniopteris*	Bennettitales	Yanliao	J_2
16	DT76	4	1.6	*Todites*	Filicales	Yangcaogou	T_3
Total		257	100.2				

Note. For biota, formational equivalents are Jehol, Yixian Formation; Yanliao, Jiulongshan Formation; Beipiao, Yangcaogou Formation. Age abbreviations are as follows: K_1 = Lower Cretaceous; J_2 = (latest) Middle Jurassic; T_3 = Upper Triassic. DT = damage type.

[a] An undescribed foliage species of a cycad.

Table 3

Insect Taxa, Morphological Data, Localities, and Literature Sources for Ovipositor Morphotypes

Taxon	Max. length (mm)	Max. width (mm)	Aspect ratio	Cross section	Incision valves	Form	Morphotype	Suppl. fig.	Affiliated DT	Locality	Reference(s)
Odonata:											
†Campterophlebiidae:											
Bellabrunetia catherinae	9.44	1.64	5.76	Lent	Single	Straight	A	A1*A*	DT54, DT293	Dao2	Fleck and Nel 2002
†Nodalulaidae:											
Nodalula dalinghensis	9.68	.78	12.41	Lent	Single	Straight	A	A1*B*	DT54, DT293	Jian	Lin et al. 2007
†Aeschnidiidae:											
Sinaeschnidia heishankowensi	21.24	1.76	12.07	Lent	Single	Straight	F	A1*D*	DT72, DT108, DT272	Huang	Ren 1995; Zhang 2000
Stylaeschnidium rarum	>33.20	2.13	15.59	Lent	Single	Straight	F	A1*C*	DT72, DT108, DT272	Huang	Zhang and Zhang 2001
Blattodea:											
†Raphidiomimidae:											
Divocina noci	1.42	.38	3.74	Circ	Double	Straight	B	A2*B*	DT292	Dao2	Liang et al. 2012
Fortiblatta cuspicolor	.50	.36	1.39	Circ	Double	Straight	B	A2*A*	DT292	Dao2	Liang et al. 2009
†Fuziidae:											
Fuzia dadao	1.86	.31	6.00	Circ	Single	Slight	C	A2*C*	DT100, DT101, DT102, DT226, DT246	Dao2	Vršanský et al. 2009
†Blattulidae:											
Elisama extenuata	1.04	.15	6.93	Circ	Single	Slight	C	A2*D*	DT100, DT101, DT102, DT226, DT246	Huang	Ren 1995; Wang et al. 2007
†Caloblattinidae:											
Colorifuzia agenora	1.77	.11	16.09	Circ	Double	Straight	B	A2*E*	DT292	Dao	Wei et al. 2013
†Mesoblattinidae:											
Karatavoblatta formosa	>7.76	.47	16.51	Circ	Single	Straight	A	A2*F*	DT54	Huang	Ren 1995
Orthoptera:											
†Haglidae:											
Allaboilus gigantus	23.05	1.03	22.38	Lent	Single	Slight	F	A3*A*	DT72, DT108, DT175, DT272	Dao1	Ren and Meng 2006; Gu et al. 2010
Allaboilus hani	11.72	2.38	4.92	Lent	Single	Straight	D	A3*E*	DT72, DT76	Huang	Gu et al. 2010
Prophalangopsidae:											
†*Aboilus cornutus*	4.06	1.31	3.10	Lent	Single	Moderate	D	A3*C*	DT72, DT76	Dao2	Li et al. 2007
†*Bacharaboilus jurassicus*	6.81	1.15	5.92	Lent	Single	Moderate	D	A3*D*	DT72, DT76	Yix	Li et al. 2007
†*Sigmaboilus peregrinus*	4.76	1.43	3.33	Lent	Single	Moderate	D	A3*B*	DT72, DT76, DT175	Dao2	Gu et al. 2009
Archaeorthoptera:											
†Chresmodidae:											
Jurachresmoda gaskelli	>5.54	1.65	3.36	Circ	Single	Straight	E	A4*B*	DT72, DT76	Dao2	Zhang et al. 2008*b*
Jurachresmoda sanyica	4.46	.69	6.46	Circ	Single	Straight	E	A4*A*	DT72, DT76	Dao2	Zhang et al. 2010
Sinochresmoda magnicornia	5.81	1.27	4.58	Circ	Single	Straight	E	A4*C*	DT72, DT76	Liu	Zhang et al. 2008*a*
Hemiptera:											
†Procercopidae:											
Anomoscytina anomala	2.58	.36	7.17	Lent	Single	Straight	G	A5*H*	DT101, DT102, DT159	Huang	Ren et al. 1998
Anthoscytina perpetua	2.88	.35	8.23	Lent	Single	Moderate	G	A5*C*	DT101, DT102, DT159	Dao1	Li et al. 2013
Jurocercopis grandis	>2.08	>.11	18.91	Lent	Single	Moderate	G	A5*A*	DT101, DT102, DT159	Dao2	Wang and Zhang 2009*a*
Stellularis aphthosa	6.51	.91	7.15	Lent	Single	Straight	D	A5*E*	DT72, DT175	Huang	Ren et al. 1998

Stellularis longirostris	2.82	.45	6.27	lent	Single	Straight	G	A5*G*	DT101, DT102	Huang	Chen et al. 2015
Stellularis macula	>1.14	.27	4.22	Lent	Single	Straight	D	A5*F*	DT72, DT76, DT159	Huang	Hu et al. 2014
†Tettigarcitidae:											
Shuraboprosbole daohugouensis	4.35	.89	4.89	Lent	Single	Moderate	G	A5*B*	DT101, DT102, DT159	Dao2	Wang and Zhang 2009*b*
Sunotettigarcta hirsuta	2.38	.40	5.95	Lent	Single	Slight	D	A5*D*	DT72, DT76, DT175	Dao2	Li et al. 2012
Cixiidae:											
†*Lapicixius decorus*	2.17	.38	5.71	Lent	Single	Straight	D	A5*I*	DT72, DT76, DT175	Huang	Ren et al. 1998
†Progonocimicidae											
Cicadocoris assimilis	.64	.18	3.56	Lent	Single	Slight	I	A5*J*	DT100, DT101, DT102	Dao1	Dong et al. 2013
†Pachymeridiidae:											
Beipiaocoris multifurcus	1.65	.18	9.17	Circ	Single	Straight	G	A6*J*	DT101, DT102, DT159	Huang	Yao et al. 2008
Corollpachymeridium heteroneurus	1.40	.12	11.67	Circ	Single	Straight	G	A6*B*	DT101, DT102, DT159	Dao2	Lu et al. 2011
Peregrinpachymeridium comitcola	1.53	.10	15.30	Circ	Single	Straight	G	A6*A*	DT101, DT102, DT159	Dao2	Lu et al. 2011
Sinopachymeridium popovi	1.62	.17	9.53	Circ	Single	Straight	G	A6*C*	DT101, DT102, DT159	Dao2	Yao et al. 2006*c*
Rhopalidae:											
†*Miracorizus punctatus*	3.01	.18	16.72	Circ	Single	Straight	G	A6*E*	DT101, DT102, DT159	Dao2	Yao et al. 2006*a*
†*Originicorizus pyriformis*	1.28	.26	4.92	Circ	Single	Straight	G	A6*F*	DT101, DT102, DT159	Dao1	Yao et al. 2006*d*
†*Quatlocellus insolentis*	1.10	.12	9.17	Circ	Single	Straight	G	A6*D*	DT101, DT102, DT159	Dao1	Yao et al. 2006*d*
†*Vescisalignus indecorus*	1.63	.06	27.17	Circ	Single	Straight	G	A8*C*	DT101, DT102	Huang	Chen et al. 2015
†Vetanthocoridae:											
Byssoidecerus levigatus	.94	.12	7.83	Lent	Single	Straight	C	A7*G*	DT100, DT101, DT102, DT226, DT246	Huang	Yao et al. 2006*b*
Collivetanthocoris rapax	2.07	.21	9.86	Lent	Single	Straight	C	A7*F*	DT100, DT101, DT102, DT226, DT246	Huang	Yao et al. 2006*b*
Curvicaudus ciliatus	1.31	.26	5.04	Lent	Single	Straight	C	A8*A*	DT100, DT101, DT102, DT226, DT246	Huang	Yao et al. 2006*b*
Curvicaudus spinosus	1.39	.14	9.93	Lent	Single	Straight	C	A7*J*	DT100, DT101, DT102, DT226, DT246	Huang	Tang et al. 2015
Longilanceolatus tenellus	1.78	.06	29.67	Circ	Single	Straight	G	A8*B*	DT101, DT102, DT159	Huang	Tang et al. 2015
Pumilanthocoris gracilis	1.05	.08	13.13	Lent	Single	Straight	G	A6*G*	DT101, DT102, DT159	Dao2	Hou et al. 2012
Pumilanthocoris obesus	1.11	.16	6.94	Lent	Single	Straight	G	A6*H*	DT101, DT102, DT159	Dao2	Hou et al. 2012
Vetanthocoris decorus	1.80	.22	8.18	Lent	Single	Straight	C	A7*I*	DT100, DT101, DT102, DT226, DT246	Huang	Yao et al. 2006*b*
Vetanthocoris longispicus	2.10	.22	9.55	Lent	Single	Straight	C	A7*H*	DT100, DT101, DT102, DT226, DT246	Huang	Yao et al. 2006*b*
†Dehiscensicoridae:											
Crassiantenninus minutus	2.43	.36	6.75	Circ	Single	Straight	G	A7*A*	DT101, DT102, DT159	Huang	Du et al. 2017
Dehiscensicoris sanctus	1.59	.11	14.46	Circ	Single	Straight	G	A6*I*	DT101, DT102, DT159	Huang	Du et al. 2017
Cydnidae:											
†*Orienicydnus hongi*	1.03	.23	4.48	Circ	Single	Straight	G	A7*B*	DT101, DT102, DT159	Huang	Yao et al. 2007
†Venicoridae:											
Clavaticoris zhengi	3.17	.13	24.39	Circ	Single	Straight	G	A7*C*	DT101, DT102, DT159	Huang	Yao et al. 2012
Halonatusivena shii	1.95	.13	15.00	Circ	Single	Straight	G	A7*D*	DT101, DT102, DT159	Huang	Du et al. 2016
Venicoris solaris	1.46	.07	20.86	Circ	Single	Straight	G	A7*E*	DT101, DT102, DT159	Huang	Yao et al. 2012
Neuroptera:											
†Kalligrammatidae:											
Oregramma illecebrosa	24.85	1.83	13.58	Lent	Single	Moderate	F	A9*A*	DT72, DT108, DT272	Huang	Yang et al. 2014

Table 3 (*Continued*)

Taxon	Max. length (mm)	Max. width (mm)	Aspect ratio	Cross section	Incision valves	Form	Morphotype	Suppl. fig.	Affiliated DT	Locality	Reference(s)
Lepidoptera:											
†Eolepidopterigidae:											
Seresilepidopteron dualis	.74	.29	2.55	Circ	Single	Straight	H	A10*A*	DT137	Dao2	Zhang et al. 2013
†Mesokristenseniidae:											
Kladolepidopteron oviformis	1.49	.52	2.87	Circ	Single	Straight	H	A10*B*	DT137	Dao2	Zhang et al. 2013
Hymenoptera:											
†Xyelotomidae:											
Abrotoma robusta	3.04	.75	4.05	Lent	Single	Slight	E	A11*C*	DT72, DT76	Dao2	Gao et al. 2009*b*
Liaotoma linearis	1.39	.55	2.53	Lent	Double	Straight	C	A12*D*	DT226, DT246	Huang	Ren 1995
Paradoxotoma tsaiae	1.05	.26	4.04	Lent	Single	Slight	C	A11*B*	DT100, DT101, DT102, DT226, DT246	Dao2	Gao et al. 2009*b*
Synaptotoma limi	1.62	.85	1.91	Lent	Single	Straight	E	A12*C*	DT72	Dawang	Gao et al. 2009*b*
Xyelocerus diaphanus	2.77	.34	8.15	Lent	Single	Straight	C	A11*A*	DT100, DT101, DT102, DT226, DT246	Dao2	Gao et al. 2009*b*
Xyelidae:											
†*Abrotoxyela multiciliata*	3.75	.75	5.00	Lent	Single	Straight	E	A11*D*	DT72, DT76	Dao1	Gao et al. 2009*a*
†*Brachyoxyela brevinodia*	.93	.21	4.43	Lent	Single	Straight	C	A12*A*	DT100, DT101, DT102, DT226, DT246	Huang	Gao et al. 2011
†*Heteroxyela ignota*	.78	.22	3.55	Lent	Single	Straight	C	A11*I*	DT100, DT101, DT102, DT226, DT246	Huang	Zhang and Zhang 2000
†*Isoxyela rudis*	1.28	.47	2.72	Lent	Single	Slight	I	A11*H*	DT100, DT101, DT102	Huang	Zhang and Zhang 2000
†*Platyxyela unica*	6.18	1.04	5.94	Lent	Single	Straight	D	A11*E*	DT72, DT76, DT175	Dao1	Wang et al. 2012
†*Sinoxyela viriosa*	1.42	.34	4.18	Lent	Single	Straight	C	A11*J*	DT100, DT101, DT102, DT226, DT246	Huang	Zhang and Zhang 2000
†Daohugoidae:											
Daohugoa tobiasi	3.15	.77	4.09	Lent	Double	Slight	C	A11*F*	DT100, DT101, DT102, DT226, DT246?	Dao1/2?	Rasnitsyn and Zhang 2004
Scoliidae:											
†*Protoscolia normalis*	2.89	.17	17.00	Circ	Single	Straight	G	A11*G*	DT101, DT102, DT159	Huang	Zhang et al. 2002
Anaxyelidae:											
†*Brachysynthexis robusta*	2.51	.47	5.34	Lent	Single	Straight	E	A12*B*	DT72?	Huang	Zhang and Rasnitsyn 2006

Note. For taxons, a dagger indicates an extinct clade. Width is a measurement indicating ovipositor depth rather than ovipositor width in some forms. Aspect ratio indicates ovipositor length divided by ovipositor width. Cross section abbreviations are as follows: lent = lenticular to ellipsoidal in cross section; circ = circular in cross section. The assignment for incision valves is based on whether the ovipositor penetrates the host plant tissue as a single unit (single) or as two paired but separate valves (double). The form of the ovipositor is whether it is straight (straight) or slightly curved (slightly) to moderately curved (moderate). The vagaries of taphonomy were taken into account. Supplementary figures A1–A12 can be found in the online appendix. Locality is an estimated measurement. DT = damage type.

DTs and frequency distributions of the 15 DTs contributing to those plant group frequencies are given in figure 3 for the three biotas. The distribution of DTs from those same oviposited plants, but at the plant species level and for each particular DT, is provided in figure 4 for the Jehol (fig. 4*A*), Yanliao (fig. 4*B*), and Beipiao (fig. 4*C*) Biotas. Photographic portrayal of the majority of these plant hosts with their DT is given in figures 5–14. These latter macrophotographic and microphotographic illustrations of ovipositional damage point to stereotyped, generalized, and other patterns that document lesion damage and tissue response relevant for DT identification.

Results

In this section, first we provide results for broad patterns of oviposition damage across all three biotas: the Jehol Biota of the Yixian Formation, the Yanliao Biota of the Jiulongshan Formation, and the Beipiao Biota of the Yangcaogou Formation. The results of the ovipositor morphotype substudy are presented as frequency distributions of ovipositor morphotypes from the Jehol and Yanliao Biotas, represented by 68 species from the eight documented insect orders presented in figure 2. Second, we evaluate the distributions and specificities of the DTs on particular host plant groups and their species. Last, we assess the preferential contribution of certain ovipositor morphotypes and their inflicted DTs to the overall pattern of ovipositional damage for the three biotas.

General Patterns

Of the 6111 total specimens examined from the Jehol, Yanliao, and Beipiao Biotas, 375 specimens, or 6.1%, exhibited one or more occurrences of oviposition. The total data set of oviposition occurrences resulted from nine ovipositor morphotypes and 15 oviposition DTs. The data also show that, of the 15 total oviposition DTs present, the Yixian megalocality had eight DTs (53.3%), the Jiulongshan megalocality had all 15 DTs (100%), and the Yangcaogou megalocality had six DTs (40%). See tables 1 and A1–A3 for data summaries.

We examined 1817 specimens from the Jehol Biota, including the rich assemblages from the Dawangzhangzi and Liutiaogou localities, representing 29.7% of the total data set, consisting of 18 plant Linnaean species or morphotypes. Of the 198 total Jehol herbivory DTs, accounting for an herbivory rate of 10.9%, 60 DTs were attributable to oviposition, representing an oviposition rate of 3.3%. The ratio of Jehol herbivory to oviposition is 30.3%, or about three-tenths the herbivory rate (tables 1, A1). By contrast, our examination of the Yanliao Biota consisted of 3886 specimens, including the specimen-rich Daohugou 1 and Daohugou 2 localities, representing 63.6% of the total data set and consisting of 38 Linnaean species or morphotypes. Of the 2646 total Yanliao herbivory DTs, accounting for an herbivory rate of a remarkable 68.1%, 296 DTs were assigned to ovipositional damage, representing an oviposition rate of 6%–7% or about a ninth of the herbivory rate. The ratio of Yanliao herbivory to oviposition rate was 11.2%, somewhat more than a fourth that of the Jehol Biota (tables 1, A2). Our examination of the Beipiao Biota, comprising 408 plant specimens, affiliated with eight Linnaean or morphotype plant taxa, consisted of 6.7% of the total data set. Of the 36 total Beipiao herbivory DTs, accounting for an herbivory rate of 8.8%, 19 DTs were assigned to oviposition, representing an oviposition rate of 4.7%. The ratio of Beipiao herbivory to oviposition is 52.7%, considerably greater than the comparable Yanliao and Jehol ratios, although the sample size of the Beipiao Biota is markedly lower (tables 1, A3). These data strongly indicate that the Yanliao flora was more highly attacked by insects than the two earlier and later floras for both overall herbivory and oviposition.

The ratio of the occurrence of ovipositional DTs to total herbivory damage is provided in table 1. Values of the oviposition–to–total herbivory ratios in the Jehol, Yanliao, and Beipiao Biotas are 30.3%, 11.2%, and 52.7%, respectively. These wildly varying values may be partly attributable to the small sample size for the Beipiao Biota, but the low value for the Yanliao Biota may be attributable to the overwhelming elevated value for nonovipositional herbivory that dwarfs the ovipositional level.

Ovipositor Morphotypes

Ovipositor morphology data were used for determining ovipositor morphotypes for the Jehol and Yanliao Biotas (table 3). Illustrations of the 68 insect species from which ovipositor data were taken are given in figures A1–A12 in the appendix. The frequency distributions of ovipositor morphotypes are provided in figure 2, where they are detailed for the Jehol (fig. 2*A*) and Yanliao (fig. 2*B*) Biotas and for each of the eight insect orders (fig. 2*C*). Ovipositor morphotype diagnoses below are based on the data from figures A1–A12 and listed in table 3.

Ovipositor morphotype A. The morphotype A ovipositor is long, narrow, straight, and lenticular to ellipsoidal in cross section, and it has a single penetrating unit of valves that have an acute but rounded terminus. The anterior to posterior ovipositor length ranges from 9 to 10 mm, and the cross-sectional outline is inferred to have been broadly lenticular along the dorsoventral plane. Morphotype A is represented mostly by extinct Odonata lineages Campterophlebiidae (fig. A1) and †Nodalulaidae (fig. A1*B*) and by Blattodea lineage Mesoblattinidae (fig. A2*F*).

Ovipositor morphotype B. The morphotype B ovipositor is a short, broad, straight structure with a circular cross section and a penetrating unit of two separate and piercing valves, each of which has a broad, chisel-like terminus. From a dorsal view, the ovipositor is generally shaped as an equilateral (broad base) or isosceles (narrower base) triangle, whose total anterior to posterior length ranges from 0.5 to 2.0 mm. Each valve cross-sectional outline is inferred to consist of a narrowly lenticular outline along the dorsoventral plane. Morphotype B is represented by extinct Blattodea lineages †Raphidiomimidae (fig. A2*A*, A2*B*) and †Caloblattinidae (fig. A2*E*).

Ovipositor morphotype C. The morphotype C ovipositor is a small or, in some cases, shorter version of a medium-length ovipositor that is narrow and straight to rarely slightly curved, and it forms a single structural unit of penetration with a rounded terminus. This common ovipositor morphotype has a length of 1.0–3.5 mm, and the cross-sectional area is circular to broadly elliptical to lenticular along the dorsoventral plane. Morphotype C

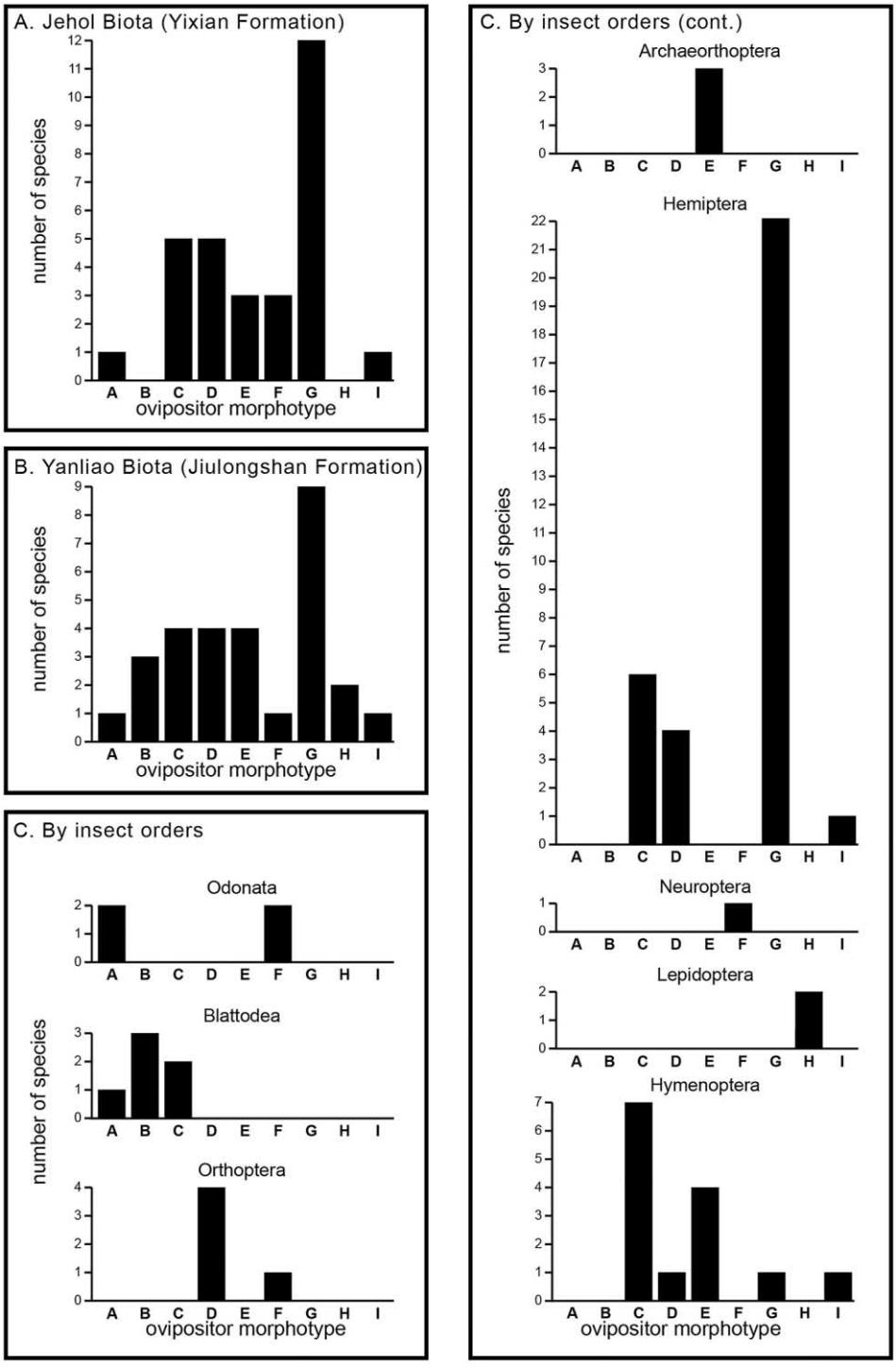

Fig. 2 Frequency distribution of ovipositor morphotypes. *A*, Distribution of morphotypes from the Jehol Biota of Yixian Formation localities (mid-Early Cretaceous). *B*, Distribution of morphotypes from the Yanliao Biota of Jiulongshan Formation localities (latest Middle Jurassic). *C*, Distribution of morphotypes by insect order for both the Jehol and Yanliao Biotas.

is represented overwhelmingly by Blattodea clades †Fuziidae (fig. A2*C*) and †Blattulidae (fig. A2*D*); by Hemiptera clade †Vetanthocoridae (figs. A7*F*–A7*J*, A8*A*); and by Hymenoptera clades Xyelidae (figs. A11*I*, A11*J*, A12*A*), †Xyelotomidae (fig. A11*A*, A11*B*, possibly A12*D*), and †Daohugoidae (fig. A11*F*).

Ovipositor morphotype D. The morphotype D ovipositor is of medium length, narrow, and from curved to moderately curved in shape, with a sharp, acuminate terminus. There is evidence for a sawtooth margin in several species (fig. A3*C*), but this feature is not commonly documented in the literature,

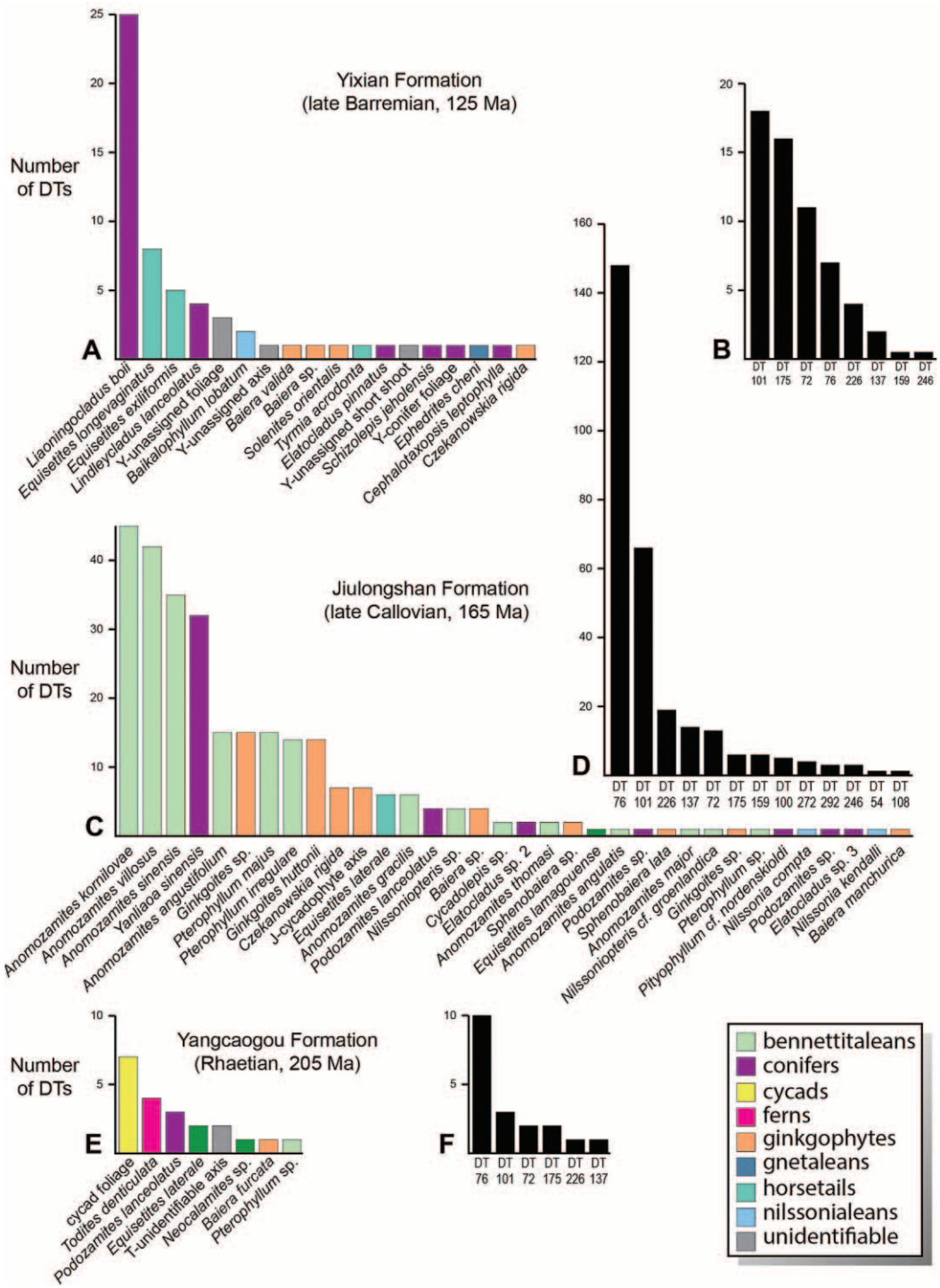

Fig. 3 Frequency distribution of plant hosts and damage types (DTs) by major locality. *A*, By plant taxon for the Jehol Biota of Yixian Formation (mid-Early Cretaceous) localities. *B*, By DT for Jehol Biota localities. *C*, By plant taxon for the Yanliao Biota of Jiulongshan Formation localities (latest Middle Jurassic). *D*, By DT for Yanliao Biota localities. *E*, By plant taxon for the Beipiao Biota of Yangcaogou Formation localities (Late Triassic). *F*, By DT for Beipiao Biota localities.

although modern taxa would indicate that a saw composed of denticles was present along one or both of the ovipositor edges. The blade-like ovipositor varies in length from 4.0 to 7.0 mm, and the cross-sectional outline is inferred to have been narrowly lenticular to somewhat more elliptical along the dorsoventral plane, as in modern grasshoppers and katydids. Morphotype D is represented by both extinct and extant Orthoptera, specifically †Haglidae (fig. A3*E*) and the currently relict Prophala-

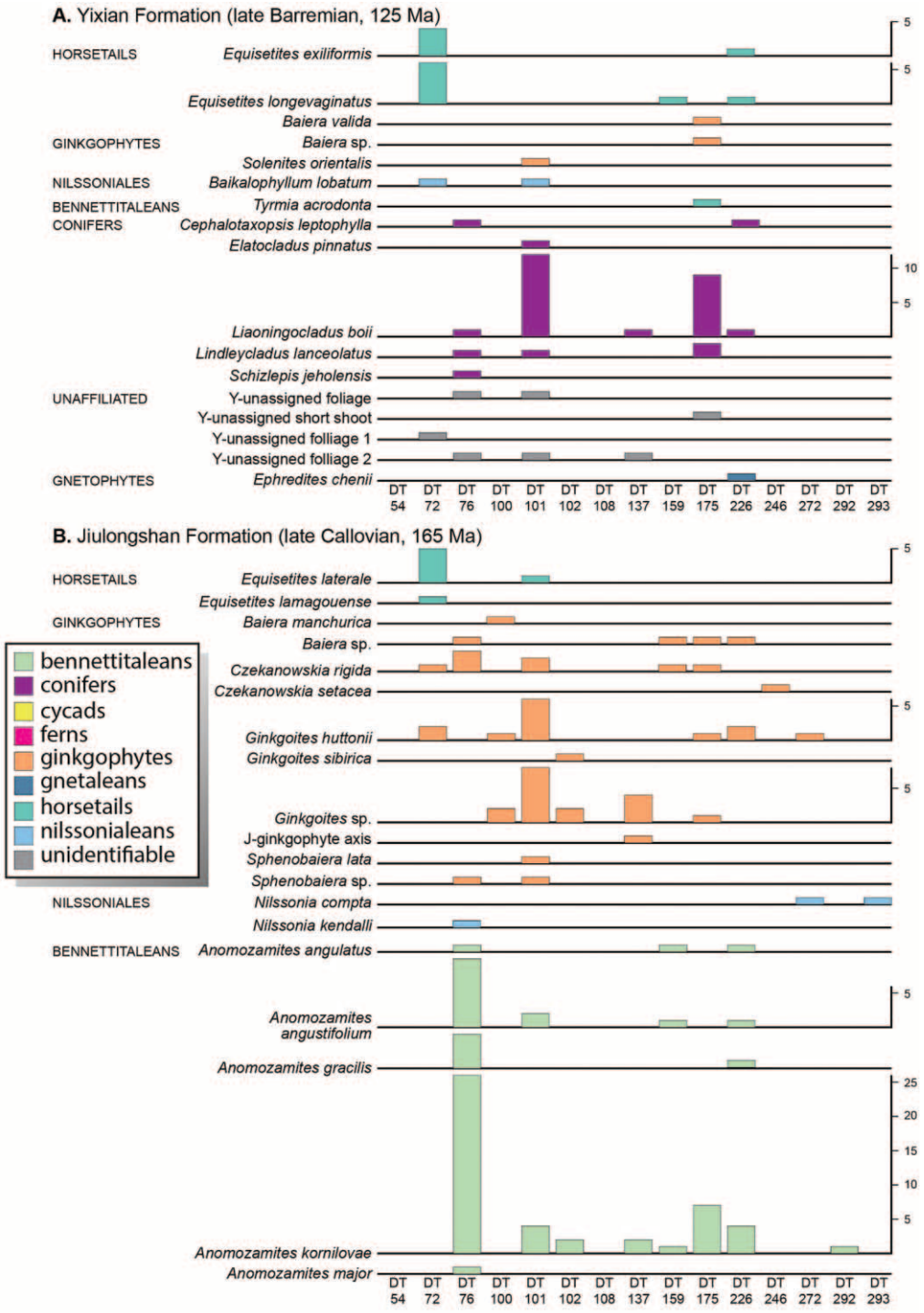

Fig. 4 Frequency distribution of oviposition damage types (DTs) by major locality and plant host. *A*, Frequency distribution of the Jehol Biota from Yixian Formation (Early Cretaceous) localities. *B*, Frequency distribution of the Yanliao Biota from Jiulongshan Formation (latest Middle Jurassic) localities. *C*, Frequency distribution of the Beipiao Biota from Yangcaogou Formation (Late Triassic) localities.

ngopsidae (fig. A3*B*–A3*D*); by Hemiptera clades †Tettigarctidae (fig. A5*D*), †Procercopidae (fig. A5*E*, A5*F*), and Cixiidae (fig. A5*I*); and by Hymenoptera clade Xyelidae (fig. A11*E*).

Ovipositor morphotype E. The morphotype E ovipositor is of medium length, basally broad to terminally narrow, straight, highly tapering, and with a single piercing device ending in an acuminate terminus. The ovipositor has the shape of an isosceles triangle in dorsal view, with the base adjoining the abdomen, represented by the shortest side. The ovipositor length is confined to a range of 4.0–6.0 mm; the cross-sectional outline is approxi-

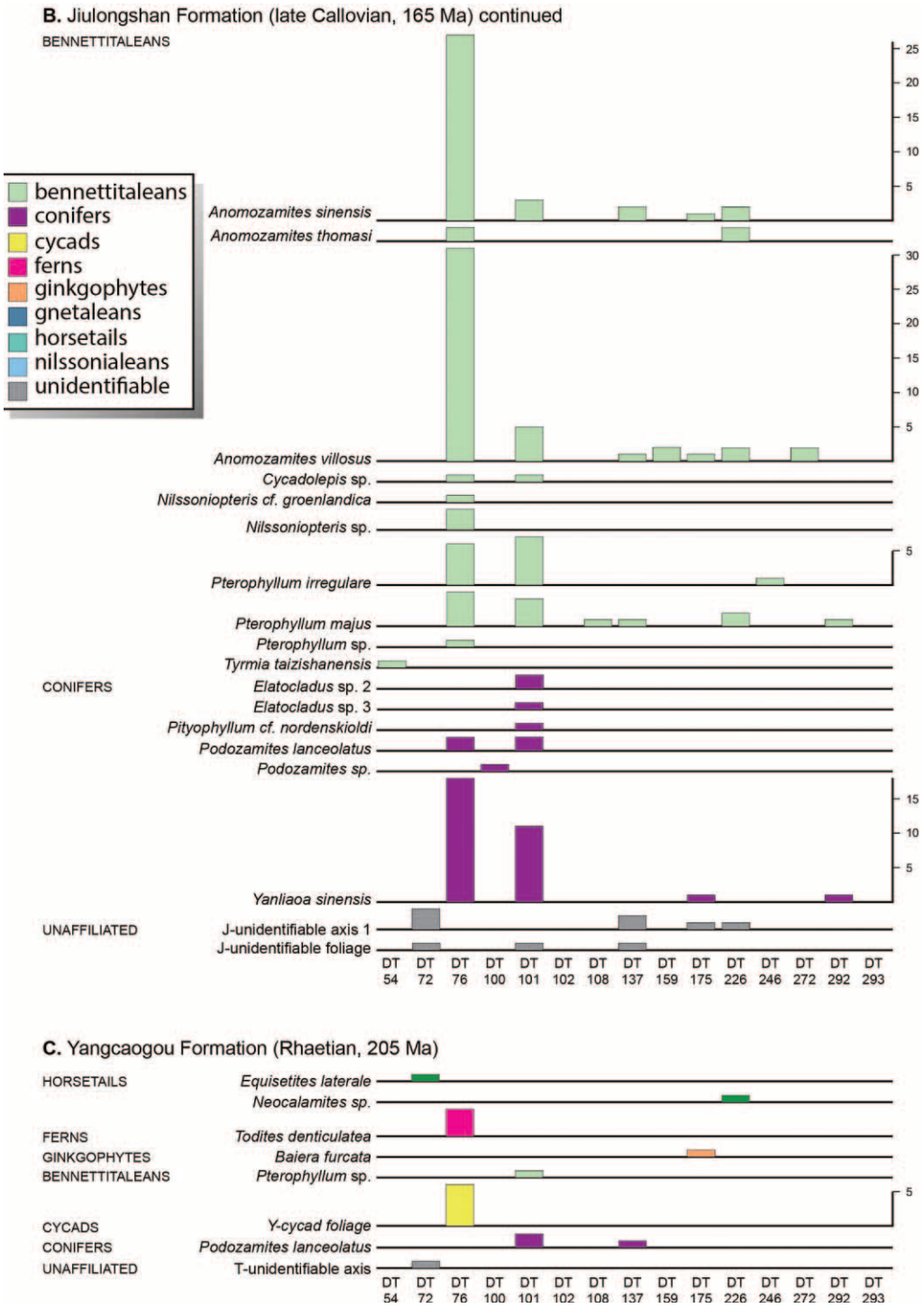

Fig. 4 (*continued*)

mately circular to broadly elliptical. Morphotype E is restricted to the extinct Chresmodida clade †Chresmodidae (fig. A4*A*–A4*C*) and Hymenoptera clades †Xyelotomidae (figs. A11*C*, A12*C*), Xyelidae (figs. A11*D*, A12*A*), and probably †Anaxyelidae (fig. A12*B*).

Ovipositor morphotype F. The morphotype F ovipositor is long to very long, moderately curved, of moderate to high depth, displays a sawtooth margin (fig. A1C), and houses a terminus that is acuminate and particularly pointed. The curved, scimitar-resembling ovipositor is very long, varying from 20 to 35 mm,

and its cross section is inferred to have consisted of a lenticular to more flattened structure oriented along the dorsoventral plane. Morphotype F ovipositors are among the largest in any mid-Mesozoic insect. Morphotype F is prominently represented by the Odonata clade †Aeschnidiidae (fig. A1*C*, A1*D*); Orthoptera clade †Haglidae (fig. A3*A*); and Neuroptera clade †Kalligrammatidae (fig. A9*A*).

Ovipositor morphotype G. The morphotype G ovipositor is a longer version of a shorter ovipositor length as well as a shorter version of the medium-length ovipositor, defined by a narrow to very narrow width, in some cases becoming threadlike. This ovipositor has a broad basal attachment in many cases and a terminus that is acute, appearing rounded. This very common ovipositor morphotype ranges from 1.5 to 4.5 mm in length and appears to retain its rigidity despite its very thin width. The cross-sectional outline of the ovipositor ranges from circular to broadly elliptical. The morphotype G ovipositor is found mostly among extinct lineages of Hemiptera, such as †Procercopidae (fig. A5*A*, A5*C*, A5*G*, A5*H*), †Tettigarcitidae (fig. A5*B*), †Pachymeridiidae (fig. A6*A*–A6*C*, A6*J*), Rhopalidae (figs. A6*D*–A6*F*, A8*C*), †Vetanthorcoridae (figs. A6*G*, A6*H*, A8*B*), †Dehiscensicoridae (figs. A6*I*, A7*A*), Cydnidae (fig. A7*B*), and †Venicoridae (fig. A7*C*–A7*E*) and in the Hymenoptera clade Scoliidae (fig. A11*G*).

Ovipositor morphotype H. The morphotype H ovipositor is highly modified, short, very broad, and straight, and it presumably had a single, peculiar structure for penetrating plant tissue, indicated by a broad and very rounded and slightly expanded terminus. The ovipositor length is 0.7–1.5 mm long, displays considerable space between the constituent valves, and probably was circular in cross section that likely left a shallow, if distinctive, ovipositor lesion on plant surfaces. The morphotype H ovipositor occurs in the extinct Lepidoptera lineages of †Eolepidopterygidae (fig. A10*A*) and †Mesokristenseniidae (fig. A10*B*).

Ovipositor morphotype I. The morphotype I ovipositor is short, very broad, and straight to perhaps slightly curved, and it contains a single piercing structure with an acute terminus for egg insertion into plant substrates. The ovipositor is 0.6–1.3 mm long and is inferred to have a broadly lenticular to elliptical cross section in the dorsoventral plane, indicating a bulb-like appearance. The morphotype I ovipositor is a mixture of extinct and extant lineages, namely from the Hemiptera clade †Progonocimicidae (fig. A5*J*) and the Hymenoptera clade Xyelidae (fig. A11*H*).

Ovipositor Morphotype Occurrences

Categorization of ovipositor structure revealed that nine morphotypes, designated as morphotypes A–I, were present in the Jehol and Yanliao Biotas, based on ovipositor structural measurements and attributes (table 3). For the mid-Early Cretaceous Jehol Biota, seven of these morphotypes were present, with morphotypes B and H absent. Morphotype G was the most abundant (12 species occurrences); morphotypes A and I were least abundant (one species occurrence each); and the remainder, morphotypes C–F, had three or five species occurrences each (fig. 2*A*).

The latest Middle Jurassic Yanliao Biota displays a similar profile, although all nine morphotypes are represented. Morphotype G, as in the Jehol Biota, shows the highest frequency (nine species occurrences); morphotypes A, F, and I have the lowest frequency (one species occurrence each); and the remaining morphotypes range from two to four species occurrences each (fig. 2*B*). (The Late Triassic Beipiao Biota lacks available insect material for ovipositor characterization.)

In contrast to the frequency distributions of ovipositor morphotypes present in the Jehol and Yanliao Biotas (fig. 2*A*, 2*B*), their occurrences among the eight insect taxonomic orders exhibit more sparing distributions (fig. 2*C*). The morphotypes are circumscribed by great differences between the highest and lowest frequencies of morphotypes within each order (Hemiptera and Hymenoptera), the presence of only one morphotype in three of the orders (Archaeorthoptera, Neuroptera, and Lepidoptera), and the occurrence of two or three morphotypes in the three remaining orders (Odonata, Blattodea, and Orthoptera).

For Odonata (dragonflies and damselflies), ovipositors consist of prominent, linear, and medium-length structures of morphotype A (fig. A1*A*, A1*B*) or very long blade-like structures of morphotype F (fig. A1*C*, A1*D*). Blattodea (cockroaches) have a morphotype A ovipositor (fig. A2*F*) or a distinctive, blunt, triangular ovipositor with double valves responsible for two parallel incisions, found in morphotype B (fig. A2*A*, A2*B*, A2*E*). Cockroaches also possess morphotype C ovipositors that have a short to very short, linear, flexible structure that houses valves resulting in a single incision slit (fig. A2*C*, A2*D*). Orthopterans (pygmy grasshoppers and relatives) support ovipositors dominated by curved, saw-like structures of considerable depth and medium length found in morphotype D (fig. A2*B*–A2*E*) and rarely express similarly structured but very long ovipositors of morphotype F (fig. A3*A*). Archaeorthopterans (chresmodids) possess ovipositors of medium length shaped as an isosceles triangle that are highly elongated into an acuminate terminus typical of morphotype E (fig. A4*A*–A4*C*).

Hemiptera (froghoppers, planthoppers, true bugs) constitute almost half (48.5%) of all insect species that bear ovipositors. The Mesozoic families Procercopidae, Pachymeridiidae, Rhopalidae, Vetanthocoridae, and Dehiscensicoridae particularly contribute to the greatest frequency of a single morphotype, morphotype G, attributed to 22 species occurrences (figs. A5*A*–A5*H*, A6*A*–A6*I*, A7*A*–A7*E*). Morphotype G is characterized as an ovipositor that is short to very short in depth, short to moderate in length, and straight to moderately curved in lateral profile. Morphotypes C (figs. A7*F*–A7*J*, A8*A*) and D (fig. A5*D*–A5*F*, A5*I*) are much less represented among Hemiptera. Morphotype I, with one hemipteran occurrence (fig. A5*J*), is small and has a distinctive, broad, rectangular, almost bulbous central region.

Neuroptera (lacewings) express one occurrence of morphotype F, consisting of a long, distinctive, moderately curved, saw-like ovipositor with an acuminate terminus (fig. A9*A*). Lepidoptera (moths) similarly had two occurrences of morphotype H that are linear and have a unique, blunt, subtly expanded, and rounded terminus (fig. A10*A*, A10*B*). Hymenoptera constitute 20.6% of all insect species in the data set and have the most broadly distributed spectrum of ovipositor morphotypes. For Hymenoptera, morphotypes C and E are most abundant, with several occurrences each, and morphotypes D, G, and I have one occurrence each (fig. A11*E*, A11*G*, A11*H*). In summary, the nine ovipositor morphotypes, representing 68 species, 61 genera, 29 families, and 8 orders of insects, likely provide a representative spectrum of the major ovipositor types in the Jehol and

Yanliao Biotas that were responsible for a variety of ovipositor-inflicted damage.

Oviposition Damage Occurrences

A plot of the DT frequency onto host plant taxa reveals several robust patterns with respect to the Jehol and Yanliao Biotas. For the Jehol Biota, the host plant with the greatest frequency of oviposition is the conifer *Liaoningocladus boii* (25 occurrences), followed by two species of *Equisetites* horsetails (13 occurrences), the conifer *Lindleycladus lanceolatus* (L et H.) Harris (four occurrences), unidentifiable foliage (three occurrences), and a series of eight other taxa of mostly ginkgophytes and conifers, with one or two occurrences each (figs. 3*A*, 4*A*; table A1). Of these Jehol plants, the host with the greatest incidence of oviposition damage is *L. boii*, which has somewhat less than half of all oviposition DT occurrences (fig. 3*A*; table A1). Of the eight oviposition DTs recorded from the Jehol Biota, DT72, DT101, and DT175 account for 79.6% of all Jehol occurrences (fig. 3*B*; table A1), about half of which occur on *L. boii* (figs. 3*A*, 4*A*; table A1). Also indicating an ovipositional predominance is the *Liaoningocladus*-DT101 association, which ranks sixth in intensity for a plant host within the entire Mesozoic data set (table 2). Similarly, although the major pattern of oviposition in the Jehol Biota indicates that conifers and, secondarily, horsetails are the principal targets (tables 2, A1), an oviposition incidence rate of 3.3% ($N = 1817$) is depressed compared to the two earlier biotas. The low rate represents a little more than a third of the total herbivory level for the same Jehol data set (table 1). This oviposition profile, however, is very different from that recorded for the older Yanliao Biota.

Oviposition frequencies for the Yanliao Biota consist of several distinctive patterns. The first and most evident pattern is the targeting of bennettitaleans. This general association especially affects the three *Anomozamites* species of *A. villosus* Pott, McLoughlin, Wu et Friis, *A. kornilovae*, and *A. sinensis* Zhang et Zheng that represent the three most oviposited taxa in the Yanliao Biota (figs. 3*C*, 4; table A2). A fourth included species, *A. angustifolium* (Nathorst), ties for the sixth-most abundantly oviposited Yanliao species. These four *Anomozamites* species represent about half (48.6%) of all incidences of oviposition in the Yanliao Biota (figs. 3*C*, 4*B*; table A2). When all bennettitalean taxa are considered, their collective representation is 60.5% of all Yanliao oviposition occurrences (fig. 4*B*; table A2). Other bennettitalean host species moderately attacked are *Pterophyllum irregulare* (14 occurrences) and *Pterophyllum* cf. *majus* (14 occurrences); those species minimally attacked are species of *Cycadolepis* and *Nilssoniopteris*, from four to one oviposition DT occurrences each (table A2). For particular DT associations spanning the entire mid-Mesozoic data set at the genus level (table 2), the *Anomozamites*-DT76 association ranks first, the *Anomozamites*-DT101 association ranks third, and the *Anomozamites*-DT226 association ranks fifth.

The second-most oviposited Yanliao plant group are ginkgophytes, accounting for 15.9% of all occurrences, and then the conifers, the third-most oviposited plant group, with 13.9% (fig. 4*B*; table A2). This latter prominence is buttressed principally by the Yanliao conifer *Yanliaoa sinensis* as the fourth-most highly ranked Yanliao plant host, with 32 oviposition DT occurrences (figs. 3*C*, 4*B*; table A2). The three taxa of *Ginkgoites* rank fifth for Yanliao associations, with 30 oviposition DT occurrences (figs. 3*C*, 4*B*; table A2). In parallel fashion from the entire Mesozoic data set, the second-most highly ranked DT interaction is the *Y. sinensis*-DT76 association, accounting for 7.4% of all data set associations; analogously, the *Ginkgoites*-DT101 association is the fourth-most highly ranked DT interaction, amounting to 5.8% of all associations (table 2). Sphenophytes, cycads, and unaffiliated taxa have minimal representation in DT associations (figs. 3C, 4C; table A2). The overall incidence of oviposition for the Yanliao Biota is 7.6% ($N = 3886$), about 2.3 times that of the Jehol Biota and about 1.7 times that of the Beipiao Biota. Although this incidence of Yanliao oviposition is high, it represents only about a ninth of the total herbivory level from the same biota (table 1).

The Beipiao Biota represents a substantially lesser number of total DT occurrences, consisting of only 19 DTs, or 6.7% of the total Mesozoic data set. However, some patterns can be discerned. There is a more even proportional representation of DTs across the spectrum of plant hosts (figs. 3*E*, 4*C*; table A3). However, the two taxa that host the greatest number of DTs are undifferentiated cycad foliage and the fern *Todites denticulata*. Cycads and ferns are not targeted in the Yanliao and Jehol Biotas, possibly indicating a broad host shift in the 40 million years between Beipiao and Yanliao times. Notably, the Beipiao DT frequency distribution (figs. 3*F*, 4*C*; table A3) remains similar to the Yanliao Biota in that DT76 and DT101 occupy the two most common DTs.

Ovipositor Morphotypes Matched with Ovipositor DTs

In this subsection, we describe particular oviposition DTs in the fossil record (figs. 5–14) and attribute to each DT the particular ovipositor morphotype or morphotypes (figs. 2, A1–A12) of the likely culprit insect creating that DT. The ovipositor morphotype assignments are based on ovipositor structures described from the literature by co-occurring Jehol and Yanliao Biotas (fig. 3). Unfortunately, insect body fossils were not available from the Late Triassic Beipiao Biota, and, consequently, potential insect culprits do not occur for these Upper Triassic deposits.

For each of the 15 oviposition DTs mentioned in this study, we provide five items of relevant data. First, prefatory remarks are given to introduce the unique features of the discussed DT. Second, a definition of the oviposition DT is given, with reference to illustrations in figures 5–14 that depict the particular DT lesion. Third, a list of the host plants and their organs is provided on which the oviposition DTs were recorded, if any, for the Jehol, Yanliao, or Beipiao Biotas, linked to the captions in figures 5–14. Fourth, one or more of the nine ovipositor morphotypes (A–I) are selected as responsible for creating the DT damage, illustrated in figures A1–A12 and listed in table 3. These ovipositor morphotypes (figs. A1–12) were abstracted from the primary literature of relevant insect taxa co-occurring in the same Yanliao and Jehol Biotas. The ovipositor morphotype most consistent with the anatomical, shape, size, and other features for each DT lesion is selected, as is the insect taxa bearing the relevant ovipositor morphotype. Fifth, an ecologically relevant modern analogue is suggested for the particular Jehol and Yanliao oviposition DT damage. It is stressed that these modern analogues provide similarly shaped oviposition lesions

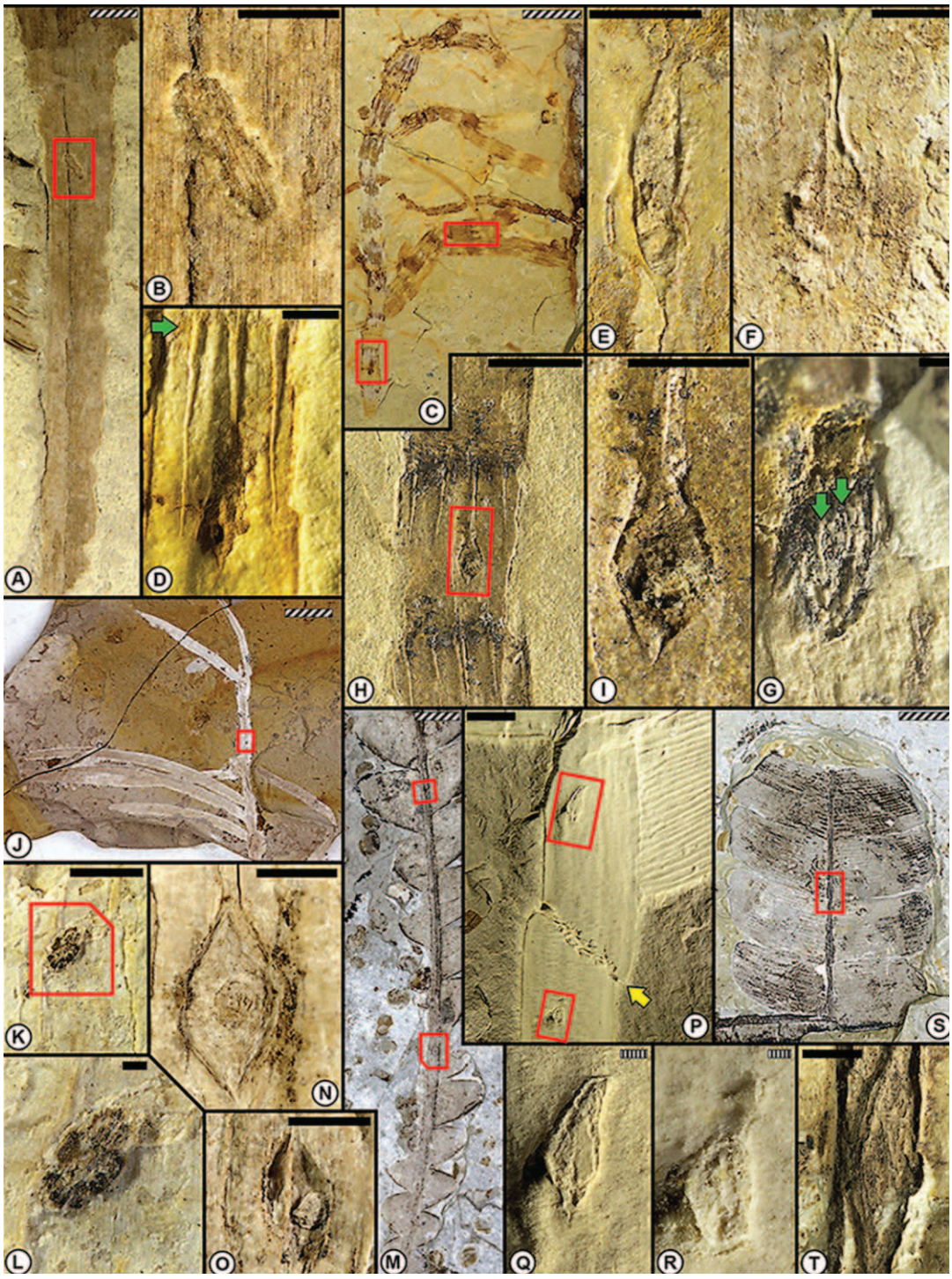

Fig. 5 Oviposition damage types (DTs) on sphenopsids, conifers, and bennettitaleans from the mid-Mesozoic of northeastern China: the generalized damage of DT72 on stems and DT76 on foliage. *A*, DT72 on the sphenopsid *Equisetites laterale* (CNU-PLA-NN-2009438, Daohugou 2). *B*, Enlargement of the unusually angulate lesion DT72 from the template outlined in *A*. *C*, Several examples of DT72 on *E. longivaginatus* (CNU-PLA-NN-2009256p, Daohugou 2). *D*, Enlargement of DT72 from the bottom template outlined in *C*. Note stem node at the uppermost margin and one vertical rib contorted by the oviposition scar. *E*, Enlargement of a second example of DT72 outlined in the upper template in *C*; the inner disturbed area may represent emplacement of an egg. *F*, DT72 occurring on *Equisetites exiliformis* (CNU-PLA-NN-2010157p, Daohugou 2), showing a vertical rib coursing through the middle of the scar. *G*, DT72 on *E. exiliformis* (CNU-PLA-NN-2009993p, Daohugou 2), with arrows pointing to inner and outer ridges. *H*, DT72 on *E. longivaginatus* (CNU-PLA-NN-2009325p, Daohugou 2). *I*, DT72 from the template in *H*, showing the partial control of oviposition shape by stem ribbing. *J*, DT72 occurring on the stem of the conifer *Liaoningocladus boii* (CNU-PLA-NN-2006292, Dawangzhangzi). *K*, Intermediate-level resolution of a DT72 lesion outlined in *J*,

that occur on modern plants. No taxonomic equivalence necessarily is implied between a suggested mid-Mesozoic ovipositing lineage, and a modern analogue that produces a similar to identical type of ovipositor damage. The confidence in the assignment is provided on a scale from 1 to 3, in which a level 1 is a very close or exact match and a level 3 is a poor match.

Oviposition DT54. Of the more complex ovipositional damage in the fossil record, DT54 is relatively common. This DT has an abundant fossil record particularly during the Paleogene (Sarzetti et al. 2009), and a few representatives extend back to the mid-Cretaceous (Krassilov et al. 2008) and very rarely earlier. DT54 represents a recurring pattern of oviposition that likely reevolved in various instances in time and space and currently is best represented by narrow-winged damselflies (Odonata: Coenagrionidae). The record of DT54 extends from the recent to the Late Triassic and may be present in the Permian (C. C. Labandeira, personal observation). Notably, only one occurrence of DT54 was documented from the data, an example of two or possibly three arcuate files of oviposition lesions on the pinnular surfaces of the bennettitalean *P. majus* Brongniart (fig. 11*A*, 11*B*). The insect responsible for this damage evidently swung its abdomen to create the row of egg-insertion lesions and moved a small increment to repeat the same process in creating the second row. Five to seven egg scars are present in each row. The accessed tissues were epidermis and deeper parenchyma, and it does not appear that major pinnular veins had an effect on the oviposition pattern. Based on similarities to recent patterns of oviposition, a coenagrionid damselfly is a strong suspect.

Definition. DT54 consists of elongate, lens-shaped to teardrop-shaped lesions on foliage, arranged with the long axes aligned subparallel to each other, as either straight rows or slightly curved arcs, and generally paralleling a midrib or major vein. Typically, there are two but sporadically three successive, generally arcuate rows, each consisting of from five to 25 lesions, many exhibiting an out-of-register patterning (fig. 11*A*–11*G*).

Host plants and organs. Jehol: No associations. Yanliao: DT54 is associated with the pinnules of the bennettitalean *P. majus* (fig. 11*A*–11*G*; Bennettitales) on a large frond-like leaf. Beipiao: No associations.

Inferred ovipositor. Ovipositor morphotype A.

Inferred insect culprits. Morphotype D culprits for this ovipositional damage are Odonata clades †Campterophlebiidae (*Bellabrunetia*) and †Nodululaidae (*Nodalula*) and probably Blattodea clade Mesoblattinidae (*Karatavoblatta*).

Modern ecological analogue. The ovipositional damage of DT54 is very similar to that of the broad-winged damselfly, *Agrion pulchellum* Van der Linden (Odonata: Agrionidae), on leaves of the water lily *Nuphar* sp. (Nympheaceae) from Germany (Wesenberg-Lund 1943, fig. 57, p. 71). The structural similarity between DT54 and its modern analogue is a level 1 match.

Oviposition DT72. The most ubiquitous ovipositional DT on stems is DT72. DT72 is especially prominent on stems of horsetails, such as species of *Equisetites*, particularly during the Mesozoic. Overall, this distinctive DT can be variable in size, ranging from 2 to 10 mm in lesion length, but the shape is variable and has a broadly ovate to narrowly lenticular shape. The DT72 pattern of oviposition on the three floras included various horsetail and seed plant hosts. However, DT72 has a much earlier legacy on floras, such as the Molteno Formation from the Late Triassic of South Africa (Labandeira et al. 2018) and a few localities from the early Permian of north-central Texas (Schachat et al. 2014, 2015; Xu et al. 2018). The earliest occurrence of DT72 may be from the Late Pennsylvanian of France (Béthoux et al. 2004), although earlier occurrences may exist.

Definition. DT72 is a lenticular to broadly oval lesion, rarely approaching a broadly ellipsoidal shape, with sharp angulate ends and whose insertion into host plant tissue is oriented parallel to or uncommonly at a slight angle to the stem axis. Typically, there is a distinct inner region of disturbed, distorted inner tissue surrounded by callus or other prominent scar tissue that rarely shows evidence of an inserted egg. DT72 is present as a single lesion and rarely occurs in clusters.

Host plants and organs. Jehol: DT72 is associated with axes of the horsetails *Equisetites exiliformis* Sun and Zheng (fig. 5*F*, 5*G*) and *Equisetites longevaginatus* Wu (fig. 5*D*, 5*E*, 5*H*, 5*I*), on stems of the conifer *L. boii* (fig. 5*K*, 5*L*), and on an unidentifiable conifer axis. Yanliao: DT72 commonly is associated with the horsetails *Equisetites laterale* Phillips (fig. 5*B*), on stems, and the ginkgophytes *Czekanowskia rigida*, on a stem, and *Ginkgoites huttonii* (Sternb.) (Ginkgoales), on a leaf petiole. DT76 also occurs on unidentifiable axes and on the petiole of unidentified foliage. Beipiao: DT72 is associated with the horsetail *E. laterale*, on stems, and on an unidentified axis.

Inferred ovipositor. Ovipositor morphotypes D, E, and F.

Inferred insect culprits. Morphotype D culprits for this ovipositional damage are Orthoptera clades †Haglidae (*Allaboilus*) and Prophalangopsidae (†*Sigmaboilus*); Hemiptera clades †Tettigarctidae (*Sunotettigarcta*), †Procercopidae (*Stellularis*), and Cixiidae (†*Lapicixius*); and Hymenoptera clade Xyelidae (†*Platyxyela*). Morphotype E culprits for the damage are †Chresmodida clade Chresmodidae (*Jurachresmoda*, *Sinochresmoda*) and Hymenoptera clades †Xyelotomidae (*Abrotoma*, *Synaptotoma*), Xyelidae (†*Abroxyela*), and probably †Anaxyelidae (*Brachysyntexis*). Morphotype F culprits for the damage are Odonata

showing its position inclined to the stem axis. *L*, High resolution of the DT72 lesion outlined in *J*, displaying a radiate pattern of tissue proliferations originating from an ellipsoidal center. *M*, DT76 on the bennettitalean *Anomozamites angustifolium* (CNU-PLA-NN-2005273, Daohugou 1). *N*, Enlargement of the lesion from the lower template in *M*, exhibiting a central circular region that presumably housed an inserted egg. *O*, Enlargement of the lesion from the upper template in *M*, displaying another circular but off-center structure. *P*, Two DT76 oviposition lesions on the bennettitalean *Pterophyllum* cf. *majus* (CNU-PLA-NN-2009009, Daohugou 2); yellow arrow indicates a break in the rachis. *Q*, Enlargement of DT76 from the upper template in *P*, showing lenticular insertion site and parallel reaction rim. *R*, Enlargement of DT76 from the lower outline in *P*, also displaying an insertion site and concentric reaction ridge. *S*, Several DT76 lesions occurring sporadically on the midrib of the trichome bearing *Anomozamites villosus* (CNU-PLA-NN-2005393, Daohugou 1). *T*, Enlargement of one of the DT76 lesions, outlined in *S*. Scale bars: vertically striped = 0.1 mm; solid white or black = 1.0 mm; back-slashed = 10.0 mm.

clade †Aeschnidiidae (*Sinaeschnidia*, *Stylaeschnidium*), Orthoptera clade †Haglidae (*Allaboilus*), and Neuroptera clade †Kalligrammatidae (*Oregramma*).

Modern ecological analogue. DT72 is very similar to an oviposition scar by the buffalo treehopper, *Stictocephala bisonia* (Hemiptera: Membracidae), on an unknown dicot twig from New York State (Funkhouser 1917, pl. XXIV, p. 223). The structural similarity between DT72 and its modern analogue is a level 1 match.

Oviposition DT76. The most common foliage DT for midrib (a primary vein of closely integrated vascular strands) or midveinal (a primary vein-like lineation of loosely affiliated vascular strands) areas, as well as prominent secondary veins, is DT76, which is lenticular and variable in size. DT76 typically occurs multiple times on the same major vein or on multiple major veins on a leaf but represents separate events that are displaced spatially during the oviposition process. By contrast, DT175 may have similar individual oviposition lesions, but their stereotyped, adjacent position, arrayed end to end on a major vein, is the product of multiple insertions of eggs and creation of lesions that are placed next to each other in a line during a single ovipositional event. Petioles, midribs, and other robust primary veins are the principal targets of insects producing DT76 damage. For most DT76 damage, a robust ovipositor penetrates from 1.0 to 4.5 mm into the thicker tissues of petioles, midribs, and stouter veins. Such penetration requires substantial insertion forces and is considerably less than the weak forces pricking surficial tissues of leaf blades, such as the ovipositor morphotypes producing DT100 and DT292 lesions. It is notable that DT76 lesions evidently are created by ovipositors that are lenticular in cross section, mostly equipped with sawtooth edges, and engaged in back-and-forth sawing through mostly vascular or structural tissues. These actions are different from lesions with circular cross-sectional areas employing an up-and-down piercing motion. The record of DT76 ranges from Permian to present.

Definition. DT76 consists of single or dispersed occurrences of lenticular to ellipsoidal-ovoidal lesions present on midribs or other major veins and small axes. Each lesion has sharply angulate to acute ends, the lesion surrounded by callus or other prominent scar tissue and inwardly containing tufts of randomly organized, disturbed tissue. DT76 is present on or adjacent to the leaf midribs or other primary veins. These lesions are oriented parallel to or at a slight angle to the leaf vein.

Host plants and organs. All three biotas—the Jehol, Yanliao, and Beipiao Biotas—show a heterogeneity of oviposition lesions (tables 2, A1–A3); however, it is the Yanliao Biota and particularly DTs on bennettitaleans that account for the major occurrences. Jehol: DT76 is associated with the midribs and major veins of the nilssonialean *Baikalophyllum lobatum* (fig. 8*Q*, 8*R*), on a pinnule; the ginkgophyte *C. rigida*, on elongate leaves; and the conifers *L. boii*, on broad-leaved foliage (fig. 5*J*–5*L*), *L. lanceolatus*, on broad-leaved foliage, *Schizolepis jeholensis*, on a scale-like leaf, and on unidentifiable conifer foliage. DT76 also occurs on unidentifiable foliage. Yanliao: DT76 is associated with the midribs, robust primary veins, and smaller axes of various seed plants. DT76 is found on the ginkgophytes *Baiera* sp. (fig. 8*I*, 8*J*), on deeply lobate leaves; *C. rigida*, on elongate leaves; and *Sphenobaiera* sp., a palmately lobed leaf. DT76 occurs on the nilssonialean *Nilssonia kendalli* Harris, on frond foliage. DT76 also occurs prominently on the foliage of several species of the bennettitalean *Anomozamites*; in particular, DT76 occurs on *A. angustifolium* (figs. 5*N*–5*R*, 6*N*), *A. gracilis* Nathorst (fig. 6*R*–6*T*), *A. kornilovae* (fig. 6*D*, 6*H*, 6*I*), *A. major* Brongn, *A. angulatus* Heer (fig. 6*J*–6*L*), *A. sinensis* (figs. 6*O*, 7*B*), *A. thomasi* Harris (fig. 7*C*, 7*D*), and *A. villosus* (figs. 5*T*, 7*E*–7*G*, 7*I*–7*K*, 8*F*, 8*G*), especially on midribs. DT76 less commonly occurs on other bennettitalean foliage and stems of *Cycadolepis* sp., a scale leaf; an unaffiliated cycadophyte axis; *Nilssoniopteris* cf. *groenlandica* (Harris) (fig. 7*O*), on a leaf; *Nilssoniopteris* sp. (figs. 7*L*–7*N*, 8*C*, 8*D*) on leaves; *P. irregulare* Stur (fig. 7*P*, 7*Q*), on leaves; *P.* cf. *majus* Brong. (figs. 5*P*–5*R*, 6*A*, 6*B*, 8*A*, 8*B*), on leaves; and *Pterophyllum* sp., on leaves. DT76 is present on the conifer *Podozamites lanceolatus*, other broad-leaved foliage, and *Y. sinensis* (fig. 8*N*–8*P*; Coniferales) and on needle leaves and their rachises. Beipiao: DT76 is associated with major veins of the fern *T. denticulata* (Brong.) Krasser on pinnules and on cycad unidentifiable foliage, on leaves.

Inferred ovipositor. Ovipositor morphotypes D and E.

Inferred insect culprits. Morphotype D culprits for this ovipositional damage are Orthoptera clades †Haglidae (*Allaboilus*) and Prophalangopsidae (†*Sigmaboilus*); Hemiptera clades †Tettigarctidae (*Sunotettigarcta*), †Procercopidae (*Stellularis*), and Cixiidae (†*Lapicixius*); and Hymenoptera clade Xyelidae (†*Platyxyela*). Morphotype E culprits for this ovipositional damage are †Archaeorthoptera clade Chresmodidae (*Jurachresmoda*, *Sinochresmoda*) and Hymenoptera clades †Xyelotomidae (*Abrotoma*, *Synaptotoma*), Xyelidae (†*Abroxyela*), and probably †Anaxyelidae (*Brachysyntexis*).

Modern ecological analogue. The midvein and petiolar oviposition-mimicking scar is very similar, made by the rostrum of *Ceutorrhynchus quadridens* Panz. (Coleoptera: Curculionidae) on collards, *Brassica oleracea* L. (Brassicaceae), from Campania, Italy (Tremblay and Bianco 1978, fig. II-2, p. 21). The structural similarity between DT76 and its modern analogue is a level 1 match.

Oviposition DT100. DT100 contrasts to the behaviorally similar end-to-end arrangement of lesions on major veins of DT175. DT100 may represent an abbreviated version of DT54, but the rows contain considerably fewer lesions, and the overall distribution of individual lesions is more clustered in DT100 compared to the looser, linear distribution of DT54. A superb example of DT100 is documented on *Sphenobaiera* sp. from the Yanliao Biota (Na et al. 2014, 2017). The geochronologic distribution of DT100 ranges from late Permian to the present.

Definition. DT100 is a cluster of several elliptical to lenticular lesions arranged as two or uncommonly more compact rows of adjacent lesions positioned side to side. The oviposition lesions are closely spaced and have tufts of distorted inner tissue and parallel major veins. Each lesion consists of a prominent, emarginate reaction rim, with length-to-width ratios of 2.5–3.5 and average dimensions of 3.0 mm by 1.0 mm. The lesions occur in compact clusters on foliage, avoiding major veins.

Host plants and organs. Jehol: No associations. Yanliao: DT100 is associated with interveinal areas of the ginkgophytes *Baiera manchurica* Yabe et Oishi (fig. 11*J*, 11*K*), on leaves; *G.*

Fig. 6 Oviposition damage of DT76 and DT226 on the rachises on various bennettitalean foliage from the mid-Mesozoic of northeastern China. *A*, DT76 on *Pterophyllum majus* (CNU-PLA-NN-2005200, Daohugou 1); also see figure 10*A* for DT108 on the same specimen. *B*, Lenticular DT76 from template in *A*; note the intact linear reaction tissue along the right edge. *C*, DT76 lesion on *Anomozamites kornilovae* (CNU-PLA-NN-2005297, Daohugou 2). *D*, Enlargement of the oviposition lesion from the template in *C*, showing a central ellipsoidal area surrounded by an outer rim of scar tissue. *E*, Pair of DT226 lesions on the petiole of *A. kornilovae* (CNU-PLA-NN-2006921, Daohugou 2). *F*, Enlargement of DT226 lesions from template in *E*, showing development of a thick black encircling callus rim. *G*, DT76 on *A. kornilovae* (CNU-PLA-NN-2011594, Daohugou 2). *H*, Enlargement of a DT76 lesion with a circular structure encircled by an upraised rim, from of the upper template in *G*. *I*, Enlargement of a DT76 lesion in *G*. *J*, Four DT76 oviposition lesions on *Anomozamites angulatus* (CNU-PLA-NN-2006233p, Daohugou 2). *K*, A narrowly lenticular DT76 lesion from the lower template in *J*, displaying elongate tufts of disturbed tissue. *L*, A second narrowly lenticular DT76 lesion from the upper template in *J*. *M*, A DT76 lesion on *Anomozamites angustifolium* (CNU-PLA-NN-2009198, Daohugou 2). *N*, Enlargement of oviposition region in the clipped template in *M*, displaying a central, broadly ellipsoidal structure. *O*, DT76 on *Anomozamites sinensis* (CNU-PLA-NN-2008186, Daohugou 2). *P*, Enlargement of DT76 from template in *O*, showing thin, delicate reaction rims and a central egg chamber. *Q*, DT76 in *Anomozamites gracilis* (CNU-PLA-NN-2009054); blue arrows indicate orientation of masses of trichomes originating from the rachis. *R*, Enlargement of DT76 from the uppermost template in *Q* shows a central domed structure. *S*, A second DT76 from the central template in *Q*. *T*, A third DT76 lesion from *Q* also displays a central dome. Scale bars: vertically striped = 0.1 mm; solid white or black = 1.0 mm; backslashed = 10.0 mm.

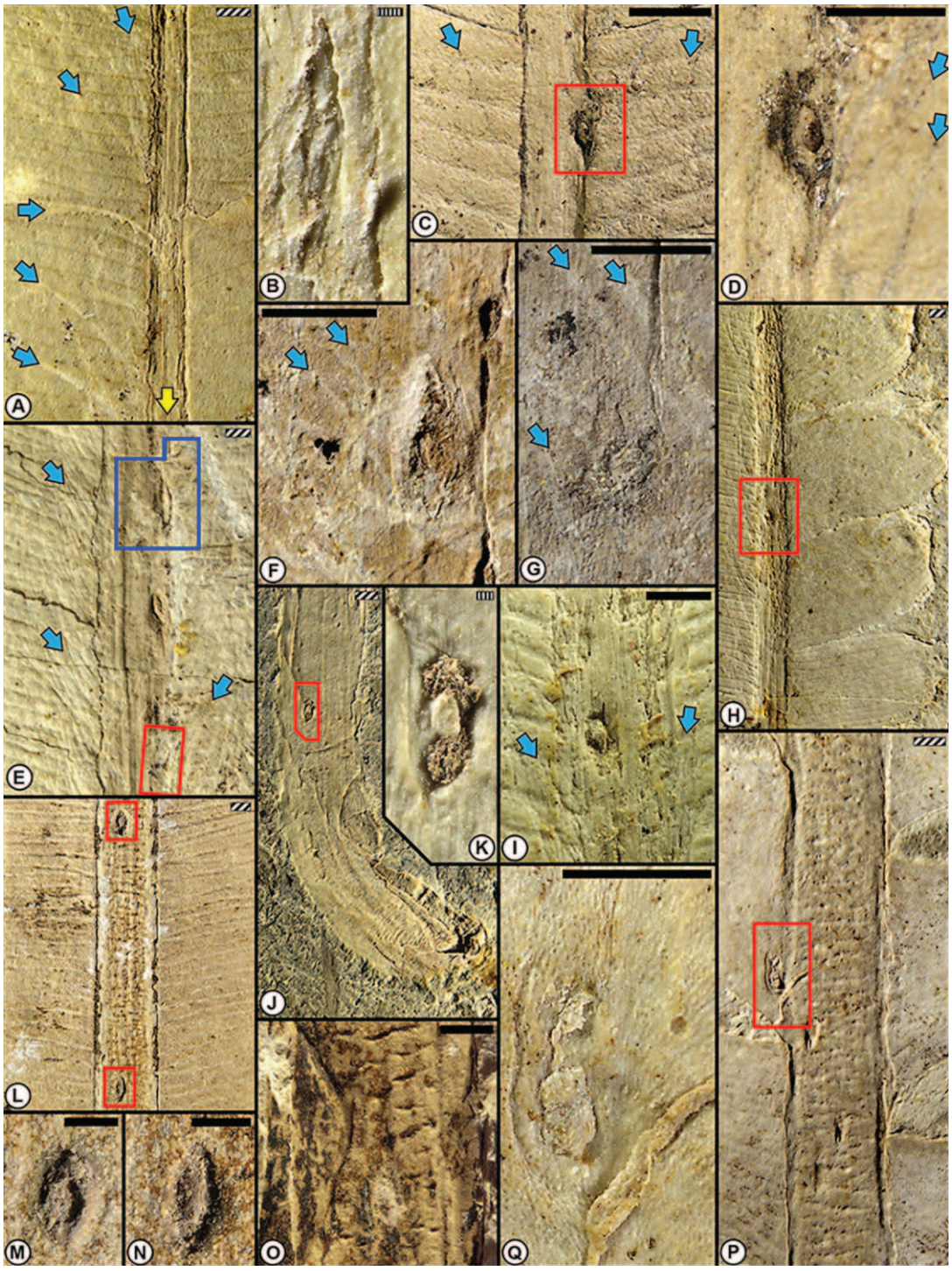

Fig. 7 Oviposition damage of DT76 on mostly trichome-defended bennettitalean foliage from the mid-Mesozoic of northeastern China. Blue arrows indicate orientation of individual trichomes originating from the rachis. *A*, DT76 on *Anomozamites sinensis* (CNU-PLA-NN-2010734, Daohugou 2) laden with rachis trichomes. *B*, Enlargement of lenticular DT76 lesion from template in *A*. *C*, DT76 on *Anomozamites thomasi* (CNU-PLA-NN-2010529p, Daohugou 2), with stiff trichomes branching at a 30° angle from rachis axis. *D*, Enlargement of DT76 adjacent two trichomes (blue arrows), indicated by the template at *C*. *E*, DT76 on *Anomozamites villosus* (CNU-PLA-NN-2006293, Daohugou 1), amid dense clusters of trichomes along each side of the rachis. Green arrows indicate oviposition lesions. *F*, Enlargement of a DT76 lesion on *E*, at the boundary between the rachis and leaf edge, adjacent the leaf midrib-blade boundary where there are fascicles of trichomes. *G*, Another example, as in *E*, with indicated spinose trichomes. *H*, DT76 on *A. villosus* (CNU-PLA-NN-2006907, Daohugou 2), nestled on a rachis surrounded by trichomes. *I*, DT76 oviposition lesion enlarged from template in *H*. *J*, DT76 on the petiole of *A. villosus* (CNU-PLA-NN-2009565p, Daohugou 2), in an area lacking trichomes. *K*, Enlargement of DT76 from the template in *J*, showing a central circular structure and surrounding disrupted

huttonii (fig. 11*O*–11*Q*), on leaves; and *Ginkgoites* sp., on leaves. DT100 also is found on the conifer *P. lanceolatus* (fig. 11*H*, 11*I*), on broad-leaved foliage. Beipiao: No associations.

Inferred ovipositor. Ovipositor morphotypes C and I.

Inferred insect culprits. Morphotype C culprits for this ovipositional damage are Blattodea clades †Fuziidae (*Fuzia*) and †Blattulidae (*Elisama*), Hemiptera clade †Vetanthocoridae (*Byssoidecerus*, *Collivetanthocoris*, *Curvicaudus*, *Vetanthocoris*), and Hymenoptera clades Xyelidae (†*Brachyoxyela*, †*Heteroxyela*, †*Sinoxyela*), †Xyelotomidae (*Paradoxotoma*, *Xyelocerus*), and perhaps †Daohugoidae (*Daohugoa*). Morphotype I culprits are Hemiptera clade †Progonocimicidae (*Cicadocoris*) and Hymenoptera clade Xyelidae (†*Isoxyela*).

Modern ecological analogue. The ovipositional damage DT100 is similar to the grasshopper *Cornops frenatum* Marschall (Orthoptera: Acrididae) on water hyacinth, *Eichhornia azurea* (Swartz) Kunth (Pontederiaceae), from Argentina (Turk 1984, fig. 3, p. 98). The structural similarity between DT100 and its modern analogue is a level 2 match.

Oviposition DT101. The occurrence of DT101 on the leaf blade is similar to that of DT76 for the leaf primary veins. DT101 and DT76 generally occur together, in some cases on the same leaf, and in some instances may represent the same or a closely related ovipositing insect species. DT101 is differentiated from DT100 by the former occurring as single lesions whereas the latter consists of clusters. Of all DTs, DT101 is the second-most abundant, accounting for 19.5% of all DT occurrences of the 16 highest-ranked DT–plant host occurrences (table 2). The distribution of DT101 extends from the latest Pennsylvanian to the present.

Definition. DT101 consists of lenticular, ovate, or elliptical lesions with prominent reaction rims surrounding inner disturbed tissue and arranged with their long axes parallel to primary venation and avoidance of primary venation. Lesion lengths are variable, from 2 to 10 mm, and generally display very prominent reaction rims. The presence of DT101 occurs singly or an unpatterned and dispersed manner in spare to dense distributions over a leaf blade surface and not in compact clusters or arcuate to linear rows.

Host plants and organs. Jehol: DT101 is associated with interveinal areas of the nilssonialean *B. lobatum* (fig. 11*M*), on a pinnule, and the ginkgophyte *Solenites orientalis* Sun, Zheng et Mei (fig. 12*F*–12*H*), on an elongate leaf. For conifers, DT101 is associated with *Elatocladus pinnatus* Sun et Zheng, on needle leaves; *L. boii* (fig. 12*V*–12*X*), on broad-leaved foliage; *L. lanceolatus*, on broad-leaved foliage; and unaffiliated conifer foliage. DT101 also occurs on unaffiliated foliage. Yanliao: DT101 is associated with horsetails and especially avoids the central vein on a nodal leaf of the horsetail *E. laterale*. Ginkgophyte associations are with *C. rigida*, on an elongate leaf; *G. huttonii* (fig. 12*C*, 12*D*), on leaves; *Ginkgoites* sp., on leaves; *Sphenobaiera lata* (Vakhrameev) Dou, on a leaf; and *Sphenobaiera* sp., on a polylobate leaf. Bennettitalean interactions are prominent and present on the four *Anomozamites* species of *A. angustifolium*, *A. kornilovae*, *A. sinensis*, and *A. villosus*, on leaves. Other bennettitalean interactions are with *Cycadolepis* sp., on a scale leaf; *P. irregulare* Nathorst, on leaves; and *P.* cf. *majus* (figs. 11*R*, 12*A*, 12*B*), on large leaves. Conifer associations are with *Elatocladus* sp. 2, on needle leaves; *Elatocladus* sp. 3, on needle leaves; *L. boii* (fig. 12*W*, 12*V*), on a broad leaf; *Pityophyllum nordenskioldi* (Heer) Seward (fig. 12*J*), on a scale bract; *P. lanceolatus*, on a broad leaf; *Y. sinensis* (figs. 12*L*, 12*N*, 12*P*–12*U*, 14*G*), on a needle leaf; and unaffiliated foliage. Beipiao: DT101 is associated with interveinal areas of the bennettitalean *Pterophyllum* sp., on a frond-like leaf, and the conifer *Podozamites eichwaldi* Schimper, on broad-leaved foliage.

Inferred ovipositor. Ovipositor morphotypes C, G, and I.

Inferred insect culprits. Morphotype C culprits for this ovipositional damage are Blattodea clades †Fuziidae (*Fuzia*) and †Blattulidae (*Elisama*), Hemiptera clade †Vetanthocoridae (*Byssoidecerus*, *Collivetanthocoris*, *Curvicaudus*, *Vetanthocoris*), and Hymenoptera clades Xyelidae (†*Brachyoxyela*, †*Heteroxyela*, †*Sinoxyela*), †Xyelotomidae (*Paradoxotoma*, *Xyelocerus*), and perhaps †Daohugoidae (*Daohugoa*). Morphotype G culprits are Hemiptera clades †Procercopidae (*Anomoscytina*, *Anthoscytina*, *Juracercopis*, *Stellularis*), †Tettigarctidae (*Shuraboprosbole*), †Pachymeridiidae (*Beipiaocoris*, *Corallopachymeridium*, *Peregrinpachymeridium*, *Sinopachymeridium*), Rhopalidae (†*Miracorizus*, †*Originicorizus*, †*Quatiocellus*), †Vetanthocoridae (*Longilanceolatus*, *Pumilanthocoris*), †Dehiscensicoridae (*Crassiantenninus*, *Dehiscensicoris*), Cydnidae (†*Orienicydnus*), and †Venicoridae (*Clavaticoris*, *Halonatusivena*, *Venicoris*) and Hymenoptera clade Scoliidae (†*Protoscolia*). Morphotype I culprits are Hemiptera clade †Progonocimicidae (*Cicadocoris*) and Hymenoptera clade Xyelidae (†*Isoxyela*).

Modern ecological analogue. Similar oviposition lesions are made by the great diving beetle, *Dytiscus marginalis* L. (Coleoptera: Dytiscidae), on semiaquatic cattail, *Typha* sp. (Typhaceae), from Germany (Wesenberg-Lund 1943, fig. 250, p. 279). The structural similarity between DT101 and its modern analogue is a level 1 match.

Oviposition DT102. DT102 is a unique combination of primary ovipositional damage and secondary fungal infection. Generally, such oviposition lesions preferentially occur along the leaf periphery and become colonized along their peripheries by a dark, surrounding rim of epiphyllous fungi that imperceptivity bleeds into the surrounding tissue. This DT occurs during the late Permian of Gondwana but is sparse thereafter, occurring intermittently in Laurasia. The presence of primary oviposition lesions resembling DT101 that are surrounded by secondary fungal colonization could make this a compound DT, but the intimate association between the oviposition colonization

tissue. *L*, Two DT76 lesions occurring on the rachis of *Nilssoniopteris* sp. (CNU-PLA-NN-2009822c, Daohugou 1). *M*, Enlargement of the DT76 lesion in the upper template in *L*. *N*, Enlargement of the DT76 lesion in the lower template in *L*. *O*, A DT76 lesion occurring on the petiole of the bennettitalean *Nilssoniopteris* cf. *groenlandica* (CNU-PLA-NN-2009402, Daohugou 1). *P*, A DT76 lesion on *Pterophyllum irregulare* (CNU-PLA-NN-2005450, Daohugou 2) occurring on the base of the petiolar blade adjacent the rachis. *Q*, Enlargement of lesion in the template at *P*, showing a central ellipsoidal structure and the distortion and wrapping of cells around the insertion scar. Scale bars: vertically striped = 0.1 mm; solid white or black = 1.0 mm; back-slashed = 10.0 mm.

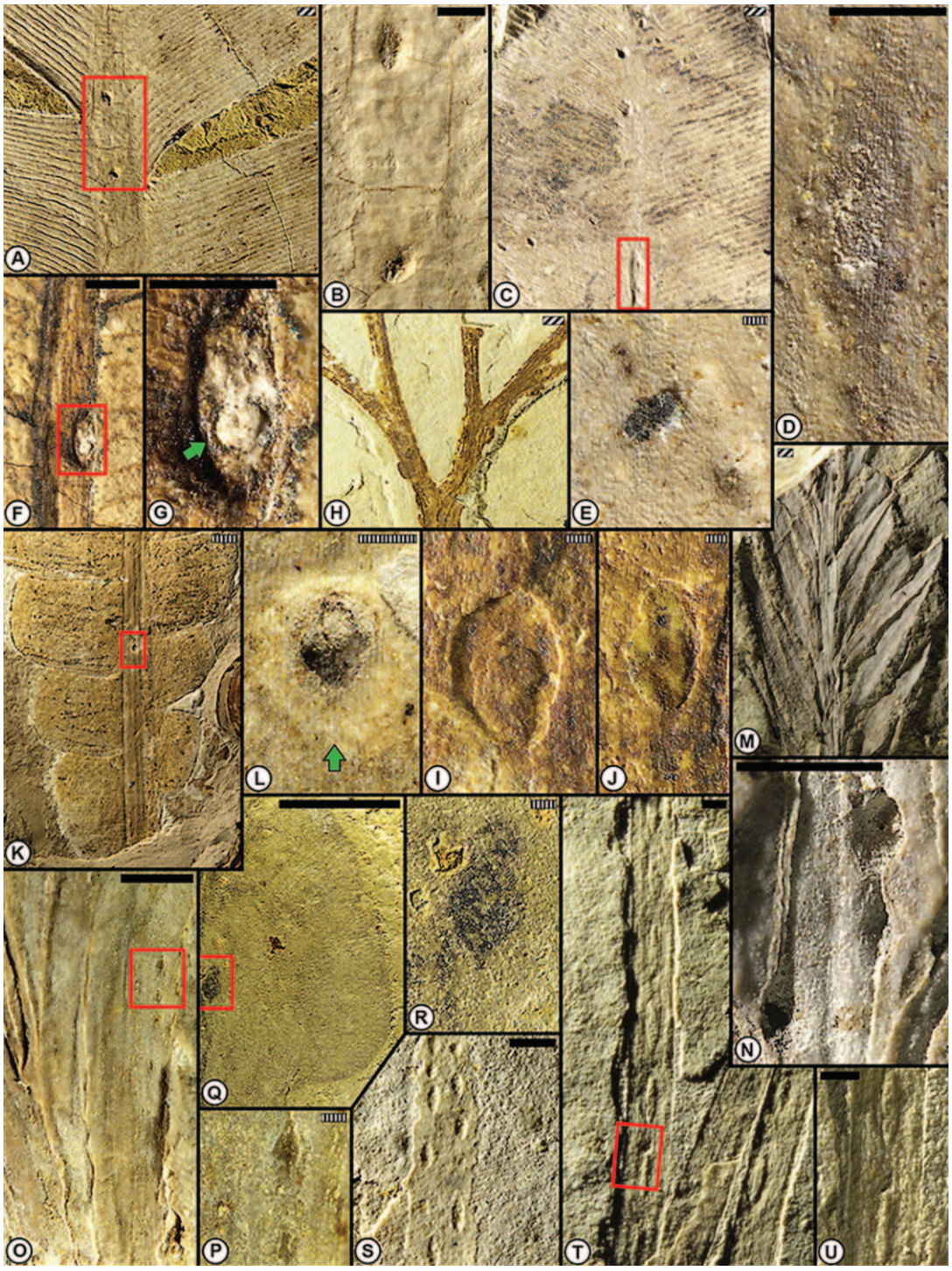

Fig. 8 Three oviposition damage types (DT76, DT137, and DT175) on the foliage of a nilssonialean, a conifer, ginkgophytes, and bennettitaleans, from the mid-Mesozoic of northeastern China. *A*, DT76 present on the midrib of the *Pterophyllum majus* (CNU-PLA-NN-2009209, Daohugou 1). *B*, Enlargement of template area in *A*, showing two lenticular oviposition lesions. *C*, DT76 occurring on *Nilssoniopteris* sp. (CNU-PLA-NN-2006244, Daohugou 2). *D*, Enlargement of DT76 lesion in *C*, showing a central egg-like structure at the green arrow. *E*, A DT137 lesion oriented 45° to rachis axis, indicated by the yellow arrow and occurring below the template in *C*. *F*, DT76 damage on *Anomozamites villosus* (CNU-PLA-NN-2006642, Daohugou 2). *G*, Enlargement of the DT76 lesion at the template in *F*, positioned at the interface of the rachis and leaf blade. *H*, Several DT76 lesions occurring on the petiolar branches of the ginkgophyte *Baiera* cf. *furcata* (CNU-PLA-NN-2011592). *I*, DT76 lesion from the upper-left template in *H*, showing a raised central area. *J*, DT76 lesion from the lower-left template in *H*. *K*, A DT76 on the rachis of *Anomozamites angustifolium* (CNU-PLA-NN-2006183, Daohugou 1). *L*, A DT76 lesion enlarged from the template in *K*, showing a central circular structure, surrounded by dark disrupted tissue and in turn enveloped by a concentric reaction ring indicated

and its fungal colonization currently is best considered as a single DT association with its plant host.

Definition. DT102 consists of an interveinal, broad to narrow lenticular DT101-like oviposition mark commonly arranged into a linear series or clusters on foliage typically along the leaf margin or near the leaf midveinal axis that is surrounded by epiphyllous necrotic tissue. Each fungal blotch has an inner zone of disrupted tissue and an outer zone of a variably wide lenticular reaction front of thick angulate reaction rims, each with its initial oviposition lesion oriented parallel to secondary venation.

Host plants and organs. Jehol: No associations. Yanliao: DT102 (not illustrated) is associated with interveinal areas and small stems of the ginkgophyte *Ginkgoites sibirica* (Heer) Seward, on a leaf; the bennettitalean *A. kornilovae*, on a leaf; and an unaffiliated cycadophyte axis. Beipiao: No associations.

Inferred ovipositor. Ovipositor morphotypes C, G, and I.

Inferred insect culprits. Morphotype C culprits for this ovipositional damage are Blattodea clades †Fuziidae (*Fuzia*) and †Blattulidae (*Elisama*), Hemiptera clade †Vetanthocoridae (*Byssoidecerus*, *Collivetanthocoris*, *Curvicaudus*, *Vetanthocoris*), and Hymenoptera clades Xyelidae (†*Brachyoxyela*, †*Heteroxyela*, †*Sinoxyela*) †Xyelotomidae (*Paradoxotoma*, *Xyelocerus*), and perhaps †Daohugoidae (*Daohugoa*). Morphotype G culprits for are Hemiptera clades †Procercopidae (*Anomoscytina*, *Anthoscytina*, *Juracercopis*, *Stellularis*), †Tettigarctidae (*Shuraboprosbole*), †Pachymeridiidae (*Beipiaocoris, Corallopachymeridium*, *Peregrinpachymeridium*, *Sinopachymeridium*), Rhopalidae (†*Miracorizus*, †*Originicorizus*, †*Quatiocellus*), †Vetanthocoridae (*Longilanceolatus*, *Pumilanthocoris*), †Dehiscensicoridae (*Crassiantenninus*, *Dehiscensicoris*), Cydnidae (†*Orienicydnus*), and †Venicoridae (*Clavaticoris*, *Halonatusivena*, *Venicoris*) and Hymenoptera clade Scoliidae (†*Protoscolia*). Morphotype I culprits are Hemiptera clade †Progonocimicidae (*Cicadocoris*) and Hymenoptera clade Xyelidae (†*Isoxyela*).

Modern ecological analogue. An example is the anthracnose leaf spot fungus *Deightoniella torulosa* (Syd.) M.B. Ellis (Capnodiales: Mycosphaerellaceae) colonizing wild banana, *Musa acuminata* Colla (Musaceae), after DT101-type oviposition marks (Photita et al. 2004, fig. 3, p. 135). The structural similarity between DT102 and its modern analogue is a level 1 match.

Oviposition DT108. This uncommon but distinctive DT is characterized by irregularly shaped, usually lobate lesions produced by an ovipositing insect on a robust stem, such as an equisetalean. The disrupted inner tissues and the shape of the damage indicate a wood-boring origin. However, the explanation preferred here is that the DT108 lesions are attributable to an insect with single overlapping oviposition events that result in an irregular pattern of tissue modification and scarring. The fossil record of DT108 evidently begins in the Late Triassic and is present sporadically to the present.

Definition. DT108 consists of distinctive, large, elliptical, and circular to more commonly irregularly polylobate oviposition lesions on stems or robust midribs, commonly reaching 8 mm in maximum dimension and merging with each other into irregular, approaching polylobate shapes, characterized by subdued reaction rims and an internal structure of extensively deformed vascular strands, parenchyma, and other tissues.

Host plants and organs. Jehol: No associations. Yanliao: DT108 is associated with large midribs of the bennettitalean *P.* cf. *majus* (fig. 10*A*–10*E*), on a large frond. Beipiao: No associations.

Inferred ovipositor. Ovipositor morphotype F.

Inferred insect culprits. Culprits for this ovipositional damage are Odonata clade †Aeschnidiidae (*Sinaeschnidia*, *Stylaeschnidium*), Orthoptera clade †Haglidae (*Allaboilus*), and especially Neuroptera clade †Kalligrammatidae (*Oregramma*).

Modern ecological analogue. Ovipositional damage of the 17-year periodical cicada, *Magicicada septendecim* (Hemiptera: Cicadidae), on stems of sugar maple, *Acer nigrum* L. (Sapindaceae), is a modern ecological analogue (Marlatt 1907, fig. 43, p. 108). The structural similarity between DT108 and its modern analogue is a level 2 match.

Oviposition DT137. The distinctive delicate scars of DT137 are recognizable by their small size, an orientation cutting across major venation, and frequent, thin, wedge-shaped lesions with a short, straight edge that substitutes for an angulate end. The small, delicate nature of this lesion is found generally on modern mosses (Glime 2017). The earliest-known example of this oviposition lesion is from a locality from South Africa, provisionally of mid-Permian age, though it should be expected in earlier Devonian- and Mississippian-age deposits.

Definition. DT137 consists of scattered foliar oviposition lesions occurring on the midvein, primary vein, midveinal region, or petioles of small axes. Each lesion is shaped as an inconspicuous, elongate, isosceles-shaped triangle, with the short segment of the "base" replacing an acuminate end but usually lenticular in shape. The aspect ratio is or is greater than 3:0, and the orientation is transverse to veins or other vascular and structural tissue.

Host plants and organs. Jehol: DT137 is associated with major veins of the conifer *L. boii*, on broad-leaved foliage and on unaffiliated foliage. Yanliao: DT137 is associated with midveins, petioles, and small axes of the ginkgophytes *Ginkgoites* sp.

by a green arrow. *M*, DT76 on the central branchlet axis of the conifer *Yanliaoa sinensis* (CNU-PLA-NN-2006139, Daohugou 2). *N*, Two successive small DT76 lesions from the template at the top of *M*, showing deep penetration of axial tissues. *O*, Four successive DT175 lesions deployed in a linear series on the leaves of *Y. sinensis* (CNU-PLA-NN-2008480, Daohugou 2). *P*, Enlargement of the upper two lesions in *O*, as indicted by the template. *Q*, DT76 occurring at the interface of the pinnular blade and its adjacent rachis on the nilssonialean *Baikalophyllum lobatum* (CNU-PLA-NN-2009863p, Liutiaogou). *R*, Enlargement of DT76 from the template in *Q*, showing a darkened area with two acuminate ends and a central circular structure. *S*, DT175 occurring on *Baiera* sp. (CNU-PLA-LL-2010331, Liutiaogou), showing two parallel sets of oviposition, one with six and the other with four successive lesions. *T*, DT175 on foliage of the conifer *Liaoningocladus boii* (CNU-PLA-NN-2010018), with one leaf exhibiting seven and the other three successive end-to-end lesions. *U*, Enlargement of three of the lesions from the template in *T*. Scale bars: vertically striped = 0.1 mm; solid white or black = 1.0 mm; back-slashed = 10.0 mm.

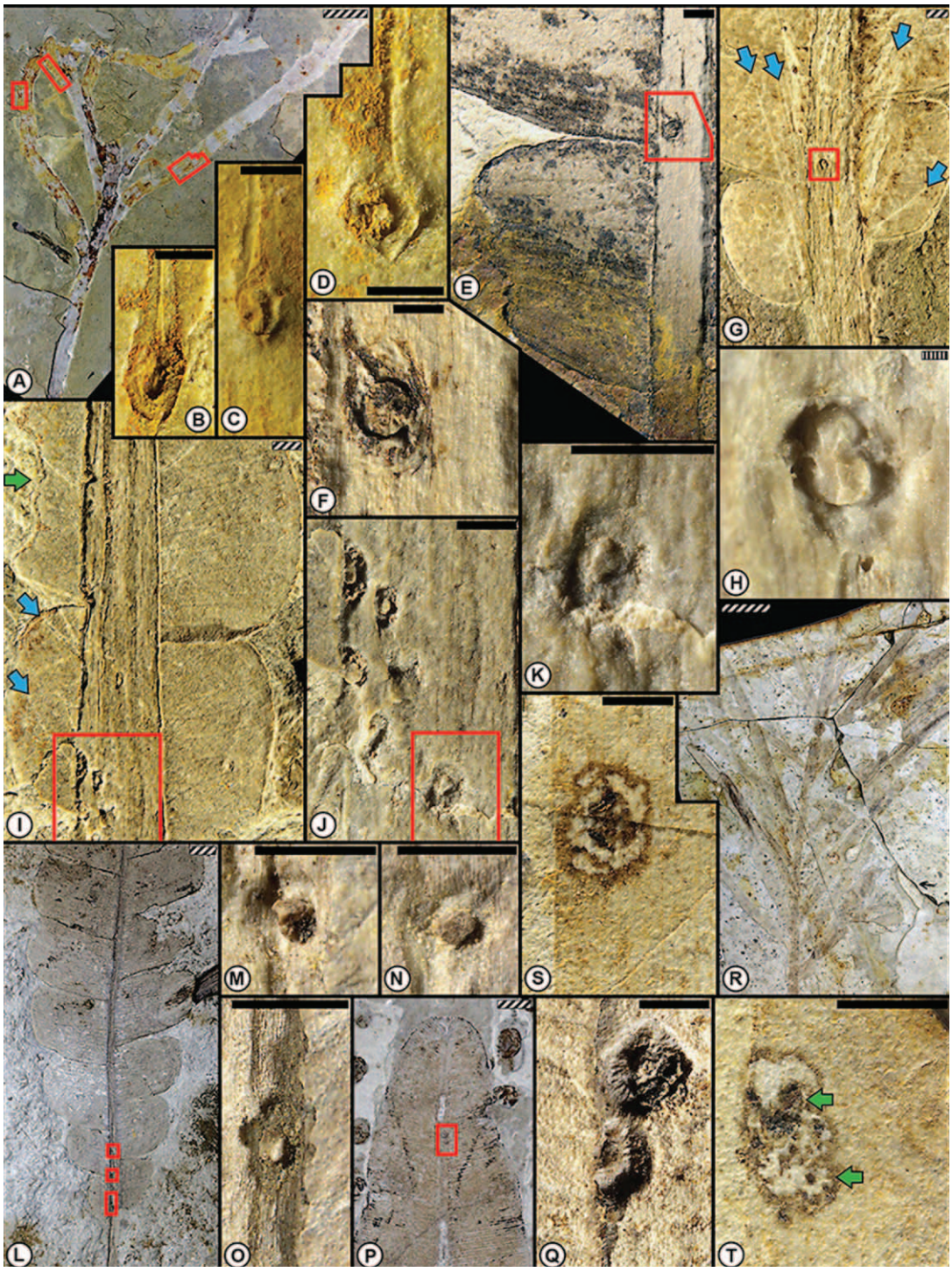

Fig. 9 DT226 oviposition damage and structural defense of sphenopsid, conifer, and bennettitalean foliage from the mid-Mesozoic of northeastern China. *A*, Several occurrences of DT226 on the stem of *Equisetites longevaginatus* (CNU-PLA-NN-2009267p, Liutiaogou). These structures are unlikely to be basal scars of leaves, as they lack vascular traces and do not originate at nodes. *B*, DT226 lesion from the template at the extreme upper left in *A*. *C*, DT226 lesion from the more centrally positioned template at upper left in *A*. *D*, DT226 lesion from the central-right template in *A*. *E*, DT226 occurring on the rachis of *Anomozamites kornilovae* (CNU-PLA-NN-2006921, Daohugou 2); same specimen as figures 4 and 5, which display DT76. *F*, DT226 lesion in *E*, showing a rounded form and an acuminate slit scar at upper left. *G*, DT226 present on the rachis of *Anomozamites villosus* (CNU-PLA-NN-2006913c), surrounded by fascicles of rigid, spine-like trichomes; blue arrows point to individual trichomes. *H*, Enlarged view of DT226 outlined in template at *G*, displaying a central ellipsoidal structure and a surrounding circular zone of disturbed tissue. This specimen is the holomorphotype for oviposition DT226 for version 4 of the forthcoming *Damage Guide*. *I*, DT226 on the rachis of *Anomozamites angustifolium* (CNU-PLA-NN-2006237, Daohugou 2). *J*, From the template in *I* is a cluster of four DT226

(fig. 10*G*), *G. huttonii* (fig. 10*J*, 10*K*), and *G. sibirica* (fig. 10*L*, 10*M*), on leaves, and on an unaffiliated ginkgophyte axis. Other associations are with the bennettitaleans *A. kornilovae* (fig. 10*H*, 10*I*), *A. sinensis* (fig. 10*O*, 10*P*), *A. villosus*, *Nilssoniopteris* sp. (fig. 8*E*), and *P.* cf. *majus* (fig. 10*R*, 10*S*), all on leaves. DT137 also is found on unaffiliated axes and foliage. Beipiao: DT137 is associated with the conifer *P. eichwaldi*, on major veins of broad-leaved foliage.

Inferred ovipositor. Ovipositor morphotype H.

Inferred insect culprits. Culprits for this ovipositional damage are Lepidoptera clades †Eolepidopterygidae (*Seresilepidopteron*) and †Mesokristenseniidae (*Kladolepidopteron*).

Modern ecological analogue. An analogue is the tree cricket *Oecanthus pellucens* Scopoli (Orthoptera: Gyrillidae) ovipositing into a taxonomically undetermined twig from Italy (Chopard 1938, fig. 156, p. 181). Also, see Fulton's (1915) illustrations of a close analogue to this DT. The structural similarity between DT137 and its modern analogue is inexact and a level 2 match.

Oviposition DT159. The miniscule oviposition mark DT159 is very similar to DT137 in overall shape. The defining feature of DT159 is an orientation parallel to the midvein, midrib, or other primary vein. Such a position is unlike the transverse lesions oriented across the midvein and similar structures in DT137 damage. The oldest occurrence of DT159 is from the Late Triassic of the Karoo Basin, and it survives to the present.

Definition. DT159 oviposition (not illustrated) consists of small, circular, ovate to lenticular lesions, ordinarily with angulate ends that have a detectable outer reaction rim enveloping a central region. Each linear lesion is 0.1–1.0 mm in length; a typical orientation is as a cluster along the medial axis of an oblong thallus or other delicate foliage that is recognizable when preserved as a group of oviposition lesions.

Host plants and organs. Jehol: DT159 is associated with surface tissues of the horsetail *E. longevaginatus*, occurring on stems. Yanliao: DT159 (not illustrated) is associated with the midribs of the bennettitaleans on *A. angustifolium* and *A. kornilovae*, on leaves, and on *P.* cf. *majus*, on leaves. Beipiao: No associations.

Inferred ovipositor. Ovipositor morphotype G.

Inferred insect culprits. Culprits for this ovipositional damage are Hemiptera clades †Procercopidae (*Anomoscytina*, *Anthoscytina*, *Juracercopis*, *Stellularis*), †Tettigarctidae (*Shuraboprosbole*), †Pachymeridiidae (*Beipiaocoris*, *Corallopachymeridium*, *Peregrinpachymeridium*, *Sinopachymeridium*), Rhopalidae (†*Miracorizus*, †*Originicorizus* †*Quatiocellus*), †Vetanthocoridae (*Longilanceolatus*, *Pumilanthocoris*), †Dehiscensicoridae (*Crassiantenninus*, *Dehiscensicoris*), Cydnidae (†*Orienicydnus*), and †Venicoridae (*Clavaticoris*, *Halonatusivena*, *Venicoris*) and Hymenoptera clade Scoliidae (†*Protoscolia*).

Modern ecological analogue. The green hawker, *Aeshna viridis* Eversmann (Aeshnidae), ovipositing delicately into the midveinal area of water pineapple, *Stratiotes aloides* L. (Hydrocharitaceae), from Germany (Wesenberg-Lund 1913*b*, fig. 4, p. 191) is an ecological analogue. The structural similarity between DT159 and its modern analogue is a level 1 match.

Oviposition DT175. Although similar to the scattered, individual lesions of DT76 that are oviposited as separate events, DT175 consists of three or more lesions oriented end to end and laid in succession within a single ovipositional event. The behavioral pattern represented by DT175 indicates elevated stereotypy on a host plant, characterized by targeting of narrow veins, avoidance of major veins, and confinement of the lesions to an approximate 1 : 3 width-to-length ratio. DT175 is present in latest Pennsylvanian and early Permian seed plants from north-central Texas, occurs in the Late Triassic Molteno Formation of South Africa, and is present today.

Definition. DT175 consists of elliptical-lenticular oviposition lesions on foliage with an aspect ratio range of 1 : 3 to 1 : 5, a length up to 1.5 mm, and with a distinct outer reaction rim and inner disturbed tissue. The scars are arranged end to end, forming a file of up to seven, probably more, lesions along venation or the margin of a leaf, usually in a parallel-veined leaf. Rarely, the lesions are deployed in two files of scars alongside each other on the same leaf specimen or adjacent to but avoiding a major vein.

Host plants and organs. Jehol: DT175 is associated with surface tissues of the ginkgophytes *Baiera valida* and *Baiera* sp. (fig. 8*S*), on leaves; on the bennettitalean *Tyrmia acrodonta*, on leaves; on the conifers *L. boii* (fig. 8*T*, 8*U*) and *L. lanceolatus*, both on broad-leaved foliage; and an unaffiliated conifer short shoot. Yanliao: DT175 is associated with surface tissues of the ginkgophytes *B. manchurica* and *Baiera* sp., on leaves; *Ginkgoites* sp., on a leaf; and the conifer *Y. sinensis*, on a needle leaf. Beipiao: DT175 is associated with surface tissues of the fern *T. denticulata*, on a pinnule; the ginkgophyte *Baiera furcata* (Lindley et Hutton) Braun, on a leaf; and unaffiliated cycad foliage.

Inferred ovipositor. Ovipositor morphotype D.

Inferred insect culprits. Culprits for this ovipositional damage are Orthoptera clades †Haglidae (*Allaboilus*) and Prophalangopsidae (†*Sigmaboilus*); Hemiptera clades †Tettigarctidae (*Sunotettigarcta*), †Procercopidae (*Stellularis*), and Cixiidae (†*Lapicixius*); and Hymenoptera clade Xyelidae (†*Platyxyela*).

Modern ecological analogue. An acceptable match is the European pine sawfly, *Neodiprion sertifer* (Geoffroy ex Fourcroy) (Hymenoptera: Tenthredinidae), on Scots pine, *Pinus sylvestris* L. (Pinaceae), from the northeastern United States (Johnson and

lesions at the base of the rachis, each showing a central raised area. *K*, Enlargement of DT226 lesion in the template at *J*, showing a central ellipsoidal eminence. *L*, Multiple occurrences of DT226 along the rachis–leaf blade boundary of *Anomozamites sinensis* (CNU-PLA-NN-2010699, Daohugou 1). *M*, Enlargement of DT226 from the middle square template in *L*, displaying a central prominence. *N*, Enlargement of DT226 from the upper square template in *L*, with a central upraised area; note continuity of vascular strands. *O*, Enlargement of DT226 from the lowermost rectangular template in *L*, showing a prominent central boss. *P*, DT226 on the leaf tip of *Nilssoniopteris* sp. (CNU-PLA-NN-2009822, Daohugou 1). *Q*, Two adjacent DT226 lesions from the template in *P*, showing a lenticular central cavity from which radiating tufts of tissue emerge. *R*, Taphonomically flattened DT226 occurring on *Liaoningocladus boii* (CNU-PLA-LL-2010223p, Liutiaogou). *S*, DT226 from a leaf in *R* outside of the image border, indicated by the yellow arrow. *T*, DT226 indicated by the template at left in *R*, showing an inner circular to ellipsoidal area (upper-left arrow) and outer scar rim (lower-right arrow). Scale bars: vertically striped = 0.1 mm; solid white or black = 1.0 mm; back-slashed = 10.0 mm.

Fig. 10 Oviposition damage types of DT108, DT137, and DT246 on sphenopsid stems and ginkgophyte and bennettitalean foliage from the mid-Mesozoic of northeastern. *A*, DT108 on the rachis of a *Pterophyllum majus* (CNU-PLA-NN-2005200, Daohugou 1) leaf. (See fig. 6*A*, 6*B* for DT76 on the same specimen.) *B*, Enlargement of a polylobate DT108 oviposition site, from the uppermost template in *A*, showing disrupted inner tissues and revealing several enigmatic rod-like features approximately parallel to the rachis axis. *C*, DT108, corresponding to the second template from the top in *A*. *D*, DT108, corresponding to the lowermost template in *A*. *E*, DT108, corresponding to the smallest template in *A*. *F*, DT137 on the ginkgophyte *Ginkgoites* sp. (CNU-PLA-NN-2008141, Daohugou 2). *G*, Two examples of DT137 occurring in the intercostal region between two secondary veins; note the bending of veins toward the upper lesion. *H*, DT137 on *Anomozamites kornilovae* (CNU-PLA-NN-2010390p, Daohugou 2). *I*, A DT137 lesion slicing across three major veins of the pinnule. *J*, A DT137 lesion on *Ginkgoites huttonii* (CNU-PLA-NN-2007528c, Daohugou 2). *K*, A nearly transverse DT137 lesion cutting across three major veins, resulting in vein distortion and convergence in *J*, very similar to *G*. *L*, A DT137 lesion on *Ginkgoites sibirica* (CNU-PLA-NN-2010175, Daohugou 2), oriented transverse to

Lyon 1976, pl. 2, fig. B, p. 19). The structural similarity between DT175 and its modern analogue is a level 2 match.

Oviposition DT226. Common occurrences on midribs, petioles, and stems are round, rather small oviposition lesions with an upraised central area. These lesions occur on a broad range of plant hosts and appear to be the least species specific of any oviposition mark from the larger data set. DT226 extends considerably back in time, recorded on Late Pennsylvanian and early Permian floras from north-central Texas (Schachat et al. 2014; Xu et al. 2018). DT226 accounts for the third-most frequent oviposition DT encountered in the larger mid-Mesozoic data set, representing 8.0% of all DT occurrences of the 16 highest-ranked DT–plant host occurrences (table 2). The geochronologic range of DT226 is from the latest Pennsylvanian (Xu et al. 2018) to the present (see "New DTs").

Definition. DT226 consists of a round, cratered lesion on a primary vein or stem, 0.5–1.5 mm in diameter, with an encircling, deep sulcus penetrating into subdermal tissue and an innermost, central, prominently raised plug of disorganized tissue. The circular lesion has surrounding scar tissue, a subtle, outermost, bordering zone with a differently appearing tissue, marked by the deflection and subsequent rejoining of surrounding vasculature around the lesion. The lesions intermittently occur as an interrupted row along the midrib.

Host plants and organs. Jehol: DT226 is associated mostly with deeper tissues of the horsetails *E. exiliformis* and *Equisetites longivaginatus* (fig. 9*A*–9*D*); the conifers *Cephalotaxopsis leptophylla* (Wu) Sun et Zheng and *L. boii* (fig. 9*R*–9*T*), on needle leaves; and the gnetophyte *Ephedrites cheniae* (Guo et Wu), on leaves. Yanliao: DT226 is associated mostly with deeper tissues on the ginkgophytes *Baiera* sp., on leaves; *Czekanowskia setacea* Heer, on elongate leaves; and *G. huttonii*, on leaves, especially midrib tissues. DT226 also is documented on the five species of the bennettitalean *Anomozamites*, namely, *A. angustifolium* (fig. 9*I*–9*K*), *A. gracilis*, *A. kornilovae* (figs. 6*E*, 6*F*, 9*E*, 9*F*), *A. sinensis* (fig. 9*M*–9*O*), and *A. villosus* (fig. 9*G*, 9*H*). Other bennettitaleans with DT226 are *Nilssoniopteris* sp. (fig. 9*P*, 9*Q*) and *P.* cf. *majus*, both on leaves, especially midribs. Beipiao: DT226 is associated with surface and deeper stem tissues on the horsetail *Neocalamites hoerensis* Schimper (Halle 1908).

Inferred ovipositor. Ovipositor morphotype C.

Inferred insect culprits. Culprits for this ovipositional damage are Blattodea clades †Fuziidae (*Fuzia*) and †Blattulidae (*Elisama*); Hemiptera clade †Vetanthocoridae (*Byssoidecerus*, *Collivetanthocoris*, *Curvicaudus*, *Vetanthocoris*); and Hymenoptera clades Xyelidae (†*Brachyoxyela*, †*Heteroxyela*, †*Sinoxyela*), †Xyelotomidae (*Paradoxotoma*, *Xyelocerus*), and perhaps †Daohugoidae (*Daohugoa*).

Modern ecological analogue. Very similar ovipositional damage is made by the spur-throat toothpick grasshopper, *Stenacris vitreipennis* Marschall (Orthoptera: Acrididae), on the giant bulrush, *Schoeneoplectus californicus* (C.A. Mey) Steud. (Cyperaceae), from Texas. The structural similarity between DT226 and its modern analogue is a level 1 match.

Oviposition DT246. Similar to DT226, DT247 is an oviposition lesion that has a circular to broadly ovate cross section, thus indicating a culprit with an ovipositor approximately circular in cross section. It also differs from DT226 by the absence of a distinct central plug in the oviposition interior, replaced by a subtle dome. Evidently, DT246 extends far into deep time, as it is recorded on seed plant leaves from the latest Pennsylvanian (Xu et al. 2018) and early Permian of north-central Texas (Schachat et al. 2014) and occurs as modern damage.

Definition. DT246 is robust, circular to broadly ovate in shape, to uncommonly wide, and has subtly lacriform scars oriented parallel to leaf venation. The enveloping scars can vary greatly in size, occurring singly or rarely clustered linearly. An upper, slightly domed, but not plug-like central surface displays a distinctly dimpled, muted pustulose or featureless surface that indicates anomalous tissue surrounded by a round to gently undulatory outer margin zone.

Host plants and organs. Jehol: DT246 is associated with the outer stem tissues of the horsetail *Equisetites longivaginatus* (fig. 5*C*, 5*H*). Yanliao: DT246 occurs on surface tissues of the bennettitaleans *A. villosus*, on leaves, and *P. irregulare*, on frond-like leaves. Beipiao: No associations.

Inferred ovipositor. Ovipositor morphotype C.

Inferred insect culprits. Culprits for this ovipositional damage are Blattodea clades †Fuziidae (*Fuzia*) and †Blattulidae (*Elisama*); Hemiptera clade †Vetanthocoridae (*Byssoidecerus*, *Collivetanthocoris*, *Curvicaudus*, *Vetanthocoris*); and Hymenoptera clades Xyelidae (†*Brachyoxyela*, †*Heteroxyela*, †*Sinoxyela*), †Xyelotomidae (*Paradoxotoma*, *Xyelocerus*), and perhaps †Daohugoidae (*Daohugoa*).

Modern ecological analogue. A very similar type of damage is the oviposition site of *Chromatomyia syngenesiae* Hardy (Diptera: Agromyzidae), on dandelion *Taraxicum officinale* (L.) Weber ex F.H. Wigg (Asteraceae), from the Netherlands (Ellis 2018, uppermost figure of first webpage). The structural similarity between DT246 and its modern analogue is a level 1 match.

Oviposition DT272. The two plant hosts of DT272 share two major features. First, DT272 occurs only on reproductive structures, in particular the fleshy seeds of *Yimaia capituliformis*. Both plant hosts from the Yanliao Biota likely had thick, fleshy to leathery tissues. Second, the ovipositor penetration of both hosts of DT272 probably traversed significant thicknesses

venation. *M*, Enlargement of DT137 in *L*, displaying an unclear dark center and a prominent surrounding scar rim transverse to venation. *N*, DT137 on *Anomozamites sinensis* (CNU-PLA-NN-2010741p, Daohugou 2). *O*, Enlargement of the DT137 lesion in *N*, showing the interruption of four major pinnular veins. *P*, Further magnification of DT137 from the template in *O*. *Q*, DT137 on *Pterophyllum magus* (CNU-PLA-NN-2009805, Daohugou 1). *R*, Approximately six narrowly lenticular lesions cutting across major pinnular veins in *Q*. *S*, A thin lenticular DT137 lesion with a prominent outer rim of scar tissue and inner disrupted tissue enlarged from *R*. *T*, Several DT246 lesions on *Equisetites longevaginatus* (CNU-PLA-NN-2009297, Daohugou 2), consisting of circular lesions that are randomly positioned on the stem, indicating that they are not leaf scars. *U*, Enlargement of a DT246 scar from the upper-right template in *T*. *V*, Enlargement of a DT246 scar from the center-left template in *T*. *W*, Enlargement of a DT246 scar from the lower-right template in *T*. *X*, Enlargement of a DT246 scar from the bottom-most, partly hidden template in *T*. Scale bars: vertically striped = 0.1 mm; solid white or black = 1.0 mm; back-slashed = 10.0 mm.

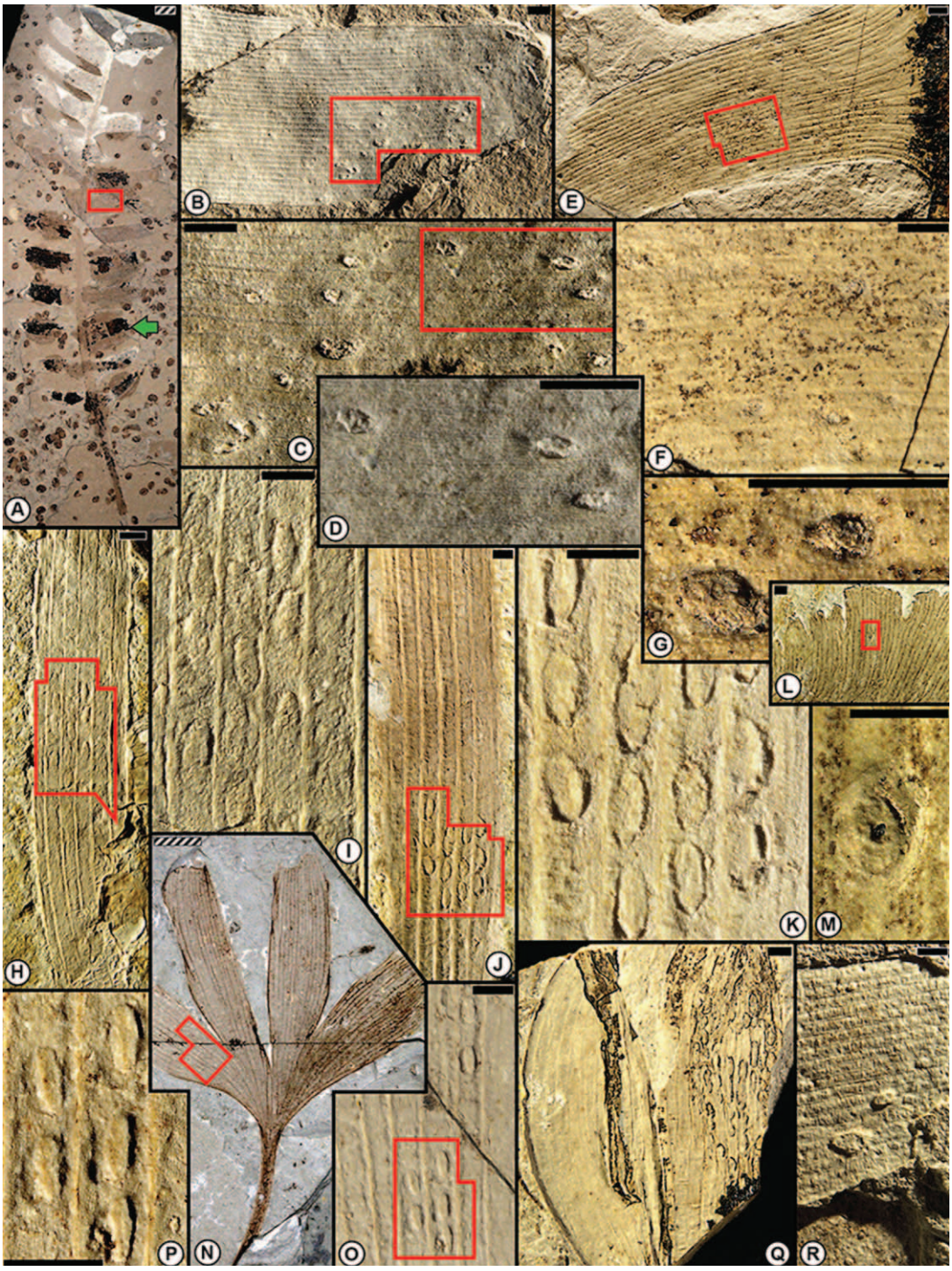

Fig. 11 Clustered oviposition damage of DT54, DT100, and DT101 on the foliage of a nilssonialean, a conifer, ginkgophytes, and bennettitaleans from the mid-Mesozoic of northeastern China. *A*, Distinctive oviposition of DT54 on *Pterophyllum majus* (CNU-PLA-NN-2005055p, Daohugou 1), a bennettitalean frond in excess of 30 cm in length. *B*, A magnified region of the distal pinnule, outlined in the template at *A*, showing the overall pattern of DT54 oviposition; the single cuspate margin represents a broken chip and not DT12 margin feeding. *C*, Enlargement of region surrounding the cuspate chip from the template in *B*, showing arcuate swaths of oviposition marks interconnected by superimposed white lines. *D*, Further enlargement, showing three oviposition lesions from the template in *C*. *E*, Counterpart specimen (CNU-PLA-NN-2005055c), showing additional DT54 damage. *F*, Enlargement of template in *E*, showing distribution of oviposition lesions. *G*, Enlargement of three lesions from the partial template at left in *F*, displaying disrupted tissue. *H*, DT100 on the conifer *Podozamites lanceolatus* (CNU-PLA-NN-2005394, Daohugou 1). *I*, Enlargement of DT100 from the template in *H*, displaying a cluster of approximately 10 lesions across three costal fields. *J*, Oviposition of DT100 on *Baiera manchurica* (CNU-PLA-NN-2011192P). *K*, Enlargement of DT100 from

of fleshy tissue. These near-identical oviposition scars indicate that thick, fleshy tissue, exposed to the ambient environment, would have been a source for larval food in these unrelated seed plant clades.

Definition. DT272 consists of a series of four to nine oviposition lesions arranged in a side-to-side manner along a subtly arcuate to linear row that is up to 9 mm long. The lenticular to ovoidal-shaped lesions are embedded in thick, parenchymatous, evidently fleshy or leathery tissue. Each penetrating incision is characterized by an inner disturbed area of tissue surrounded by a minimal rim of dark reaction tissue, displaying a width-to-length ratio of 1:1.2 to 1:2.5 and forming overall a distinctly stereotyped pattern.

Host plants and organs. Jehol: No associations. Yanliao: DT272 is associated with penetration of thick, fleshy tissue and the underlying ovular tissue of the ginkgophyte ovulate organ *Y. capituliformis* (fig. 13*A*–13*H*), reproduced from Meng et al. (2017). Meng and colleagues (2017) provide documentation and a discussion of DT272 on *Y. capituliformis*. Beipiao: No associations.

Inferred ovipositor. Ovipositor morphotype F.

Inferred insect culprits. Culprits for this ovipositional damage are Odonata clade †Aeschnidiidae (*Sinaeschnidia*, *Stylaeschnidium*), Orthoptera clade †Haglidae (*Allaboilus*), and particularly Neuroptera clade †Kalligrammatidae (*Oregramma*).

Modern ecological analogue. Oviposition scars by the spotted wing pomace fly, *Drosophila suzukii* Matsumura (Diptera: Drosophilidae), on cherry, *Prunus cerasus* L. (Rosaceae), from California (Walsh et al. 2011, fig. 4, p. 3). The structural similarity between DT272 and its modern analogue is a level 2 match.

Oviposition DT292. Perhaps the most distinctive oviposition marks in the total Mesozoic northwestern China data set are the isolated occurrences of DT292. This singular and uncommon surface damage of DT292 occurs overwhelmingly on *Y. sinensis* of the Yanliao Biota. To our knowledge, DT292 occurs nowhere else in the fossil record, indicating that a unique ovipositor structure inflicted this damage. DT292 consists of a shallow modification of plant epidermal tissue inflicted by an ovipositor with a pair of piercing valves, each with an elongate cutting edge, resulting in characteristic, delicate paired incisions (see "New DTs").

Definition. DT292 consists of a distinctive oviposition lesion characterized by a single occurrence of two small, slit-like, lenticular, parallel lesions that indicate a unique ovipositor structure. The lesions occur on surface tissue of foliage such as conifer needles, away from major veins. Each lesion is about 0.2 mm long, formed from a doublet of the two parallel, elongate incisions surrounded by a circular to broadly ellipsoidal to squarose field of altered tissue about 0.5–0.7 mm in maximum dimension and, in turn, surrounded by a subtle, depressed, discolored reaction zone.

Host plants and organs. Jehol: No associations. Yanliao: DT292 is associated with surface tissues of the bennettitaleans *A. kornilovae*, on leaves, and *P.* cf. *majus*, on leaves, and especially the conifer *Y. sinensis* (fig. 14*C*–14*F*), on needle leaves. Beipiao: No associations.

Inferred ovipositor. Ovipositor morphotype B.

Inferred insect culprits. Culprits for this ovipositing clade are Blattodea clades †Raphidiomimidae (*Divocina*, *Fortiblatta*) and †Caloblattinidae (*Colorifuzia*). It also is probable that currently undocumented mid-Mesozoic representatives of treehoppers (Hemiptera: Membracidae) similar to modern *Enchenopa*, *Stictocephala*, and related taxa may have made this stereotypical damage, resembling the damage of these modern analogues (Sorenson 1928; Armstrong et al. 1979).

Modern ecological analogue. Very similar ovipositional damage is made by the planthopper, *Taosa longula* Remes Lenicov (Hemiptera: Dictyopharidae), on common water hyacinth, *Eichhornia crassipes* (Mart.) Solms (Pontederiaceae), from Argentina (Remes Lenicov and Hernández 2010, fig. 6*d*, p. 339). The structural similarity between DT292 and its modern analogue is a level 1 match.

Oviposition DT293. DT293 is a distinctive ovipositional pattern of approximately eight scars probably made by an odonatan, such as a damselfly, based on the pattern of occurrence on the leaf surface. The position of a row of oviposition lesions oriented side by side scars adjacent the midrib of a large, pinnate bennettitalean frond suggests anchorage of the insect fabricator's body to the midrib and movement of the entire abdomen of the ovipositing insect incrementally to scarify the surface and insert eggs into deeper tissue. This latest Middle Jurassic occurrence is the earliest example of DT293 (see "New DTs").

Definition. DT293 is a linear series of side-to-side-placed lesions, in which adjacent lesions are separated by narrow, submillimeter-long intervening spaces. The row of lesions occurs about 1.0–1.5 mm from the edge of the frond midrib at the pinnular bases, where each adjacent pinnule contains from one to three lenticular to elliptical-shaped lesions, each of which is encircled by a thick callus. Each lesion occurs parallel to venation and individually ranges from 1.5–2.0 mm wide to 2.5–4.0 mm long. The entire ensemble consists of a linear row of approximately 10 ovipositional scars.

Host plants and organs. Jehol: No associations. Yanliao: DT293 is associated with surface and deep tissues of the nilssonialean *Nilssonia compta* (Phillips) (fig. 14*H*–14*O*), on pinnular bases of a large leaf. Beipiao: No associations.

Inferred ovipositor. Ovipositor morphotype A.

the template in *J*, showing a cluster of 13 lesions across four costal fields. *L*, DT101 on the nilssonialean *Baikalophyllum lobatum* (CNU-PLA-NN-2009364c, Liutiaogou). *M*, Enlargement of DT101 from template in *L*, showing a black ellipsoidal central structure, a surrounding zone of disturbed tissue, and outer scar tissue lodged between adjacent primary veins. *N*, DT100 on *Ginkgoites huttonii* (CNU-PLA-NN-2011383, Daohugou 2). *O*, Enlargement of DT100 from the template in *N*, showing a separated cluster of nine lesions occupying three costal fields. *P*, Further enlargement of the bottom cluster from the template in *O*, showing oviposition details. *Q*, DT100 on *Ginkgoites huttonii* (CNU-PLA-NN-2009629c, Daohugou 2), showing a cluster of approximately 40 lesions across nine costal fields. *R*, Four isolated DT101 lesions on a *Pterophyllum majus* pinnule (CNU-PLA-NN-2005019, Daohugou 2). Note avoidance of primary pinnule veins. Scale bars: vertically striped = 0.1 mm; solid white or black = 1.0 mm; back-slashed = 10.0 mm.

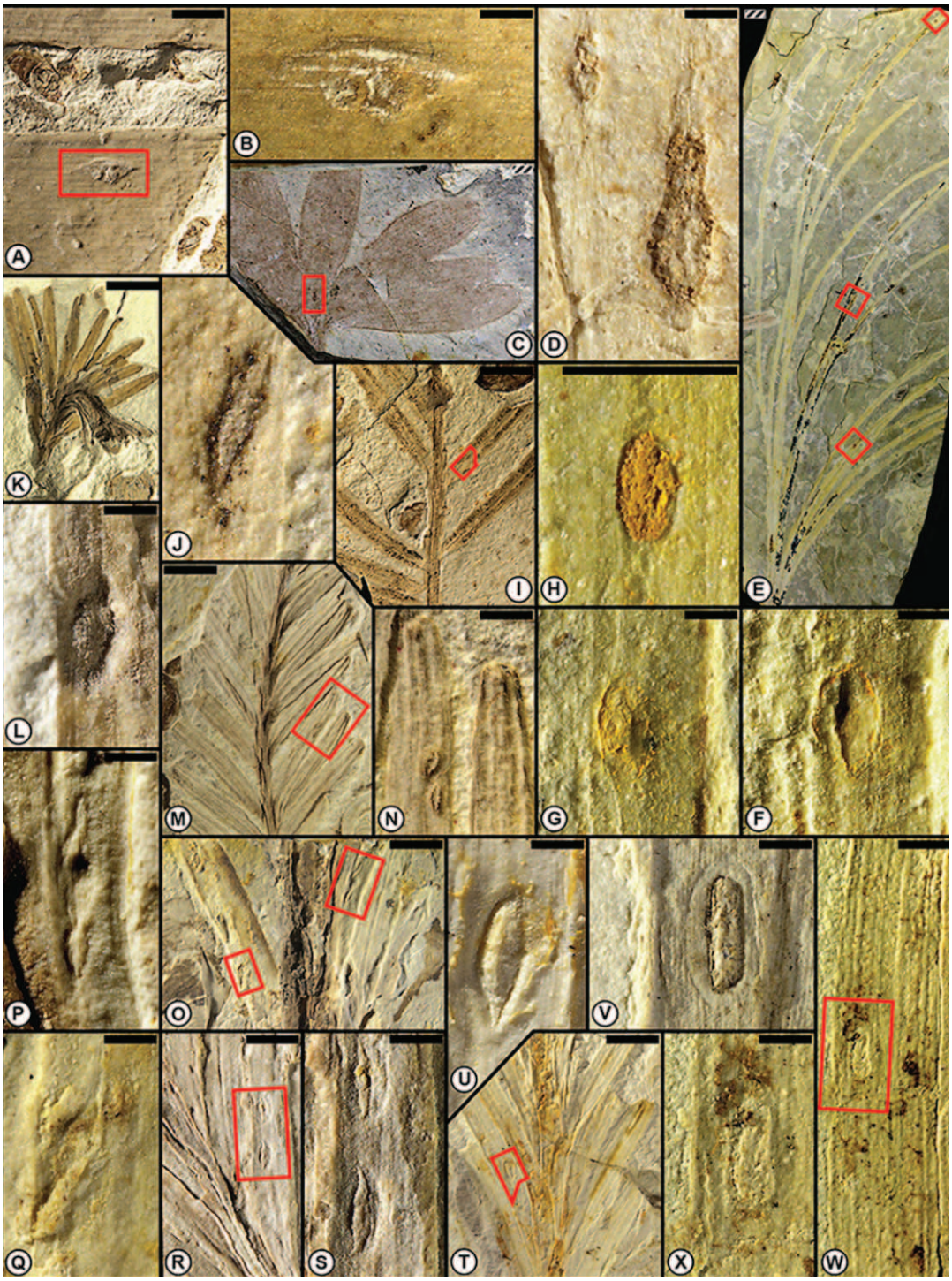

Fig. 12 Oviposition damage of DT101 on conifer foliage from the mid-Mesozoic of northeastern China. *A*, Oviposition of DT101 paralleling the primary veins of *Pterophyllum majus* (CNU-PLA-NN-2009805p, Daohugou 1). *B*, Enlargement of DT101 from the template in *A*, showing lenticular outline, malformed inner tissue, and a possible egg insertion site. *C*, DT101 on *Ginkgoites huttonii* (CNU-PLA-NN-2010396, Daohugou 2). *D*, Two DT101 oviposition marks indicted by the template at *C*; each is located on a primary vein, contains significant malformed tissue, and has a centrally placed egg insertion site. *E*, The czekanowskialean ginkgophyte *Solenites orientalis* (CNU-PLA-NN-2009925p, Liutiaogou) with DT101. *F*, DT101 from center-right template in *E*, showing broad, ovoidal shape of this oviposition type. *G*, Another very similar DT101 from the upper-right template in *E*. *H*, A third similar broadly ellipsoidal DT101 from the lower-right template in *E*, displaying bulbous tufts of teratologic tissue. *I*, DT101 on the conifer *Pityophyllum* cf. *nordenskioldi* (CNU-PLA-NN-2009468p, Daohugou 1). *J*, Enlargement of a DT101 lesion along the leaf margin from the template in *I*, showing an incision inclined to venation. *K*, DT101 on *Yanliaoa sinensis* (CNU-PLA-NN-2008566, Daohugou 1), consisting of a branchlet terminus. *L*, Enlargement of DT101 from a template in *K*, showing

Inferred insect culprits. Culprits for this ovipositing clade are Odonata clades †Campterophlebiidae (*Bellabrunetia*) and †Nodalulaidae (*Nodalula*; Fleck and Nel 2002; Lin et al. 2007).

Modern ecological analogue. There is no verified modern ecological analogue for DT293, indicating level 4, or the absence of an association.

New DTs

Fifteen DTs are attributable to insect oviposition from the three mid-Mesozoic deposits of northeastern China. In the course of examining fossil specimens, we found three new oviposition types: DT226, DT292, and DT293. Below, we provide documentation that summarizes the occurrence, associational relationships, ichnotaxonomic placement, modern ecological analogue, and other features of the three DTs. These new data will be added as new entries to version 4 of the forthcoming *Guide to Insect (and Other) Damage Types on Compressed Plant Fossils*, the succeeding volume to Labandeira et al. (2007).

New Damage Type DT226. *Description*. DT226 consists of a round cratered lesion on a primary vein or stem, 0.5–1.5 mm in diameter, with an encircling deep sulcus penetrating into subdermal tissue and an innermost, central, prominently raised plug of disorganized tissue. The circular lesion has surrounding scar tissue, a subtle, outermost bordering zone with a differently appearing tissue, marked by the deflection and subsequent rejoining of surrounding vasculature around the lesion. Some lesions typically occur as an interrupted row along the midrib.

Holomorphotype specimen for DT226. Figure 9*G* and 9*H* (CNU-PLA-NN-2006913p/c) of this article.

Functional feeding group. Oviposition.

Ichnotaxonomy. *Costaveon* cf. *adnatum* Krassilov (Krassilov et al. 2008).

Specialization level. 3.

Host plant. *Anomozamites villosus* Pott, McLoughlin, Wu and Friis (Williamsoniaceae) (Pott et al. 2012).

Inferred culprit. The ovipositor morphotype for DT226 damage was of short length, 1–3.5 mm long and straight, gracile, circular in cross section, and ending in an acute or acuminate terminus. There are 15 late Middle Jurassic sympatric taxa whose ovipositor morphology is consistent with the fabrication of DT226. Representative taxa include *Curvicaudus ciliatus* (Hemiptera: †Vetanthocoridae), *Xyelocerus diaphanus* Rasnitsyn, 1968 (Hymenoptera: †Xyelotomidae), and *Isoxyela rudis* Zhang et Zhang (Hymenoptera: Xyelidae) (Zhang and Zhang 2000). A very similar convergent ovipositor lesion is made by the Mexican boll weevil *Anthonomus grandis* Boheman (Coleoptera: Curculionidae) on cotton *Gossypium hirsutum* L. (Malvaceae). However, the organ of host plant penetration is the rostrum, with a circular cross section, and not the ovipositor, which is an egg-laying but not a penetrative organ in weevils.

Occurrences. Yixian Formation, Liutiaogou locality, Liaoning Province, northeastern China, and the Jiulongshan Formation, Daohugou 2 locality, Inner Mongolia Autonomous Region, northeastern China.

Figured specimens. Other than the holotype, the following specimens are illustrated: CNU-PLA-NN-2006921, from Daohugou 2, on *A. kornilovae* (fig. 6*E*, 6*F*); CNU-PLA-NN-2009267p, from Liutiaogou, on *Equisetites longivaginatus* (fig. 9*A*–9*D*); CNU-PLA-NN-2006921, from Daohugou 2, on *A. kornilovae* (fig. 9*E*, 9*F*); CNU-PLA-NN-2006237, from Daohugou 2, on *A. angustifolium* (fig. 9*I*–9*K*); CNU-PLA-NN-2010699, from Daohugou 1, on *A. sinensis* (fig. 9*L*–9*O*); CNU-PLA-NN-2009822, from Daohugou 1, on *Nilssoniopteris* sp. (fig. 9*P*, 9*Q*); and CNU-PLA-NN-2010223p, from Liutiaogou, on *L. boii* (fig. 9*R*–9*T*).

Remarks. With the exception of the considerably more abundant DT101 and the slightly more abundant DT72, the ovipositor-affiliated DT226 has one of the most eclectic host plant preferences of any DT in the broader mid-Mesozoic data set (table 3). The abundance of DT226 in the Yanliao Biota and other circular oviposition lesions are belied by their general absence elsewhere in the fossil record. One extensive review (Gnaedinger et al. 2014) lists two relevant examples from 42 provided, of oviposition lesions that are circular in surface appearance. One example of such oviposition is from the Barakar Formation from the early Permian of India that includes lesions that are apparently circular to very broadly ovate in surface view (Srivastava and Agnihotri 2011). These DT226-like occurrences are found on *Glossopteris indica* Schimper but on a leaf lamina rather than a midrib. DT226 also occurs in other recently evaluated floras from the late Permian of South Africa. The second example is *Paleoovoidus megaovoidius* Gnaedinger, Adami-Rodrigues et Gallego, hosted by *Equisetum nuwejaarensis* Anderson et Anderson, from the Late Triassic of South Africa (Labandeira 2006*b*; Anderson and Anderson 2018). These disparate occurrences in time and space indicate that ovipositors with circular cross-sectional areas were of sufficient length to penetrate the vascular and structural tissues in midribs of various unrelated plant hosts, including horsetails and glossopterid and bennettitalean seed plants.

prominent reaction rim scar. *M*, Several narrowly lenticular examples of DT101 on *Y. sinensis* (CNU-PLA-NN-2005389, Daohugou 1). *N*, Enlargement of DT101 from the template in *M*, exhibiting two oviposition marks wedged between major veins and with prominent outer scars. *O*, DT101 on *Y. sinensis* (CNU-PLA-NN-2006112, Daohugou 1), with three prominent DT101 occurrences on the upper-left leaf. *P*, Enlarged view of DT101 from the center-right template in *O*, showing acuminate ends of ovipositor sliced foliar tissue. *Q*, Enlarged view of DT101 from the lower-left template in *O*, revealing the same pattern in *P*. *R*, DT101 on another *Y. sinensis* (CNU-PLA-NN-2008480, Daohugou 1). *S*, Two elongate DT101 oviposition lesions from the template in *R*, showing acuminate ends and a surrounding zone indicating a plant response. *T*, DT101 on *Y. sinensis* (CNU-PLA-NN-2009420p, Daohugou 1). *U*, A distinctive DT101 scar outlined in the template in *T*, showing a broad reaction rim spanning most of the leaf blade width. *V*, A stereotypical DT101 oviposition scar on *Liaoningocladus boii* (CNU-PLA-NN-2010149p, Dawangzhangzi), reproduced from Ding et al. (2014). *W*, DT101 on *L. boii* (CNU-PLA-LL-2010388, Dawangzhangzi). *X*, Enlargement of the DT101 lesion from the template in *W*, very similar in structure to the lesion in *V* on the same host. Scale bars: vertically striped = 0.1 mm; solid white or black = 1.0 mm; back-slashed = 10.0 mm.

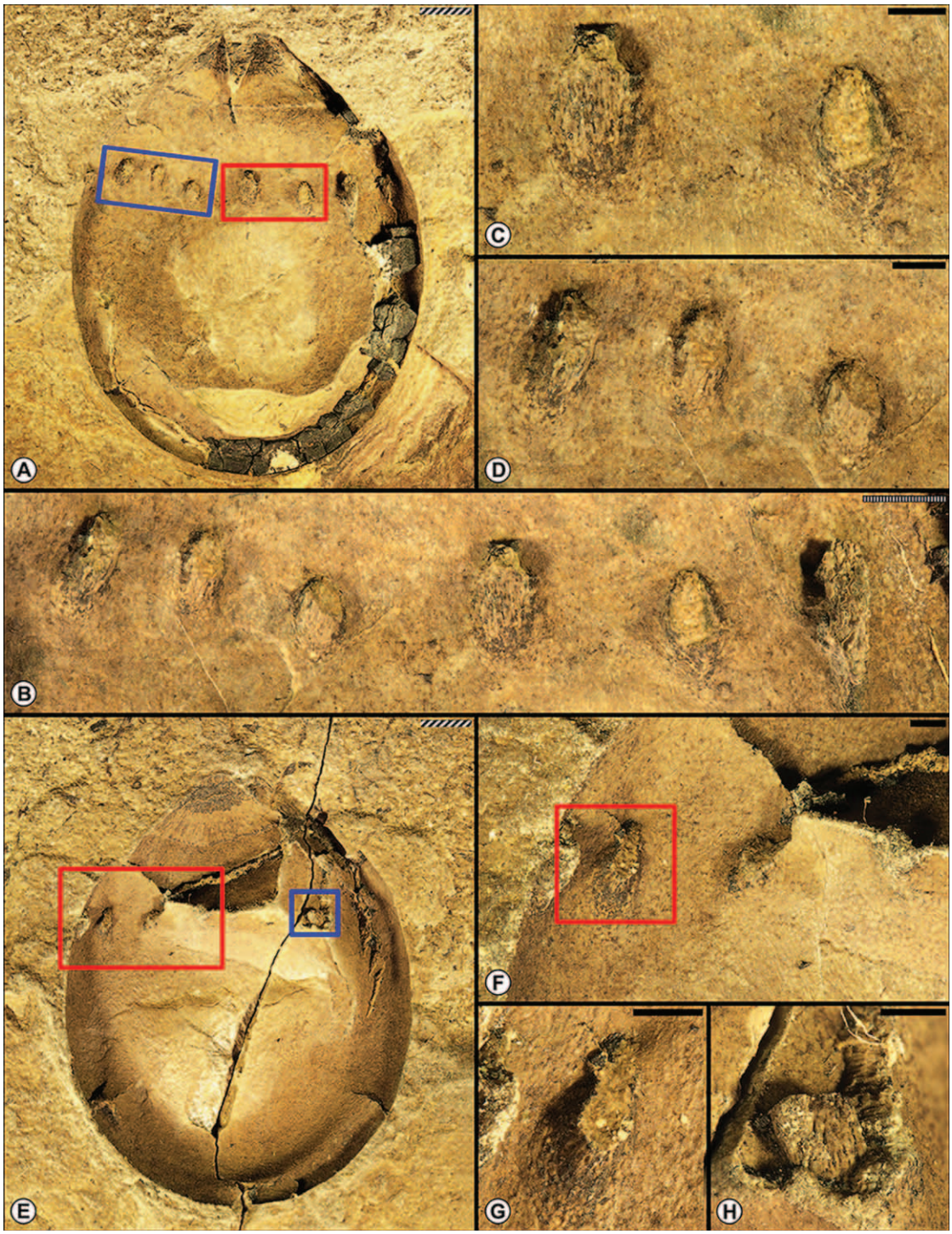

Fig. 13 Oviposition damage of DT272 on a *Yimaia capituliformis* ovule from the mid-Mesozoic of northeastern China. *A*, Entire ovule with the fleshy outer ovulate coat compressed as a black carbonized zone along the margin (CNU-PLA-NN-2011663p). *B*, Enlargement of all oviposition lesions occurring on the part. *C*, Enlargement of two oviposition lesions occurring on the part, denoted in *A* as a red rectangle. *D*, Enlargement of three oviposition lesions occurring on the part, denoted in *A* as a blue rectangle. *E*, Entire ovule with the fleshy outer seed coat compressed as a black carbonized zone along the margin (CNU-PLA-NN-2011663c). *F*, Enlargement of three oviposition lesions occurring on the counterpart, denoted in *E* as a red rectangle. *G*, Enlargement of an oviposition lesion occurring on the counterpart, denoted in *F* as a red rectangle. *H*, Enlargement of an oviposition lesion occurring on the counterpart, denoted in *E* as blue rectangle. See Meng et al. (2017) for additional details regarding this interaction. Scale bars: solid black = 0.5 mm; vertically striped = 1 mm; back-slashed = 2 mm.

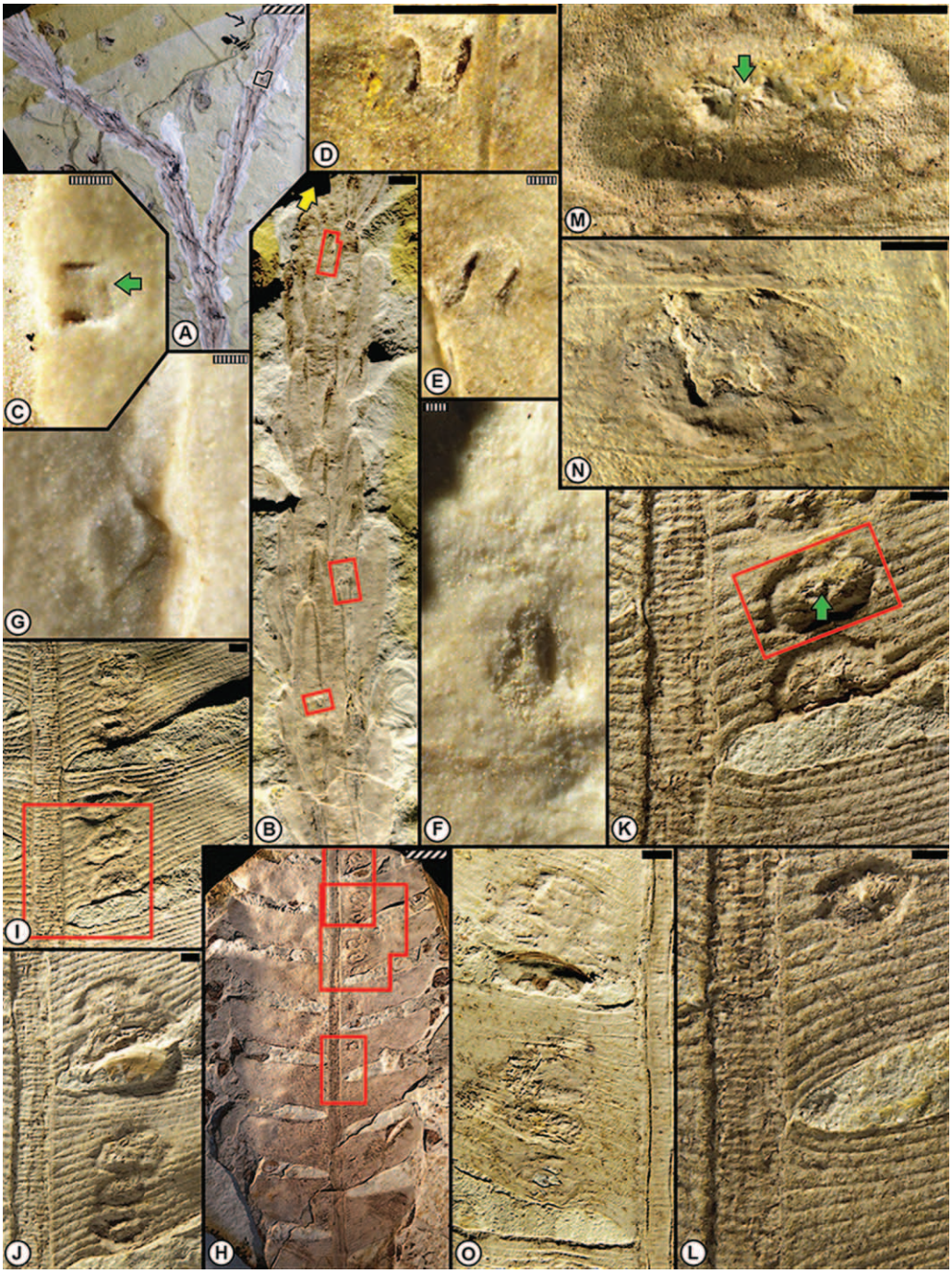

Fig. 14 New oviposition damage types DT292 (*A*–*G*) and DT293 (*H*–*O*) on two gymnosperm species from the mid-Mesozoic of northeastern China. *A*, New oviposition DT292 on the conifer *Yanliaoa sinensis* (CNU-PLA-NN-2009797p, Daohugou 1). *B*, Enlargement of the branch section at the upper right in *A* that harbors four occurrences of DT292. *C*, The distinctive DT292 lesion with two parallel incisions occurs beyond the branchlet tip in *B*, indicated by the yellow arrow. *D*, A second example of the DT292 lesion, occurring in the bottommost template in *B*. *E*, A third DT292, present in one of the upper templates in *B*, that overlaps below that of the template for *F*. *F*, A fourth example of DT292, occurring in the uppermost template in *B*. *G*, A probable DT292 from template at the upper-right template in *A*. *H*, New oviposition DT293 on the nilssonialean *Nilssonia compta* (CNU-PLA-NN-2009487p, Daohugou 1). *I*, Enlargement of the central six-sided template in *H*, showing the essential feature of multiple lesions at the base of adjacent pinnules. *J*, Enlargement of the uppermost template in *H*, demonstrating continuation of the series of lesions along the bases of three successive pinnules. *K*, Enlargement of the template at *I*, showing three successive oviposition marks, with the middle one displaying reaction tissue (green arrow), detailed in *M*. *L*, Enlargement of the lowermost template in *H*, showing an isolated lenticular lesion. *M*, Enlargement of the lesion in *K*, showing radiating files of proliferating tissue at the green arrow. *N*, Enlargement of a lesion on the counterpart of *O*. *O*, Section of the more poorly preserved counterpart (CNU-PLA-NN-2009797c), showing approximately three lesions. Scale bars: vertically striped = 0.1 mm; solid white or black = 1.0 mm; back-slashed = 10.0 mm.

New Damage Type DT292. *Description*. DT292 consists of a distinctive oviposition lesion characterized by a single occurrence of two small, slit-like, lenticular, parallel lesions that indicate a unique ovipositor structure. The lesions occur on surface tissue of foliage such as conifer needles, away from major veins. Each lesion is about 0.2 mm long, formed from a doublet of two parallel, elongate incisions surrounded by a circular to broadly ellipsoidal to squarose field of altered tissue about 0.5–0.7 mm in maximum dimension and, in turn, surrounded by a subtle discolored reaction zone.

Holomorphotype specimen for DT292. CNU-PLA-NN-2009797p/c (fig. 14*A*, 14*B*, 14*D*–14*F*).

Functional feeding group. Oviposition.

Ichnotaxonomy. No ichnotaxonomic designation exists for DT292.

Specialization level. 1.

Host plant. *Yanliaoa sinensis* Pan emend. Tan, Dilcher, Wang, Zhang, Na, Li, Li et Sun (Pan 1977; Tan et al. 2018).

Inferred culprit. A robustly constructed ovipositor that was medium in length and circular in cross section likely produced this type of oviposition. Probable late Middle Jurassic sympatric candidates for this type of oviposition were the cockroaches *Divocina noxi* (Liang et al. 2012) and *Fortiblatta cuspicolor* (Liang et al. 2009) (Blattodea: †Raphidiomimidae) and *Colorifuzia agenora* (Blattodea: †Caloblattinidae) (table 3). This distinctive type of oviposition evidently does not occur in modern plants, although there is a resemblance to oviposition scarring by *Lestes sponsa* Hansemann (Odonata: Lestidae) on rush *Juncus* sp. (Juncaceae) (Hellmund and Hellmund 2002*b*). Similarities also exist between DT292 and ovipositional damage made by *Taosa* dictyopharid planthoppers on pontederiaceous *Eichhornia* water hyacinth (Remes Lenicov and Hernández 2010).

Occurrence. Jiulongshan Formation, Daohugou 1 locality, Inner Mongolia Autonomous Region, northeastern China.

Figured specimen. The only figured specimen bearing distinctive DT293 is CNU-PLA-NN-2009797p, the holomorphotype (fig. 14*A*–14*G*).

Remarks. DT292 represents a unique style of ovipositional damage that likely was confined to the cockroach lineages of Raphidiomimidae and Caloblattinidae (table 3). These three lineages bore very stout, triangular ovipositors from 0.5 to 2.0 mm in length, characterized by two separate valves, each with a terminus for penetrating plant surface tissue, characterized as morphotype B (fig. A2*A*, A2*B*, A2*E*). The termini of these ovipositor valves match the double lesion damage of DT292. Notably, morphotype B and associated DT292 damage are very different from the gracile, linear, and much longer ovipositors of other related lineages of Mesozoic Blattodea, such as some Raphidiomimidae, Fuziidae, and possibly Mesoblattinidae. These latter lineages bore morphotype C that were gracile, linear, circular in cross section, and up to 20 mm long (Vishniakova 1968; Ren 1995). These lineages did not bear oothecae (Gao et al. 2018) but rather oviposited into plant tissues by retaining the ancient condition penetrating into plant tissues with stylate ovipositors circular in cross section. In contrast to the long ovipositors borne by some ovipositor-bearing lineages (fig. A2*C*, A2*D*, A2*F*), the shallow, truncate ovipositors of some Raphidiomimidae and Caloblattinidae (fig. A2*A*, A2*B*, A2*E*) provided DT292 damage to surface tissues that likely represents an extinct oviposition DT confined to certain Mesozoic blattodean lineages. However, some modern broad-headed bugs (Hemiptera: Alydidae) may produce similar lesions based on an ovipositor structure (Ventura and Panizzi 2000) similar to morphotype B, a lineage whose presence is recorded in the mid-Mesozoic (Yao et al. 2008).

New Damage Type DT293. *Description*. DT293 is a linear series of side-to-side placed lesions, in which adjacent lesions are separated by narrow, submillimeter-long intervening spaces. The row of lesions occurs about 1.0–1.5 mm from the edge of the frond midrib at the pinnular bases, where each adjacent pinnule contains from one to three lenticular to elliptical-shaped lesions, each of which is encircled by a thick callus. Each lesion occurs parallel to venation and individually ranges from 1.5–2.0 mm wide to 2.5–4.0 mm long. The entire ensemble consists of a linear row of approximately 10 ovipositional scars.

Holomorphotype specimen for DT293. CNU-PLA-NN-2009487p/c (fig. 14*H*–14*O*).

Functional feeding group. Oviposition.

Ichnotaxonomy. *Paleoovoidus* cf. *megaovoidius* Gnaedinger, Adami-Rodrigues and Gallego (Gnaedinger et al. 2014).

Specialization level. 1.

Host plant. *Nilssonia compta* (Phillips) Brongniart (Nilssoniaceae) (Brongniart 1828).

Inferred culprit. We infer that this type of oviposition was made by an odonatan bearing a linear, highly tapering ovipositor of medium length, approximately 10 mm long, and consisting of an acute, blunt terminus characteristic of ovipositor morphotype A. The likely late Middle Jurassic sympatrically occurring candidates were *Bellabrunetia catherinae* (Fleck and Nel 2002) (†Campterophlebiidae) and *Nodalula dalinghensis* (Lin et al. 2007) (†Nodalulaidae). Modern oviposition resembling DT293 plant damage is produced by the predaceous diving beetle *Colymbetes fuscus* L. (Coleoptera: Dytiscidae) ovipositing on great spearwort *Ranunculus ligua* (Ranunculaceae) (Wesenberg-Lund 1943), although this match is inexact.

Occurrence. Jiulongshan Formation, Daohugou 1 locality, Inner Mongolia Autonomous Region, northeastern China.

Figured specimen. The only specimen bearing distinctive DT293 is CNU-PLA-NN-2009487, the holomorphotype (fig. 14*H*–14*O*).

Remarks. The distinctiveness of DT293 is matched closely in the fossil record by *P. megaovoidius* (Gnaedinger et al. 2014), a prominent pattern of oviposition on *Taeniopteris* sp. B, from the Las Breas Formation, Upper Triassic of Elqui Province of Chile (Gnaedinger et al. 2014). Features in common are the single row of similarly positioned oviposition lesions oriented lengthwise and parallel to the leaf blade venation adjacent to the leaf midrib. The host plant, *Taeniopteris* sp. B, is a robust leaf of very similar structure to *N. compta* that bears DT293. Oviposition similar to DT293 could not be found in other host plants upon an examination of mid-Mesozoic oviposition literature. Consequently, DT293 may represent a past interaction between an extinct odonatan lineage and extinct groups of plant hosts with large, robust, pinnately veined leaves, such as the nilssonialean *Nilssonia* and a possible pentoxylalean that bears *Taeniopteris*-like leaves (Anderson and Anderson 2003; Taylor et al. 2009). Alternatively, DT293 may currently exist but remains undiscovered or has not been recognized formally in the literature.

Discussion

The study of insect use of plants in the fossil record overwhelmingly has been the study of herbivory and, to a much lesser extent, examinations of pollination (Labandeira 2006*a*, 2013). Notably fewer accounts have considered oviposition as a source of data for understanding how insects use plants as resources in deep time (Scheirs and De Bruyn 2002). Just as arthropod terrestrial herbivores consume plants on a dietary spectrum from polyphagy (host generalization) to monophagy (host specialization), patterns of ovipositor structure and ovipositional damage on plants reveal that there are analogous plant preferences (Guido and Perkins 1975; Thompson and Pellmyr 1991; Singer 2004; Matushkina and Gorb 2007). These predispositions can take the form of egg-laying habits that target certain host plant taxa (Resetarits 1996; Ventura and Panizzi 2000), the exophytic versus endophytic oviposition mode (Liebermann 1957; Hilliard 1982; Turk 1984), or the choice of a particular plant internal tissue for promoting ideal egg development (Waage 1987; Singh and Singh 2005). These options are tempered by negative feedback that affects the ovipositing insect, such as the production of wound-induced volatile compounds by the plant host, which attract parasitoids that decrease the fitness of the ovipositing insect (Renwick 1989; Meiners and Hilker 2000; Hilker et al. 2005). There is evidence for understanding some of these features of oviposition biology in the results from our study of the mid-Mesozoic Jehol, Yanliao, and Beipiao Biotas of northeastern China.

For the Jehol Biota, the most important associations were DT101 and DT175, present on the broad-leaved conifer *Liaoningocladus boii* (figs. 3*A*, 4*A*; tables 2, A1). Including a few other minor oviposition associations, *L. boii* was the recipient of 41.7% of all Jehol oviposition activity (fig. 4*A*; table A1). Of all oviposition interactions in the total data set, the *Liaoningocladus*-DT101 relationship was only the sixth-most intensely ranked interaction (table 2). *Liaoningocladus boii* also was a major host to herbivores (Ding et al. 2015), such as leaf miners (Ding et al. 2014) and gallers (C. C. Labandeira, personal observation). Considering the Jehol Biota as a whole, DT101 and DT175 attack overwhelmingly was directed toward *L. boii* (figs. 3*A*, 3*B*, 4*A*; table A1), constituting 56.7% of all oviposition interactions for these two DTs. Interactions DT101 and DT175 were linked to ovipositor morphotypes C and G that were induced by an assemblage of hemipteran insects (fig. 4*A*; tables 3, A1). These insects mostly included the families Procercopidae, Rhopalidae, Vetanthocoridae, Dehiscensicoridae, Cydnidae, and Venicoridae. Collectively, these relationships indicate that *L. boii* housed the most diverse component community (Futuyma and Mitter 1996) of ovipositing insects and probably herbivores in the Jehol Biota (Ding et al. 2015). Jehol plant hosts with the next most diverse associations were the two *Equisetites* horsetail species (fig. 4*A*; table A1). The two *Equisetites* horsetails had 13 oviposition associations, 10 of which were DT72 (figs. 3*A*, 3*B*, 4*A*; table A1), accounting for 21.7% of all Jehol oviposition activity, about half the value of *L. boii*, and ranking tenth of all mid-Mesozoic interactions (table 2). The comparatively high rates of oviposition on Yixian *Equisetites* are not attributable to elevated specimen abundances and are supported by a rank of tenth in overall frequency for the *Equisetites*-DT72 interaction. Data for other oviposition associations were minor and apparently unimportant. Although about half of all examined Jehol species were conifers, the data point to *L. boii* as the most heavily targeted taxon and *Equisetites* horsetails as the secondarily most used taxon. Based on photographic detail of the oviposition lesions (figs. 5*J*–5*L*, 8*S*, 8*T*, 9*R*–9*T*, 12*W*, 12*Y*), stem epidermal and vascular tissue was accessed, as was foliar epidermal, mesophyll, and vascular tissue, indicating significant ovipositional penetration of tissues. The presence of *L. boii* as the single most oviposited and likely herbivorized plant suggests that this conifer (Tan et al. 2018) played a central role in plant-insect associations in at least some locales of the Jehol Biota. For the Jehol Biota, the evidence strongly indicates that ovipositing insects were partitioning their plant resource world by taxon, organ, and tissue, analogous to the modern condition.

The Yanliao Biota represents about twice the number of examined plant specimens, 13 times the number of DTs of total herbivory, and about five times the number of DTs of oviposition compared to the Jehol Biota (tables 1, A1, A2). By every index we have used, bennettitalean taxa, in particular, several species of *Anomozamites*, overwhelmingly had the highest frequency of ovipositional damage throughout the larger data set (fig. 4; tables A1–A3). In rank order, four of the five most heavily attacked taxa by ovipositing insects in the Yanliao Biota were four species of *Anomozamites*—*A. kornilovae* (45 DTs), *A. villosus* (42 DTs), *A. sinensis* (35 DTs), and *A. angustifolium* (15 DTs)—collectively representing 46.6% of all oviposition interactions (figs. 3*C*, 4*B*; tables 2, A2). The overwhelming amounts of oviposition DTs responsible for elevated *Anomozamites* damage were, in rank order, DT76, DT101, and DT226 (figs. 3*C*, 3*D*, 4*B*; table A2). For rank order of the 16 most frequent associations in the total data set (table 2), the *Anomozamites*-DT76 interaction prominently ranked first and represented 40.1% of all interactions, the *Anomozamites*-DT101 interaction ranked third and represented 7.4%, and the *Anomozamites*-DT226 interaction ranked fifth and represented 5.1%. The collective representation of these three *Anomozamites* associations constituted 52.6% of the 16 most highly ranked associations in the total data set (table 2). Three other Yanliao bennettitalean interactions, the *Pterophyllum*-DT76, *Pterophyllum*-DT101, and *Nilssoniopteris*-DT75 interactions, ranking seventh, eighth, and fifteenth, respectively (table 2), collectively contributed an additional 10.6%, representing a cumulative contribution of 63.2% for the top 16 ovipositional associations in the total data set that were attributable to Yanliao bennettitaleans. The principal DT spectrum harbored by *Anomozamites* was predominantly DT76 and secondarily DT101 and DT226 (figs. 3*D*, 4*B*; tables 2, A2). These data indicate that *Anomozamites* in particular and bennettitaleans in general were overwhelmingly the principal targets of ovipositing insects. The herbivore targeting of bennettitaleans, such as *Anomozamites* taxa, remains enigmatic, although in angiosperms the connection between pollinator and herbivore networks on the same plant species promotes broader community stability (Sauve et al. 2016).

A broad spectrum of insect herbivores were using bennettitalean tissues. Associated with DT76 were ovipositor morphotypes D and E (table 3). Both morphotypes involved prophalangopsid orthopterans, chresmodid archaeorthopterans, and, more sporadically, procercopid, tettigarcitid, and cixiid hemipterans and xyelid hymenopterans (table 3). For DT101, associated

ovipositor morphotypes were C and especially G, which collectively were linked to a broad variety of insect taxa, typically procercopid, pachymeridiid, rhopalid, vetanthocorid, dehiscensicorid, cydnid, and venicorid hemipterans, as well as xyelid, daohugoid, and scoliid hymenopterans (table 3). This spectrum of ovipositor C, D, E, and G morphotypes indicates that bennettitalean foliar and stem tissues were probed and used by a wide variety of insects possessing different but deeply penetrating blade-like ovipositors that produced, for example, DT76 and DT101 damage patterns throughout stem and leaf tissues. One reason for the exceptionally high oviposition levels by the above taxa on bennettitaleans may have to do with their connection with pollination by groups such as long-proboscid Mecoptera (scorpionflies), Diptera (flies), and Neuroptera (lacewings; Ren et al. 2009; Labandeira 2010) and perhaps Lepidoptera (moths). It is possible that some of these pollinator groups would have had conspecific, externally feeding larvae present on the same hosts as the adult pollinators. This is a feature documented in modern cycad-weevil pollinator and herbivore interactions (Norstog and Nicholls 1997). Alternatively, some bennettitalean taxa, such as *A. villosus*, are well defended by spines (Pott et al. 2012) that would hinder foliar oviposition, a consequence that is contrary to the pattern seen in modern cycads and Yanliao bennettitaleans.

Two other plant hosts of the Yanliao Biota, the cupressaceous conifer *Yanliaoa sinensis*, and three taxa of the ginkgoalean *Ginkgoites* had subdominant levels of ovipositional damage that were important secondary recipients of insect egg laying. Contrary to the situation with bennettitalean oviposition, the DT frequencies of *Yanliaoa* and *Ginkgoites* were modest and their DT spectrum was somewhat different. The dominant pattern for *Yanliaoa* was DT76 (19 occurrences) and DT101 (11 occurrences), and species of *Ginkgoites* had DT101 (15 occurrences), DT137 (4 occurrences), and DT100 (3 occurrences). These data suggest lower levels of oviposition and a moderately different distribution of insects ovipositing on *Yanliaoa* and *Ginkgoites* than compared to those on *Anomozamites* (figs. 3*C*, 4*B*). The likely culprits for *Yanliaoa* and *Ginkgoites* were members that collectively possessed five different ovipositor morphotypes that inflicted four major DTs on their host plants (table 3). Significant remaining ovipositor-plant relationships in the Yanliao Biota may include the *Czekanowskia rigida* ginkgophyte and *Equisetites* horsetails, both with seven DTs. Remaining species and morphotypes of cycads, ginkgophytes, bennettitaleans, conifers, and undetermined plants exhibit a low level of oviposition activity. These data, again, indicate that ovipositing insects in the Yanliao Biota were intricately partitioning plant resources. Bennettitaleans were highly targeted, whereas conifers and ginkgophytes were moderately affected.

The sampled Beipiao Biota represents 22.5% that of the sampled Jehol Biota and 10.5% that of the sampled Yanliao Biota (table 1), indicating that inferences regarding oviposition are preliminary until sample size is substantively increased. Unfortunately, insect fossils are not known from the Beipiao Biota (Ren 1995), obviating the reconstruction of ovipositor morphotypes. Nonetheless, certain DT patterns do stand out. The spectrum of oviposition DTs on plants of the Beipiao Biota emphasizes cycad and fern foliage (figs. 3*E*, 4*C*; table A3), two plant groups that virtually are lacking as hosts to oviposition in the Yanliao and Jehol Biotas. The substantial amount of oviposition on ferns in the Beipiao Biota is at considerable variance with the lack of ferns as resources for oviposition in the subsequent Yanliao and Jehol Biotas, where they are common (Sun et al. 2001; Huang 2016). The reason for this underutilization is enigmatic but could involve the delicate and thin foliage of especially ground-dwelling ferns that would provide insufficient tissue support for oviposition (Boughton et al. 2011), or possibly the presence of major chemical deterrents to ovipositing insects (Smith et al. 2016). Additionally, the spectrum of damage is rather even across the plant groups compared to the two younger biotas. A point of similarity between the Beipiao Biota and its younger counterparts is the predominance of DT76 and the subordinate presence of DT101 (figs. 3*F*, 4*C*).

It appears that the Late Triassic spectrum of oviposition was much more eclectic and resulted in minimal targeting of particular plant hosts, a pattern that was reversed during the late Middle Jurassic with the overwhelming targeting of bennettitaleans and to a lesser extent conifers and ginkgophytes. The late Middle Jurassic pattern was followed by a shift toward elevated targeting of conifers and subordinately horsetails during the mid-Early Cretaceous. This time series of changing oviposition DT levels and the targeting of plant hosts resemble similar shifts in the extent of the herbivory spectra for broad-leaved conifers during the same three time slices (Ding et al. 2015). Although comprehensive arthropod herbivory studies are lacking, one task for future research would be a parallel examination to test the hypothesis that Beipiao cycads, Yanliao bennettitaleans, and Jehol conifers were the most highly herbivorized and targeted plant groups.

Summary

Several major points summarize this study on the ecology of insect ovipositor structure and vascular plant ovipositional damage for three slices of time during the Mesozoic of northeastern China. This study will require follow-up collections of fossil specimens and data analysis to further test some of the following conclusions.

1. *Testing hypotheses involving oviposition data from the fossil record*. The fossil record of oviposition offers a rich archive of data that can be extracted to understand how plant resources are used by egg-laying insects in deep time. This oviposition record of using host plant resource parallels the herbivory record, allowing one mode of host plant resource use to be applied as a test of the other mode.

2. *Raw data*. Vascular plant and associated insect fossils were examined for the Jehol Biota (Yixian Formation, mid-Early Cretaceous, ~125 Ma), consisting of 1817 specimens; the Yanliao Biota (Jiulongshan Formation, latest Middle Jurassic, ~165 Ma), consisting of 3886 specimens; and the Beipiao Biota (Yangcaogou Formation, Late Triassic, ~205 Ma), consisting of 408 specimens. The Beipiao Biota lacked insect fossils.

3. *Insect ovipositor morphotypes*. Ovipositors of insect specimens documented in the fossil insect literature that cooccurred in the Jehol and Yanliao Biotas provided structural features that were categorized into nine fundamental morphotypes. The greatest ovipositor diversity was Hymenoptera (morphotypes C, D, E, G, and I), which contrasted with the single ovipositor morphotypes present in Archaeorthoptera (morphotype E), Neuroptera (morphotype F), and Lepidoptera (morphotype H).

4. *Plant oviposition DTs*. Of all specimens examined, 60 specimens (16.0%) from the Jehol Biota, 296 (78.9%) from the Yanliao Biota, and 19 (5.1%) from the Beipiao Biota had oviposition lesions that were further analyzed. Fifteen identifiable DTs were distributed on horsetails, ferns, ginkgophytes, cycads, bennettitaleans, conifers, gnetophytes, and unaffiliated plants.

5. *Linkage of insect ovipositor morphotypes to plant oviposition DTs*. The nine basic ovipositor morphotypes were linked to 15 documented DTs on the basis of lesion features anatomically consistent with host plant damage patterns based on ovipositor structure. This procedure linked (i) the plant host, (ii) the DT interaction, and (iii) the ovipositor-bearing culprit insect.

6. *Patterns of oviposition targeting of plant groups*. Conifers, especially *Liaoningocladus boii* and subordinately horsetails were the most ovipositor-damaged groups in the Jehol Biota. By contrast, ovipositor-bearing insects in the Yanliao Biota overwhelmingly attacked bennettitaleans, particularly several species of *Anomozamites*. Subordinate levels of Yanliao oviposition were documented for the conifer *Yanliaoa* and ginkgophyte *Ginkgoites*. For the Beipiao Biota, cycad foliage and subordinately ferns received the highest oviposition, although sample size was low.

7. *An unanswered question*. Why were Yanliao Biota bennettitaleans highly targeted? The most notable feature of plant resource use among the three slices of time in northeastern China was the extensive oviposition on *Anomozamites* bennettitaleans in the Yanliao Biota, suggesting that other insect interactions, such as herbivory, may have had a promoting role.

Acknowledgments

Finnegan Marsh adeptly produced figures 2–12 and 14. This research is supported by grants from the National Natural Science Foundation of China (31730087, 41688103, and 31672323), Program for Changjiang Scholars and Innovative Research Team in University (IRT-17R75), and Support Project of High-Level Teachers in Beijing Municipal Universities in the Period of the 13th Five-Year Plan (IDHT20180518). Xiaodan Lin is supported by the Graduate Student Program for International Exchange and the Joint Supervision at Capital Normal University (028175534000). This is contribution 324 of the Evolution of Terrestrial Ecosystems consortium at the National Museum of Natural History in Washington, DC.

Literature Cited

Adami-Rodrigues K, R Iannuzzi, ID Pinto 2004*a* Permian plant-insect interactions from a Gondwana flora of southern Brazil. Foss Strat 51: 106–125.

Adami-Rodrigues K, PA Souza, R Iannuzzi, ID Pinto 2004*b* Herbivoria em floras Gonduânicas do Neopaleozóico: análise quantitative. Rev Bras Paleontol 7:93–102.

Anderson HM, JM Anderson 2018 Molteno sphenophytes: Late Triassic biodiversity I southern Africa. Palaeontol Afr 53:1–391.

Anderson JM, HM Anderson 2003 Heyday of the gymnosperms: systematics and biodiversity of the Late Triassic Molteno fructifications. National Botanical Institute, Pretoria, South Africa.

Armstrong JE, WH Kearby, EA McGinnes Jr 1979 Anatomical response and recovery of twigs of *Juglans nigra* following oviposition injury inflicted by the two-spotted treehopper, *Enchenopa biontata*. Wood Fiber 11:29–37.

Ash S 2005 A new Upper Triassic flora and associated invertebrate fossils from the basal beds of the Chinle Formation, near Cameron, Arizona. PaleoBios 25:17–34.

——— 2009 Late Triassic flora and associated invertebrate fossils from the beds of the Chinle Formation in Dinnebito Wash, east-central Arizona, USA. Palaeontogr Abt B 282:1–37.

Backus E 1985 Anatomical and sensory mechanisms of leafhopper and planthopper feeding behavior. Pages 163–194 *in* LR Nault, JG Rodriguez, eds. The leafhoppers and planthoppers. Wiley, New York.

Banerji J 2004 Evidence of insect-plant interactions from the Upper Gondwana Sequence (Lower Cretaceous) in the Rajmahal Basin, India. Gondwana Res 7:205–210.

Barker MS, SW Shaw, RJ Hickey, JE Rawlins, JW Fetzner Jr 2005 Lepidopteran soral crypsis on Caribbean ferns. Biotropica 37:314–316.

Beamer RH 1928 Studies on the biology of Kansas Cicadidae. Univ Kans Sci Bull 18:155–263.

Beattie R 2007 The geological setting and palaeoenvironmental and palaeoecological reconstructions of the Upper Permian insect beds at Belmont, New South Wales, Australia. Afr Invertebr 48:41–57.

Bechly G, C Brauckmann, W Zessin, E Gröning 2001 New results concerning the morphology of the most ancient dragonflies (Insecta: Odonatoptera) from the Namurian of Hagen-Vorhalle (Germany). J Zool Syst Evol Res 39:209–226.

Béthoux O, J Galtier, A Nel 2004 Earliest evidence of insect endophytic oviposition. Palaios 19:408–413.

Bogdanov-Kat'kov NN 1947 Guide for practical training in general entomology. Sel'khozgiz, Moscow. (In Russian.)

Boughton AJ, GR Buckingham, CA Bennett, R Zonneveld, JA Goolsby, RW Pemberton, TD Center 2011 Laboratory host range of *Austromusotima camptozonale* (Lepidoptera: Crambidae), a potential biological control agent of Old World climbing fern, *Lygodium microphyllum* (Lygodiaceae). Biocon Sci Tech 21:643–676.

Braker HE 1989 Oviposition on host plants by a tropical forest grasshopper (*Microtylopteryx hebardi*: Acrididae). Ecol Entomol 14:141–148.

Brongniart A 1828 Histoire des végétaux fossiles ou recherches botaniques et géologiques sur les végétaux renfermés dans les diverse couches du globe. 1st ed. Prodromus d'une histoire des végétaux fossiles. Dufour & d'Ocagne, Paris.

Bronstein JL, ed 2015 Mutualism. Oxford University Press, New York.

Bugdaeva EV 1983 A new leaf genus from the Cretaceous sediments of eastern Transbaikalia. Pages 44–47 *in* VA Krassilov, ed. Palaeobotany and phytostratigraphy of the Far East of the USSR. Akademia Nauk SSSR, Vladivostok.

Carbonell CS 1957 Observaciones bio-ecologicas sobre *Marellia remipes* Uvarov (Orthoptera, Acridioidea) en le Uruguay, con especial referencia a su modo de oviposition. Invest Estud Fac Hum Cienc Univ Repub Urug Biol 4:1–12.

Cariglino B 2018 Patterns of insect-mediated damage in a Permian *Glossopteris* flora from Patagonia (Argentina). Palaeogeogr Paleoclim Palaeoecol 507:39–51.

Cariglino B, PR Gutiérrez 2011 Plant-insect interactions in a *Glossopteris* flora from the La Golondrina Formation (Guadalupian-Lopingian), Santa Cruz Province, Patagonia, Argentina. Ameghiniana 48:103–112.

Carpenter FM 1970 Adaptations among Paleozoic insects. Pages 1236–1251 *in* EL Yochelson, ed. Proceedings of the First North American Paleontological Convention. Allen, Lawrence, KS.

Chaudonneret J 1990 Les Pieces Buccales des Insectes: Thème et variations. Berthier, Dijon.

Chen D, YZ Yao, D Ren 2015 A new species of fossil Procercopidae (Hemiptera, Cicadomorpha) from the Lower Cretaceous of northeastern China. Cretac Res 52:402–406.

Chen W, Q Ji, DY Liu, Y Zhang, B Song, XY Liu 2004 Isotope geochronology of the fossil-bearing beds in the Daohugou area, Ningcheng, Inner Mongolia. Geol Bull China 23:1165–1169.

Chew FS, RK Robbins 1984 Egg laying in butterflies. *In* RI Vane-Wright, PR Ackery, eds. The biology of butterflies. Symp R Entomol Soc Lond 11:65–79.

Childers CC 1997 Feeding and oviposition injuries to plants. Pages 505–537 *in* T Lewis, ed. Thrips as crop pests. CAB International, Wallingford.

Childers CC, DS Achor 1991 Feeding and oviposition injury to flowers and developing floral buds of "navel" orange by *Frankliniella bispinosa* (Thysanoptera: Thripidae) in Florida. Ann Entomol Soc Am 84:272–282.

Chisholm IF, T Lewis 1984 A new look at thrips (Thysanoptera) mouthparts, their action and effects of feeding on plant tissue. Bull Entomol Res 74:663–675.

Chopard L 1938 Les orthoptères qui se construisent un abri. Pages 126–138 *in* L Chopard, ed. La biologie des orthoptères. Lechevalier, Paris.

Constant B, S Grenier, G Febvay, G Bonnot 1996 Host plant hardness in oviposition of *Macrolophus caliginosus* (Hemiptera: Miridae). J Econ Entomol 89:1446–1452.

Corbet PS 1999 Dragonflies: behaviour and ecology of Odonata. Harley, Great Horkesley, UK.

Craig TP, JK Itami, PW Price 1988 Plant wound compounds from oviposition scars used in host discrimination by a stem galling sawfly. J Insect Behav 1:343–356.

Decaro Júnior ST, NM Martinelli, DHB MacCagnan, ESDBP Ribeiro 2012 Oviposition of *Quesada gigas* (Hemiptera: Cicadidae) in coffee plants. Rev Colomb Entomol 38:1–5.

Denno RF, HJ Dingle 1981 Considerations for the development of a more general life history theory. Pages 1–6 *in* RF Denno, HJ Dingle, eds. Insect life history patterns: habitat and geographic variation. Springer, New York.

Ding QH, LD Zhang, SZ Guo, CJ Zhang, YD Peng, B Jia, SW Chen, DH Xing 2003 Study on the paleoecology of Yixian Formation in Beipiao area, western Liaoning Province, China. Geol Resour 12:9–18.

Ding QL, CC Labandeira, QM Meng, D Ren 2015 Insect herbivory, plant-host specialization and tissue specialization and tissue partitioning on mid-Mesozoic broadleaved conifers of northeastern China. Palaeogeogr Palaeoclimat Palaeoecol 440:259–273.

Ding QL, CC Labandeira, D Ren 2014 Biology of a leaf miner (Coleoptera) on *Liaoningocladus boii* (Coniferales) from the Early Cretaceous of northeastern China and the leaf-mining biology of possible insect culprit clades. Arthropod Syst Phylogeny 72:281–308.

Dong QP, YZ Yao, D Ren 2013 A new species of Progonocimicidae (Hemiptera, Coleorrhyncha) from the Middle Jurassic of China. Alcheringa 37:31–37.

Du SL, YZ Yao, D Ren 2016 New fossil species of the Venicoridae (Heteroptera: Pentatomomorpha) from the Lower Cretaceous of northeast China. Cretac Res 68:21–27.

Du SL, YZ Yao, D Ren, WT Zhang 2017 Dehiscensicoridae fam. nov. (Insecta: Heteroptera: Pentatomomorpha) from the Upper Mesozoic of northeast China. J Syst Palaeontol 15:991–1013.

Dwumfour EF 1992 Volatile substances evoking orientation in the predatory f1owerbug *Anthocoris nemorum* (Heteroptera: Anthocoridae). Bull Entomol Res 82:465–469.

Ellis WM 2018 Egg-oviposition within the leaf. https://bladmineerders.nl/introduction/mines/life-stages/egg/.

Feeny P, L Rosenberry, M Carter 1983 Chemical aspects of oviposition behavior in butterflies. Pages 27–76 *in* S Ahmed, ed. Herbivorous insects. Academic Press, New York.

Fleck G, A Nel 2002 The first isophlebioid dragonfly (Odonata: Isophlebioptera: Campterophlebiidae) from the Mesozoic of China. Palaeontology 45:1123–1136.

Forget PM, JE Lambert, PE Hulme 2004 Seed fate: predation, dispersal and seedling establishment. Commonwealth Agriculture Board International, London.

Freeman TP, JS Buckner, DR Nelson, CC Chu, TJ Henneberry 2001 Stylet penetration by *Bemisia argentifolii* (Homoptera: Aleyrodidae) into host leaf tissue. Ann Entomol Soc Am 94:761–768.

Friis EM, KR Pederson, PR Crane 2011 Early flowers and angiosperm evolution. Cambridge University Press, Cambridge.

Fulton BB 1915 The tree crickets of New York: life history and bionomics. N Y Agric Exp Stn Tech Bull 42:1–47.

Funkhouser WD 1917 Biology of the Membracidae of the Cayuga Lake basin. Cornell Univ Agric Exp Stn Mem 11:173–445.

Futuyma DJ, C Mitter 1996 Insect-plant interactions: the evolution of component communities. Philos Trans R Soc B 351:1361–1366.

Gallego J, RN Cúneo, I Escapa 2014 Plant-arthropod interactions in gymnosperm leaves from the Early Permian of Patagonia, Argentina. Geobios 47:101–110.

Gao TP, D Ren, CK Shih 2009*a* *Abrotoxyela* gen. nov. (Insecta, Hymenoptera, Xyelidae) from the Middle Jurassic of Inner Mongolia, China. Zootaxa 2094:52–59.

——— 2009*b* The first Xyelotomidae (Hymenoptera) from the Middle Jurassic in China. Ann Entomol Soc Am 102:588–596.

Gao TP, CK Shih, CC Labandeira, X Liu, ZQ Wang, YL Che, XC Yin, D Ren 2018 Maternal care by Early Cretaceous cockroaches. J Syst Palaeontol 17:379–391.

Gao TP, YY Zhao, D Ren 2011 New fossil Xyelidae (Insecta, Hymenoptera) from the Yixian Formation of western Liaoning, China. Acta Geol Sin 85:528–532.

Genç H 2016 Infestations of olive fruit fly, *Bactrocera oleae* (Rossi) (Diptera: Tephritidae), in different olive cultivars in Çanakkale, Turkey. Int J Agric Biosyst Eng 10:439–442.

Geyer G, KP Kelber 1987 Flügelreste und Lebensspuren von Insekten aus dem Unteren Keuper Mainfrankens. Neues Jarhb Miner Abh 174:331–355.

Givulescu R 1984 Pathological elements on fossil leaves from Chuizbaia (galls, mines and other insect traces). D S Inst Geol Geofiz 68:123–133.

Glime JM 2017 Terrestrial insects: Holometabola-Lepidoptera biology and ecology. Pages 12-13-1–12-13-32 *in* JM Glime. Bryophyte ecology. Vol 2. Bryophyte interaction. Michigan Technological University and the International Association of Bryologists. http://digitalcommons.mtu.edu/bryophyte-ecology2/.

Gnaedinger SC, K Adami-Rodrigues, OF Gallego 2007 Evidencias de trazas de oviposición de insectos (Odonata) en hojas del Triásico de Chile. Ameghiniana Suppl 44:94–95 (abstract).

——— 2014 Endophytic oviposition on leaves from the Late Triassic of northern Chile: ichnotaxonomic, palaeobiogeographic and palaeoenvironment considerations. Geobios 47:221–236.

Grauvogel-Stamm L, KP Kelber 1996 Plant-insect interactions and coevolution during the Triassic in western Europe. Paleontol Lomb 5:5–23.

Grunert H 1995 Eiblageverhalten und Substratnutzung von *Erythromma najas* (Odonata: Coenagrionidae). Braun Naturkund Schr 4:769–794.

Gu JJ, GX Qiao, D Ren 2010 Revision and new taxa of fossil Prophalangopsidae (Orthoptera: Ensifera). J Orth Res 19:41–56.

Gu JJ, YY Zhao, D Ren 2009 New fossil Prophalangopsidae (Orthoptera, Hagloidea) from the Middle Jurassic of Inner Mongolia, China. Zootaxa 2004:16–24.

Guido AS, BD Perkins 1975 Biology and host specificity of *Cornops aquaticum* (Bruner) (Orthoptera: Acrididae), a potential biological control agent for water hyacinth. Environ Entomol 4:400–404.

Günthart H, MS Günthart 1983 *Aguriahana germari* (Zett.) (Hom. Auch. Cicadellidae, Typhlocybinae): breeding and specific feeding behaviour on pine needles. Mitt Schweiz Entomol Ges 56:33–44.

Gwynne DT 2001 Katydids and bush-crickets: reproductive behavior and evolution of the Tettigoniidae. Cornell University Press, Ithaca, NY.

Halle TG 1908 Zur Kenntniss mesozoischen Equisetales Schwedens. Kung Sven Vetetenskap Handl 43:1–56.

He HY, XL Wang, ZH Zhou, RX Zhu, F Jin, F Wang, X Ding, A Boven 2004 $^{40}Ar/^{39}Ar$ dating of ignimbrite from Inner Mongolia, northeastern China, indicates a post-Middle Jurassic age for the overlying Daohugou Bed. Geophys Res Lett 31:1–4.

Hellmund M 1987 Hennef-Rott, eine Fossilfundstelle von Weltgeltung im Rhein-Sieg-Kreis. Jahrb Rhein-Sieg-Kreises 1988:152–157.

——— 1988 Porzellanite—eine neue fossilführende Kieselsteinmodifikation aus Rott im Siebengebirge. Decheniana 141:319–326.

Hellmund M, W Hellmund 1993 Neufunde fossile Kleinlibellen (Odonata, Zygoptera) aus dem Oberoligozän von Rott im Siebengebirge. Decheniana 146:348–351.

——— 1996*a* Fossile Zeugnisse zum Verhalten von Kleinlibellen aus Rott. Pages 57–60 *in* W von Koenigswald, ed. Fossillagerstätte Rott bei Hennef im Siebengebirge Rheinlandia. Rheinlandia, Bonn.

——— 1996*b* Zum Fortpflanzungsmodus fossiler Kleinlibellen (Insecta, Odonata, Zygoptera). Palaeontol Zeit 70:153–170.

——— 1996*c* Zur endophytischen Eiablage fossiler Kleinlibellen (Insecta, Odonata, Zygoptera), mit Beschreibung eines neuen Gelgetyps. Mitt Bayer Staat Palaeontol Hist Geol 36:107–115.

——— 1998 Eilogen von Zygopteren (Insecta, Odonata, Coenagrionidae) in unteroligozänen Maarsedimenten von Hammerunterwiesenthal (Freistaat Sachsen). Abh Staat Mus Mineral Geol Dresd 43/44:281–292.

——— 2002*a* Eigelge fossilier Zygopteren aus dikotylenblättern aus dem Mittelmiozän von Salzhausen (Vogelsberg, Hessen, Deutschland). Odonatologica 31:253–272.

——— 2002*b* Erster Nachweis von Kleinlibellene-Eilogen (Insecta, Zygoptera, Lestidae) in der mitteleozänen Braunkohle des ehemaligen Tagebaues Mücheln, Bfd. Neumark-Nord (Geiseltal, Sachsen-Anhalt, Deutschland). Halles Jarb Geowiss B 24:47–55.

——— 2002*c* Neufunde und Ergänzungen zur Fortpflanzungsbiologie fossiler Kleinlibellen (Insecta, Odonata, Zygoptera). Stutt Beit Naturk 319:1–26.

Hilker M, C Stein, R Schröder, M Varama, R Mumm 2005 Insect egg deposition induces defence responses in *Pinus sylvestris*: characterization of the elicitor. J Exp Biol 208:1849–1854.

Hilliard JR Jr 1982 Endophytic oviposition by *Leptysma marginicollis marginicollis* and *Stenacris vitreipennis* (Orthoptera: Acrididae: Leptysminae) with life history notes. Trans Am Entomol Soc 108:153–180.

Hinton HE 1981 Biology of insect eggs. Vols 1–3. Pergamon, Oxford.

Hori K 1968 Feeding behavior of the cabbage bug, *Eurydema rugosa* Motschulsky (Hemiptera: Pentatomidae) on the cruciferous plants. Appl Entomol Zool 3:26–36.

Horn YM, K Adami-Rodrigues, LM Anzótegui 2011 Primeras evidencias de interacción insecto-planta en el Neógeno del Noroeste de la Argentina. Rev Bras Paleontol 14:87–92.

Hörnig MK, C Haug, JW Schneider, JT Haug 2018 Evolution of reproductive strategies in dictyopteran insects—clues from ovipositor morphology of extinct roachoids. Acta Palaeontol Pol 63:1–24.

Hou WJ, YZ Yao, WT Zhang, D Ren 2012 The earliest fossil flower bugs (Heteroptera: Cimicomorpha: Cimicoidea: Vetanthocoridae) from the Middle Jurassic of Inner Mongolia, China. Eur J Entomol 109:281–288.

Hu HJ, YZ Yao, D Ren 2014 New fossil Procercopidae (Hemiptera, Cicadomorpha) from the Cretaceous of northeastern China. Acta Geol Sin 88:725–729.

Huang DY 2016 The Daohugou biota. Shanghai Scientific and Technical, Shanghai. (In Chinese.)

Isenhour DJ, KV Yeargan 1982 Oviposition sites of *Orius insidiosus* (Say) and *Nabis* spp. in soybean (Hemiptera: Anthocoridae and Nabidae). J Kans Entomol Soc 55:65–72.

Janz N 2002 Evolutionary ecology of oviposition strategies. Pages 349–376 *in* M Hilker, T Meiners, eds. Chemoecology of insect eggs and egg deposition. Blackwell, Berlin.

Jiang BY 2006 Non-marine *Ferganoconcha* (Bivalvia) from the Middle Jurassic in Daohugou area, Ningcheng County, Inner Mongolia, China. Acta Palaeont Sin 45:259–264.

Johnson WT, HH Lyon 1976 Insects that feed on trees and shrubs. Cornell University Press, Ithaca, NY.

Johnston JE 1993 Insects, spiders and plants from the Tallahatta Formation (middle Eocene) in Benton County, Mississippi. Miss Geol 14:71–82.

Kelber KP 1988 Was ist *Equisetites foveolatus*? Pages166–184 *in* H Hagdorn, ed. Neue Forschung zur Erdgeschichte von Crailshem. 1. Goldschneck, Stuttgart.

Kelber KP, G Geyer 1989 Lebensspuren von Insekten an Pflanzen des unteren Keupers. Cour Forsch-Inst Senck 109:165–174.

Krassilov VA, S Shuklina 2008 Arthropod trace diversity on fossil leaves from the mid-Cretaceous of Negev, Israel. Alavesia 2:239–245.

Krassilov VA, N Silantieva, Z Lewy 2008 Traumas on fossil leaves from the Cretaceous of Israel. Pages 7–187 *in* V Krassilov, AP Rasnitsyn, eds. Plant-arthropod interactions in the early angiosperm history: evidence from the Cretaceous of Israel. Pensoft & Brill, Moscow.

Krausel R 1958 Die Juraflora von Sassendorf der Bamberg. Senck Leth 29:87–103.

Laaß M, C Hoff 2015 The earliest evidence of damselfly-like endophytic oviposition in the fossil record. Lethaia 48:115–124.

Labandeira CC 2002*a* The history of associations between plants and animals. Pages 26–74, 248–261 *in* C Herrera, O Pellmyr, eds. Plant-animal interactions: an evolutionary approach. Blackwell Science, Oxford.

——— 2002*b* Paleobiology of middle Eocene plant-insect associations from the Pacific Northwest: a preliminary report. Rocky Mt Geol 37:31–59.

——— 2006*a* The four phases of plant-arthropod associations in deep time. Geol Acta 4:409–438.

——— 2006*b* Silurian to Triassic plant and hexapod clades and their associations: new data, a review, and interpretations. Arthropod Syst Phylogeny 64:53–94.

——— 2010 The pollination of mid-Mesozoic seed plants and the early history of long-proboscid insects. Ann Mo Bot Gard 97:469–513.

——— 2013 A paleobiological perspective on plant-insect interactions. Curr Opin Plant Biol 16:414–421.

——— 2014 Why did terrestrial insect diversity not increase during the angiosperm radiation? mid-Mesozoic, plant-associated insect lineages harbor clues. Pages 261–299 *in* P Pontarotti, ed. Evolutionary biology: genome evolution, speciation, coevolution, and the origin of life. Springer, Cham.

Labandeira CC, JM Anderson, HM Anderson 2018 Arthropod herbivory in Late Triassic South Africa: the Molteno Biota, the Aasvoëlberg 411 locality and the developmental biology of a gall. *In* L Tanner, ed. The Late Triassic world: Earth in a time of transition. Top Geobiol 46:623–719.

Labandeira CC, ED Currano 2013 The fossil record of plant-insect dynamics. Annu Rev Earth Planet Sci 41:287–311.

Labandeira CC, E Kustatscher, T Wappler 2016 Floral assemblages and patterns of insect herbivory during the Permian to Triassic of northeastern Italy. PLoS ONE 11:e0165295.

Labandeira CC, P Wilf, KR Johnson, F Marsh 2007 Guide to insect (and other) damage types on compressed plant fossils, version 3.0, spring 2007. Smithsonian Institution, Washington, DC.

Lambret P, A Besnard, N Matushkina 2015 Initial preference for plant species and state during oviposition site selection by an odonate. Entomol Sci 18:377–382.

Le Pape H, R Bronner 1987 The effects of *Ceutorrhynchus napi* (Curculionidae, Coleoptera) on stem tissues of *Brassica napus* var. *oleifera*. Pages 207–212 *in* V Labeyrie, G Fabres, D Lachaise, eds. Proceedings of the Sixth International Symposium on Insect-Plant Relation. Junk, Dordrecht.

Lewis SE 1992 Insects of the Klondike Mountain Formation, Republic, Washington. Wash Geol 20:15–19.

Lewis SE, MA Carroll 1991 Coleopterous egg deposition on alder leaves from the Klondike Mountain Formation (middle Eocene), northeastern Washington. J Paleontol 65:334–335.

Li LM, D Ren, ZH Wang 2007 New prophalangopsids from late Mesozoic of China (Orthoptera, Prophalangopsidae, Aboilinae). Acta Zootaxon Sin 32:412–422.

Li S, CK Shih, C Wang, H Pang, D Ren 2013 Forever love: the hitherto earliest record of copulating insects from the Middle Jurassic of China. PLoS ONE 8:e78188.

Li S, Y Wang, D Ren, H Pang 2012 Revision of the genus *Sunotettigarcta* Hong, 1983 (Hemiptera, Tettigarctidae), with a new species from Daohugou, Inner Mongolia, China. Alcheringa 36:501–507.

Liang JH, P Vršanský, D Ren 2012 Variability and symmetry of a Jurassic nocturnal predatory cockroach (Blattida: Raphidiomimidae). Rev Mex Cien Geol 29:411–421.

Liang JH, P Vršanský, D Ren, CK Shih 2009 A new Jurassic carnivorous cockroach (Insecta, Blattaria, Raphidiomimidae) from the Inner Mongolia in China. Zootaxa 1974:17–30.

Liebermann J 1957 Sistematica de la oviposición epidafica en acridoideos (Orth. Caelif. Acrid.). Rev Soc Entomol Argent 20:41–44.

Lin QB, DY Huang, A Nel 2007 A new family Cavilabiata from the Lower Cretaceous Yixian Formation, China (Odonata: Anisoptera). Zootaxa 1469:59–64.

Liu SW 1987 Conchostracan fossils from the Yangcaogou Formation in western Liaoning and their age significance. Geol Rev 33:115–121.

Lodos N 1967 Contribution to the biology of and damage caused by the cocoa coreid, *Pseudotheraptus devastans* Dist. (Hemiptera-Coreidae). Ghana J Sci 7:87–102.

Lokesh S, R Singh 2005 Influence of leaf vein morphology in okra genotypes (Malvaceae) on the oviposition of the leafhopper species *Amrasca biguttula* (Hemiptera: Cicadellidae). Entomol Gen 28: 103–114.

Lopez-Abella D, RHE Bradley, KF Harris 1988 Correlation between stylet paths made during superficial proving and the ability of aphids to transmit nonpersistent viruses. Adv Disease Vector Res 5:251–285.

Lu Y, YZ Yao, D Ren 2011 Two new genera and species of fossil true bugs (Hemiptera: Heteroptera: Pachymeridiidae) from northeastern China. Zootaxa 2835:41–52.

Marlatt CL 1907 The periodical cicada. USDA Bull 71:1–181, pls. 1–6.

Martens A 1992 Egg deposition rates and duration of oviposition in *Platynemis pennipes* (Pallas) (Insecta, Odonata). Hydrobiologia 230:63–70.

Matushkina NA, SN Gorb 2007 Mechanical properties of the endophytic ovipositor in damselflies (Zygoptera, Odonata) and their oviposition substrates. Zoology 110:167–175.

McClure MS 1974 Biology of *Erythroneura lawsoni* (Homoptera: Cicadellidae) and coexistence in the sycamore leaf-feeding guild. Environ Entomol 3:59–68.

McLoughlin S 2011 New records of leaf galls and arthropod oviposition scars in Permian-Triassic Gondwanan gymnosperms. Aust J Bot 59:156–169.

McLoughlin S, SK Martin, R Beattie 2015 The record of Australian Jurassic plant-arthropod interactions. Gondwana Res 27:940–959.

Meiners T, M Hilker 2000 Induction of plant synomones by oviposition of a phytophagous insect. J Chem Ecol 26:221–232.

Meng QM, CC Labandeira, QL Ding, D Ren 2017 The natural history of oviposition on a ginkgophyte fruit from the Middle Jurassic of northeastern China. Insect Sci 26:171–179.

Mickoleit G 1973 Über den Ovipositor der Neuropteroidea und Coleoptera und seine phylogenetische Bedeutung (Insecta, Holometabola). Z Morph Tiere 74:37–64.

Moisan P, CC Labandeira, NA Matushkina, T Wappler, S Voigt, H Kerp 2012 Lycopsid-arthropod associations and odonatopteran oviposition on Triassic herbaceous *Isoetites*. Palaeogeogr Palaeoclimatol Palaeoecol 344–345:6–15.

Mugrabi-Oliveira E, GRP Moreira 1996 Conspecific mimics and low host plant availability reduce egg laying by *Heliconius erato phyllis* (Fabricius) (Lepidoptera, Nymphalidae). Rev Bras Zool 13:929–937.

Mumm R, K Schrank, R Wegener, S Schulz, M Hilker 2003 Chemical analysis of volatiles emitted by *Pinus sylvestris* after induction by insect oviposition. J Chem Ecol 29:1235–1252.

Na YL, CL Sun, T Li, Y Li 2014 The insect oviposition firstly discovered on the Middle Jurassic Ginkgoales leaf from Inner Mongolia, China. Acta Geol Sin 88:18–28.

Na YL, CL Sun, HS Wang, DL Dilcher, ZY Yang, T Li, YF Li 2017 Insect herbivory and plant defense on ginkgoalean and bennettitalean leaves of the Middle Jurassic Daohugou Flora from northeast China and their paleoclimatic implications. Palaeoworld 27:202–210.

Norstog KJ, TJ Nicholls 1997 The biology of the cycads. Cornell University Press, Ithaca, NY.

O'Dowd DJ, MF Willson 1989 Leaf domatia and mites on Australasian plants: ecological and evolutionary implications. Biol J Linn Soc 37:191–236.

Ostry ME, NA Anderson 1983 Infection of trembling aspen by *Hypoxylon mammatum* through cicada oviposition wounds. Phytopathology 73:1092–1096.

Pan K 1977 Jurassic conifer, *Yanliaoa sinensis*, gen. et sp. nov. from Yanliao Region. Acta Phytotaxon Sin 15:69–71.

Peñalver E, X Delclòs 2004 Insectos del Mioceno inferior de Ribelsalbes (Castellón, España). Interacciones planta-insecto. Treb Mus Geol Barc 12:69–95.

Petrulevičius JF, T Wappler, A Nel, J Rust 2011 The diversity of Odonata and their endophytic ovipositions from the Upper Oligocene Fossillagerstätte of Rott (Rhineland, Germany). ZooKeys 130: 67–89.

Photita W, S Lumyong, P Lumyong, EHC McKenzie, KD Hyde 2004 Are some endophytes of *Musa acuminata* latent pathogens? Fungal Divers 16:131–140.

Popa ME, A Zaharia 2011 Early Jurassic ovipositories on bennettitalean leaves from Romania. Acta Palaeontol Rom 7:285–290.

Potonié H 1893 Die Flora des Rothliegenden von Thüringen. Abh Koenig Preuss Geol Landes 9:1–298, pls. 1–34.

Pott C, CC Labandeira, M Krings, H Kerp 2008 Fossil insect eggs and ovipositional damage on bennettitalean leaf cuticles from the Carnian (Upper Triassic) of Austria. J Paleontol 82:778–789.

Pott C, S McLoughlin, S Wu, EM Friis 2012. Trichomes on the leaves of *Anomozamites villosus* sp. nov. (Bennettitales) from the Daohugou beds (Middle Jurassic), Inner Mongolia, China: mechanical defence against herbivorous arthropods. Rev Palaeobot Palynol 169:48–60.

Prevec R, RA Gastaldo, J Neveling, SB Reid, CV Looy 2010 An autochthonous glossopterid flora with latest Permian palynomorphs and its depositional setting in the Dicynodont Assemblage Zone of the southern Karoo Basin, South Africa. Palaeogeogr Palaeoclimatol Palaeoecol 292:391–408.

Prevec R, CC Labandeira, J Neveling, RA Gastaldo, CV Looy, M Bamford 2009 Portrait of a Gondwanan ecosystem: a new late Permian fossil locality form KwaZulu-Natal, South Africa. Rev Palaeobot Palynol 156:454–493.

Rasnitsyn AP 1968 New Mesozoic sawflies (Hymenoptera, Symphyta). Pages 190–236 *in* BB Rohdendorf, ed. Jurassic insects of Karatau. Nauka, Moscow.

Rasnitsyn AP, H Zhang 2004 A new family, Daohugoidae fam. n, of siricomorph hymenopteran (Hymenoptera = Vespida) from the Middle Jurassic of Daohugou in Inner Mongolia (China). Proc Russ Entomol Soc 75:12–16.

Readio PA 1922 Ovipositors of Cicadellidae (Homoptera). Kans Univ Sci Bull 14:212–298.

Remes Lenicov AM, MC Hernández 2010 A new species of *Taosa* (Hemiptera: Dictyopharidae) from South America associated with water hyacinth. Ann Entomol Soc Am 103:332–340.

Ren D 1995 Faunae and stratigraphy of Jurassic-Cretaceous in Beijing and the adjacent areas. Seismic, Beijing. (In Chinese.)

Ren D, KQ Gao, ZG Guo, SA Ji, JJ Tan, Z Song 2002 Stratigraphic division of the Jurassic in the Daohugou Area, Ningcheng, Inner Mongolia. Geol Bull China 21:584–591.

Ren D, CC Labandeira, JA Santiago-Blay, AP Rasnitsyn, CK Shih, A Bashkuev, MAV Logan, CL Hotton, DL Dilcher 2009 A probable pollination mode before angiosperms: Eurasian, long-proboscid scorpionflies. Science 326:840–847.

Ren D, XM Meng 2006 New Jurassic protaboilins from China (Orthoptera: Prophalangopsidae, Protaboilinae). Acta Zootaxon Sin 31: 513–519. (In Chinese.)

Ren D, JC Yin, WX Dou 1998 New planthoppers and froghoppers from the Late Jurassic of northeast China (Homoptera: Auchenorrhyncha). Acta Zootaxon Sin 23:281–288.

Renwick JAA 1989 Chemical ecology of oviposition in phytophagous insects. Experientia 45:223–228.

Resetarits WJ Jr 1996 Oviposition site choice and life history evolution. Am Zool 36:205–215.

Roselt G 1954 Ein neuer Schachtelhalm aus dem Keuper und Beiträge zur Kenntnis von *Neocalamites meriani* Brongn. Geologie 3:617–643.

Roversi PF, M Covassi, P Toccafondi 1989 Danni da *Haematoloma dorsatum* (Ahrens) su conifer (Homoptera, Cercopidae). II. Indagine microscopa sulle vie de penetrazione degli stiletto boccali. Redia 72:595–608.

Sanford KH 1964 Eggs and oviposition sites of some predacious mirids on apple trees (Miridae: Hemiptera). Can Entomol 96:1185–1189.

Sankaran T, D Srinath, K Krishna 1966 Studies on *Gesonula punctifrons* Stål (Orthoptera; Acrididae: Cyrtacanthacridinae) attacking water-hyacinth in India. Entomophaga 11:433–440.

Sarzetti LC, CC Labandeira, J Muzón, P Wilf , NR Cúneo, KR Johnson, JF Genise 2009 Odonatan endophytic oviposition from the Eocene of Patagonia: the ichnogenus *Paleoovoidius* and implications for behavioral stasis. J Paleontol 83:431–447.

Sauve AMC, E Thébault, MJO Pocock, C Fontaine 2016 How plants connect pollination and herbivory networks and their contribution to community stability. Ecology 97:908–917.

Schaarschmidt F 1992 The vegetation: fossil plants as witnesses of a warm climate. Pages 27–52 *in* S Schaal, W Ziegler, eds. Messel: an insight into the history of life and of the earth. Clarendon, Oxford.

Schachat SR, CC Labandeira 2015 Evolution of a complex behavior: the origin and initial diversification of foliar galling by Permian insects. Sci Nat 102:14.

Schachat SR, CC Labandeira, DS Chaney 2015 Insect herbivory from early Permian Mitchell Creek Flats of north-central Texas: opportunism in a balanced component community. Palaeogeogr Palaeoclimatol Palaeoecol 440:830–847.

Schachat SR, CC Labandeira, J Gordon, D Chaney, S Levi, MN Halthore, J Alvarez 2014 Plant–insect interactions from Early Permian (Kungurian) Colwell Creek Pond, north-central Texas: the early spread of herbivory in clastic environments. Int J Plant Sci 175:855–890.

Scheirs J, L De Bruyn 2002 Integrating optimal foraging and optimal oviposition theory in plant-insect research. Oikos 96:187–191.

Scott AC, JM Anderson, HM Anderson 2004 Evidence of plant-insect interactions in the Upper Triassic Molteno Formation of South Africa. J Geol Soc Lond 161:401–410.

Scudder GGE 1961 The comparative morphology of the insect ovipositor. Trans R Entomol Soc Lond 113:25–40.

——— 1971 Comparative morphology of insect genitalia. Annu Rev Entomol 16:379–406.

Severson RF, DM Jackson, AW Johnson, VA Sisson, MG Stephenson 1991 Ovipositional behavior of tobacco budworm and tobacco hornworm. Pages 264–277 *in* PA Hedin, ed. Naturally occurring pest bioregulators. American Chemical Society, Washington, DC.

Shah BA 2004 Gondwana lithostratigraphy of Peninsula India: comment. Gondwana Res 7:600–607.

Shen YB, PJ Chen, DY Huang 2003 Age of the fossil conchostracans from Daohugou of Ningcheng, Inner Mongolia. J Stratigr 27:311–313. (In Chinese with English abstract.)

Shively AW 1948 Role of oviposition in plant gall production. Proc Penn Acad Sci 22:94–98.

Sinclair WA, H Lyon, WT Johnson 1987 Diseases of trees and shrubs. Cornell University Press, Ithaca, NY.

Singer MC 1984 Butterfly-host plant relationships: host quality, adult choice, and larval success. Pages 81–88 *in* RI Vane-Wright, PR Ackery, eds. The biology of butterflies. Academic Press, London.

——— 2004 Oviposition preference: its definition, measurement and correlates, and its use in assessing risk of host shifts. Pages 235–244 *in* Proceedings of the XI International Symposium on Biological Control of Weeds. Plant Protection Research Institute, Canberra.

Singh L, R Singh 2005 Influence of leaf vein morphology in okra genotypes (Malvaceae) on the oviposition of the leafhopper species *Amrasca biguttula* (Hemiptera: Cicadellidae). Entomol Gen 28: 103–114.

Smith EL 1969 Evolutionary morphology of external insect genitalia. 1. Origin and relationships to other appendages. Ann Entomol Soc Am 62:1051–1079.

Smith FF, RG Linderman 1974 Damage to ornamental trees and shrubs resulting from oviposition by periodical cicada. Environ Entomol 3:725–732.

Smith MC, EC Lake, GS Wheeler 2016 Oviposition choice and larval performance of *Neomusotima conspurcatalis* on leaflet types of the invasive fern, *Lygodium microphyllum*. Entomol Exp Appl 160:11–17.

Snodgrass RE 1933 Morphology of the insect abdomen. II. The genital ducts and the ovipositor. Smithson Misc Coll 85:1–148.

——— 1935 Principles of insect morphology. McGraw-Hill, New York.

Sorenson CJ 1928 Treehopper injury in Utah orchards. Utah Agric Exp Stn 206:1–18.

Spooner-Hart R, L Tesoriero, B Hall 2007 Field guide to olive pests, diseases and disorders in Australia. Rural Industries Research and Development Corporation, Canberra.

Srivastava AK 1987 Lower Barakar flora of Raniganj coalfield and insect/plant relationship. Palaeobotanist 36:138–142.

Srivastava AK, D Agnihotri 2011 Insect traces on Early Permian plants of India. Paleontol J 45:200–206.

St Quentin D 1962 Der Eilegeapparat der Odonaten. Zeit Morphol Oekol 51:165–189.

Straus A 1977 Gallen, Minen und andere Frasspuren im Pliozän von Willershausen am Harz. Verhand Botan Ver Prov Brandenbg 113:43–80.

Sun G, DL Dilcher, S Zheng, Z Zhou 1998 In search of the first flower: a Jurassic angiosperm *Archaefructus* from northeast China. Science 282:1692–1695.

Sun G, SL Sheng, DL Dilcher, YD Wang, SW Mei 2001 Early angiosperms and their associated plants from western Liaoning, China. Shanghai Scientific and Technological Education, Shanghai.

Sun KQ, JZ Cui, SJ Wang 2016 Fossil gymnosperms in China. Vol 3, pt 1. Higher Education, Beijing.

Swisher CC, YQ Wang, XL Wang, X Xu, Y Wang 1999 Cretaceous age for the feathered dinosaurs of Liaoning, China. Nature 400:58–61.

Tan X, DL Dilcher, HS Wang, Y Zhang, YL Na, T Li, YF Li, CL Sun 2018 *Yanliaoa*, an extinct genus of Cupressaceae s. l. from the Middle Jurassic, northeastern China. Palaeoworld 27:360–373.

Tang D, YZ Yao, D Ren 2015 New fossil flower bugs (Heteroptera: Cimicomorpha: Cimicoidea: Vetanthocoridae) with uniquely long ovipositor from the Yixian Formation (Lower Cretaceous), China. Cretac Res 56:504–509.

Taylor TN, EL Taylor, M Krings 2009 Paleobotany: the biology and evolution of fossil plants. 2nd ed. Academic Press, Burlington, VT.

Thompson JN, O Pellmyr 1991 Evolution of oviposition behavior and host preference in Lepidoptera. Annu Rev Entomol 36:65–89.

Tower DG 1914 The mechanism of the mouth parts of the squash bug *Anasa tristis*. Psyche 21:99–108.

Tremblay E, M Bianco 1978 Punteruoli del cavolfiore in Campania. Istituto di Entomología Agraria della Università di Napoli, Portici.

Turk SZ 1984 Acridios del NOA VI: Ciclo de vida de *Cornops frenatum cannae* Roberts y Carbonell (Acrididae, Leptysminae) con especial referencía su oviposición endofitica. Rev Soc Entomol Argent 43:91–102.

van Konijnenburg-van Cittert JHA, S Schmeißner 1999 Fossil insect eggs on Lower Jurassic plant remains from Bavaria (Germany). Palaeogeogr Palaeoclimatol Palaeoecol 152:215–223.

Vasilenko DV 2005 Damages on Mesozoic plants from the Transbaikalian locality Chernovskie Kopi. Paleontol J 39:628–633.

——— 2008 Insect ovipositions on aquatic plant leaves *Quereuxia* from the upper Cretaceous of the Amur Region. Paleontol J 42:514–521.

——— 2011 The first record of endophytic insect oviposition from the Tatarian of European Russia. Paleontol J 45:333–334.

Vasilenko DV, AP Rasnitsyn 2007 Fossil ovipositions of dragonflies: review and interpretation. Paleontol J 41:1156–1161.

Ventura MU, AR Panizzi 2000 Oviposition behavior of *Neomegalotomus parvus* (West.) (Hemiptera: Alydidae): daily rhythm and site choice. An Soc Entomol Bras 29:391–400.

Vidano C 1963 Eccezionali strozzature anulari caulinari provocate da *Ceresa bubalus* Fabricius in Vitis. Ann Fac Sci Agr Univ Studi Torino 2:57–108.

Vincent JFV 1990 Fracture properties of plants. Adv Bot Res 17: 235–287.

Vishniakova VN 1968 Mesozoic cockroaches with an external ovipositor and the specific relations of their reproduction (Blattodea). Pages 55–86 *in* BB Rohdendorf, ed. Jurassic insects of Karatau. Academy of Sciences, Moscow. (In Russian.)

Vjalov OS 1975 Fossil remains of insect feeding. Paleontol Sbor 1:147–155.

Vršanský P, JH Liang, D Ren 2009 Advanced morphology and behaviour of extinct earwig-like cockroaches (Blattida: Fuziidae fam. nov.). Geol Carpat 60:449–462.

Waage JK 1987 Choice and utilization of oviposition sites by female *Calopteryx maculata* (Odonata: Calopterygidae): influence of site size and the presence of other females. Behav Ecol Sociobiol 20:439–446.

Walker JD, JW Geissman, SA Bowring, LE Babcock 2013 The Geological Society of America geologic time scale. Geol Soc Am Bull 125:259–272.

Walsh DB, MP Bolda, RE Goodhue, AJ Dreves, J Lee, DJ Bruck, VM Walton, SD O'Neal, FG Zalom 2011 *Drosophila suzukii* (Diptera: Drosophilidae): invasive pest of ripening soft fruit expanding its geographic range and damage potential. J Integr Pest Manag 2: G1–G7.

Wang B, HC Zhang 2009*a* A remarkable new genus of Procercopidae (Hemiptera: Cercopoidea) from the Middle Jurassic of China. C R Palevol 8:389–394.

——— 2009*b* Tettigarctidae (Insecta: Hemiptera: Cicadoidea) from the Middle Jurassic of Inner Mongolia, China. Geobios 42:243–253.

Wang M, CK Shih, D Ren 2012 *Platyxyela* gen. nov. (Hymenoptera, Xyelidae, Macroxyelinae) from the Middle Jurassic of China. Zootaxa 3456:82–88.

Wang SJ, JZ Cui, Y Yang, KQ Sun 2016 Fossil gymnosperms in China. Vol 3, pt II. Higher Education, Beijing.

Wang SS, HG Hu, PX Li 2001 The geological age of Yixian Formation in western Liaoning, China. Bull Mineral Petrol Geochem 20:189–291. (In Chinese with English abstract.)

Wang T, D Ren, JH Liang, CK Shih 2007 New Mesozoic cockroaches (Blattaria: Blattulidae) from Jehol Biota of western Liaoning in China. Ann Zool 57:483–495.

Wappler T 2010 Insect herbivory close to the Oligocene-Miocene transition: a quantitative analysis. Palaeogeogr Palaeoclimatol Palaeoecol 292:540–550.

Webb JA 1982 Triassic species of *Dictyophyllum* from eastern Australia. Alcheringa 6:79–91.

Weber H 1928 Sklett, Muskulatur und darm der schwarzen Blattlaus *Aphis fabae* Scop. mit besonderer Berücksichtigung des Funktion des Mundwerkzeuge und des Darms. Zoologica 76:1–120.

Wei DD, JH Liang, D Ren 2013 A new fossil genus of Fuziidae (Insecta, Blattida) from the Middle Jurassic of Jiulongshan Formation, China. Geodiversitas 35:335–343.

Weiss CE 1876 Steinkohlen-Calamarien, mit besonderer Berücksichtigung ihrer Fructificationen. Neumann'sche Kartenhandlung, Berlin.

Weltz CE, L Vilhelmsen 2014 The saws of sawflies: exploring the morphology of the ovipositor in Tenthredinoidea (Insecta: Hymenoptera), with emphasis on Nematinae. J Nat Hist 48:133–183.

Wesenberg-Lund C 1913*a* Fortpflanzungsverhältnisse: Paarung und Eiblage der Süsswasserinsekten. Fortsch Naturwiss Forsch 8:161–286.

——— 1913*b* Odonaten-Studien. Mitt Biol Súßwasser Hill Lyngby 16:155–228.

——— 1943 Biologie der Süsswasserinsekten. Springer, Berlin.

Wilf P 2008 Insect-damaged leaves record food web response to ancient climate change and extinction. New Phytol 178:486–502.

Xing DH, CL Sun, YW Sun, LD Zhang, YD Peng, SW Chen 2005 New knowledge on Yixian Formation. Acta Geosci Sin 26:25–30.

Xu Q, J Jin, CC Labandeira 2018 Williamson Drive: herbivory of a north-central Texas flora of latest Pennsylvanian age showing discrete component community structure, early expansion of piercing and sucking, and plant counterdefenses. Rev Palaeobot Palynol 251:28–72.

Yang J, H Zhou, H Cao 2000 Stratigraphical Monographs of China: Triassic. Geologic Publishing House, Beijing.

Yang Q, YJ Wang, CC Labandeira, CK Shih, D Ren 2014 Mesozoic lacewings from China provide phylogenetic insight into evolution of the Kalligrammatidae (Neuroptera). BMC Evol Biol 14:126.

Yao YZ, WZ Cai, D Ren 2006*a* The first discovery of fossil rhopalids (Heteroptera: Coreoidea) from Middle Jurassic of Inner Mongolia, China. Zootaxa 1269:57–68.

——— 2006*b* Fossil flower bugs (Heteroptera: Cimicomorpha: Cimicoidea) from the Late Jurassic of northeast China, including a new family Vetanthocoridae. Zootaxa 1360:1–40.

——— 2006*c* *Sinopachymeridium popovi* gen. and sp. nov.: a new fossil true bug (Heteroptera: Pachymeridiidae) from the Middle Jurassic of Inner Mongolia, China. Ann Zool 56:753–756.

——— 2007 The first fossil Cydnidae (Hemiptera: Pentatomoidea) from the Late Mesozoic of China. Zootaxa 1388:59–68.

——— 2008 New Jurassic fossil true bugs of the Pachymeridiidae (Hemiptera: Pentatomomorpha) from northeast China. Acta Geol Sin 82:35–47.

Yao YZ, WZ Cai, D Ren, CK Shih 2006*d* New fossil rhopalids (Heteroptera: Coreoidea) from the Middle Jurassic of Inner Mongolia, China. Zootaxa 1384:41–58.

Yao YZ, D Ren, DA Rider, WZ Cai 2012 Phylogeny of the infraorder Pentatomomorpha based on fossil and extant morphology, with description of a new fossil family from China. PLoS ONE 7:e37289.

Yothers MA 1934 Biology and control of tree hoppers injurious to fruit trees in the Pacific Northwest. USDA Tech Bull 402:1–46.

Yuan CX, HB Zhang, M Li, XX Ji 2004 Discovery of a Middle Jurassic fossil tadpole from Daohugou Region, Ningcheng, Inner Mongolia, China. Acta Geol Sin 78:145–148.

Zhang HC, AP Rasnitsyn 2006 Two new anaxyelid sawflies (Insecta, Hymenoptera, Siricoidea) from the Yixian Formation of western Liaoning, China. Cretac Res 27:279–284.

Zhang HC, AP Rasnitsyn, JF Zhang 2002 The oldest known scoliid wasps (Insecta, Hymenoptera, Scoliidae) from the Jehol biota of western Liaoning, China. Cretac Res 23:77–86.

Zhang HC, JF Zhang 2000 Xyelid sawflies (Insecta, Hymenoptera) from the Upper Jurassic Yixian Formation of western Liaoning, China. Acta Palaeontol Sin 39:476–492.

Zhang JF 2000 The discovery of aeschnidiid nymphs (Aeschnidiidae, Odonata, Insecta). Chin Sci Bull 45:1031–1038.

Zhang JF, HC Zhang 2001 New findings of larval and adult aeschnidiids (Insecta: Odonata) in the Yixian Formation, Liaoning Province, China. Cretac Res 22:443–450.

Zhang WT, CK Shih, CC Labandeira, JC Sohn, DR Davis, JA Santiago-Blay, O Flint, D Ren 2013 New fossil Lepidoptera (Insecta: Amphiesmenoptera) from the Middle Jurassic Jiulongshan Formation of northeastern China. PLoS ONE 8:e79500.

Zhang XW, D Ren, H Pang, CK Shih 2008*a* A new genus and species of Chresmodidae (Insecta: Gryllones) from Upper Jurassic–Lower Cretaceous of Yixian Formation, Inner Mongolia, China. Zootaxa 1702:26–40.

——— 2008*b* A water-skiing chresmodid from the Middle Jurassic in Daohugou, Inner Mongolia, China (Polyneoptera: Orthopterida). Zootaxa 1762:53–62.

——— 2010 Late Mesozoic chresmodids with forewing from Inner Mongolia, China (Polyneoptera: Archaeorthoptera). Acta Geol Sin 84:38–46.

Zherikhin VV 2002 Insect trace fossils. Pages 303–324 *in* AP Rasnitsyn, DLJ Quick, eds. History of insects. Kluwer, Dordrecht.

Zhou HQ 1981 Discovery of the Upper Triassic flora from Yangcaogou of Beipiao, Liaoning. Pages 147–152 *in* Paleontological Society of China, ed. Selected Papers of the Twelfth Annual Conference of the Palaeontological Society of China. Science, Beijing.

Zhou Z, PM Barrett, J Hilton 2003 An exceptionally preserved Lower Cretaceous ecosystem. Nature 421:807–814.